



HAL
open science

Etude numérique et asymptotique des écoulements dans des domaines minces

Abdesselam Nachit

► **To cite this version:**

Abdesselam Nachit. Etude numérique et asymptotique des écoulements dans des domaines minces. Mathématiques générales [math.GM]. Université Jean Monnet - Saint-Etienne, 2010. Français. NNT : 2010STET4005 . tel-00674436

HAL Id: tel-00674436

<https://theses.hal.science/tel-00674436>

Submitted on 27 Feb 2012

HAL is a multi-disciplinary open access archive for the deposit and dissemination of scientific research documents, whether they are published or not. The documents may come from teaching and research institutions in France or abroad, or from public or private research centers.

L'archive ouverte pluridisciplinaire **HAL**, est destinée au dépôt et à la diffusion de documents scientifiques de niveau recherche, publiés ou non, émanant des établissements d'enseignement et de recherche français ou étrangers, des laboratoires publics ou privés.

THESE

Pour obtenir le grade de

DOCTEUR DE L'UNIVERSITÉ JEAN MONNET DE SAINT-ÉTIENNE

Discipline : Mathématiques Appliquées

Présentée et soutenue publiquement le vendredi 10 décembre 2010

par

Abdesselam NACHIT

Etude numérique et asymptotique des écoulements dans des domaines minces

Directeur de thèse :

Grigory PANASENKO et Abdelmalek ZINE

Jury de Thèse :

Rapporteurs : **Youcef AMIRAT**, Professeur, Université Blaise Pascal, Aubière
Ruxandra STAVRE, Directeur de Recherche, Institut de Mathématique "Simion Stoilow" de Roumanie

Examineurs : **Jerôme POUSIN**, Professeur, INSA de Lyon
Alexandre ELBERT, Chargé de recherche, Institut de Mathématique et Mécanique des Sciences de la Russie, Ekaterinburg, Russie

Directeur : **Grigory PANASENKO**, Professeur, Université de Saint-Étienne
Abdelmalek ZINE, Maître de Conférences, HDR, École centrale de Lyon

Table des matières

1	Introduction	5
2	Problèmes d'écoulement de fluides newtoniens et non newtoniens	9
2.1	Problème de Stokes	9
2.1.1	Le problème continu	10
2.2	Problème de Stokes non linéaire	11
3	M.A.P.D.D : Method of Asymptotic Partial Domain Decomposition	13
3.1	Flows in tube structures	13
3.1.1	Definitions. One bundle structure	13
3.1.2	Tube structure with m bundles of tubes	25
3.2	Decomposition of a flow in a tube structure	28
4	Asymptotic analysis of a periodic flow in a thin channel with two viscoelastic walls	36
4.1	Introduction :	36
4.2	The Description of the physical problem :	37
4.3	Modeling the problem :	38
4.4	Variational approach of the problem	40
4.4.1	Variational formulation	40
4.5	Asymptotic approach :	41
4.6	Introducing functions :	42
4.6.1	Proposition :	43
4.7	Problem Resolution :	45

4.7.1	Proposition :	46
4.7.2	Proposition :	48
4.7.3	Proposition :	49
4.8	A priori Estimates :	50
4.8.1	Proposition :	53
4.9	Error estimates : rigorous justification of the asymptotic expansion . .	53
4.9.1	Proposition :	54
5	Parallelization of the asymptotic partial decomposition for flows in thin structures	60
5.1	Introduction	60
5.2	MAPDD for newtonian flows	61
5.2.1	One-bundle tube structure	61
5.2.2	Multi-bundle tube structure	61
5.2.3	General case	62
5.3	MAPDD for non-newtonian fluid flows	63
5.4	Numerical simulations	65
5.4.1	introduction :	65
5.4.2	The complete T-Geometry	65
5.4.3	MAPDD for non-Newtonian flow in T-Geometry	68
5.4.4	The complete Y-Geometry	71
5.4.5	MAPDD for non-Newtonian flow in Y-Geometry	74
5.4.6	The complete T-Y-Geometry	78
5.4.7	MAPDD for non-Newtonian flow in T-Y-Geometry	81
5.4.8	The complete Geometry of three bifurcations	83
5.4.9	MAPDD for non-Newtonian flow in three bifurcations	86
5.4.10	The complete Geometry of quadruple bifurcations	88
5.4.11	MAPDD for non-Newtonian flow in quadruple bifurcations	91
5.4.12	The complete Geometry of Semi-Triangle	93
5.4.13	MAPDD for non-Newtonian flow in Semi-Triangle-Geometry	96

5.4.14	The complete Geometry of Triangle	98
5.4.15	MAPDD for non-Newtonian flow in Triangle-Geometry	99

A	Rappels sur la discrétisation des problèmes de Stokes linéaire et non linéaire	104
A.1	Problème de Stokes linéaire	104
A.1.1	Cadre fonctionnel :	105
A.1.2	Existence et unicité :	106
A.1.3	Le problème discret :	107
A.2	Problème de Stokes non linéaire	108
A.2.1	Remarque :	109
A.3	Choix des éléments :	110
A.3.1	élément finis P2-P1 de Taylor-Hood :	110
A.3.2	Base nodale pour la pression :	111
A.3.3	Base nodale pour la vitesse :	112
	Bibliographie	115

Remerciements :

Mes premiers remerciements s'adressent au professeur Grigory Panasenکو et Monsieur Zine qui m'ont dirigé tout au long de ce travail, à mes rapporteurs Ruxandra Stavre et Youcef Amirat pour leurs remarques et suggestions et mes examinateurs : Professeur Jerome Pousin et Alexandre Elbert.

Je remercie l'aide financière aux études du Québec.

Je remercie l'ensemble du Laboratoire de Mathématiques de l'Université de Saint-Etienne (LAMUSE) au sein duquel j'ai effectué ce travail, particulièrement Alain LARGILLIER et Mario Ahues pour leur aide.

Mes remerciements personnels vont à Pascale Villet, Roula, Imanne, Benoit, Marthe, Hamza, Ahmed, Boualam, Aziz.

à ma mère, mes frères, mes soeurs et à la mémoire de mon père

Chapitre 1

Introduction

D'un point de vue mécanique, le sang a un comportement non newtonien c'est à dire que sa viscosité n'est pas constante, mais varie dans des proportions considérables (de 1 à 1000). Ces variations sont liées à des modifications de sa structure : agrégation/désagrégation globulaire, mais aussi de son comportement mécanique lors de l'écoulement : variations de la structure et interaction avec les parois des vaisseaux sanguins.

Un des objectifs de cette thèse est d'étudier, dans le chapitre 4, l'analyse asymptotique d'un problème d'interaction fluide–structure dans une structure tubulaire mince avec deux parois élastiques, dans le chapitre 5, d'appliquer la Méthode de Décomposition Asymptotique Partielle du Domaine dans des géométries contenant des bifurcations de divers types (T,Y, etc).

La Méthode de Décomposition Asymptotique Partielle du Domaine (M.A.P.D.D.) est une méthode numérique récente, apparue en 1998, développée par G. Panasenko dans le but de traiter des problèmes dépendant d'un petit paramètre ε qui intervient dans le problème soit au niveau des équations soit au niveau du domaine. La résolution numérique de ces équations est souvent rendue plus compliquée par la présence de ce paramètre. L'étude du comportement de la solution lorsque le petit paramètre tend vers zéro est généralement traitée en utilisant des méthodes asymptotiques. Malheureusement, du point de vue de la mise en oeuvre numériques, ces méthodes sont souvent difficiles à traiter. Des méthodes se basant sur le comportement asymptotique

ont été développées.

Les premiers travaux datent de 1999 [2], ils étudient l'application de la Méthode Asymptotique Partielle de Décomposition du Domaine (M.A.P.D.D.) au problème de Stokes dans des structures tubulaires minces. Le développement asymptotique de la solution est construit et justifié. Les problèmes de couches limites sont étudiés. Cette approche permet de réduire la géométrie initiale à une partie, seulement, du domaine où les problèmes de couches limites sont concentrées.

En 2004 [3], les auteurs étudient l'écoulement dans une structure tubulaire ondulée : analyse asymptotique et résolution numérique. Ils considèrent le mouvement bidimensionnel et stationnaire d'un fluide incompressible à l'intérieur d'un domaine constitué de tubes ondulés. La méthode de décomposition asymptotique partielle du domaine est mise en place et des résultats numériques, obtenus pour la modélisation de procédés d'extrusion sont présentés afin de justifier l'application de cette méthode. En effet, cette analyse consiste à étudier l'écoulement d'un fluide à l'intérieur d'un domaine constitué de deux tubes ondulés dépendant d'un petit paramètre $\varepsilon > 0$. Le problème de départ est la modélisation des phénomènes mécaniques qui interviennent au cours de l'extrusion d'un polymère. L'analyse asymptotique du problème permet de mettre en évidence le caractère périodique du phénomène et de construire un problème cellulaire permettant d'approcher la solution. En considérant les effets de couche limite, des estimations d'erreur sont montrées afin de justifier la solution asymptotique. La méthode numérique développée dans ce travail met en place la méthode de décomposition asymptotique partielle du domaine. Cette méthode consiste à écrire le problème initial variationnel sur un espace plus régulier, construit à partir du comportement asymptotique de la solution. Des estimations d'erreur permettent de justifier la solution partiellement décomposée comme approximation de la solution initiale.

Dans les travaux de 1999, le problème de Stokes dans une structure tubulaire constituée de cylindres fins a été considéré, en utilisant la méthode de décomposition asymptotique partielle du domaine (M.A.P.D.D.). Cette méthode consiste à séparer le problème initial en petits sous-problèmes afin de réduire le coût total de la résolution numérique.

Dans ce travail, nous appliquerons la M.A.P.D.D. L'idée principale consiste à construire une solution asymptotique pour le problème afin de décrire et de justifier l'application de la M.A.P.D.D. Cette analyse confirme la localisation des effets de couches limites au voisinage des zones de transition ainsi que la convergence de la solution asymptotique vers une solution à l'intérieur des tubes. La justification numérique proposée ici, est l'application de cette méthode pour simuler un procédé d'écoulement non newtonien. En effet, la méthode consiste à résoudre le problème initial sur une petite partie du domaine (correspondant généralement à un voisinage où les couches limites apparaissent) et de simplifier le problème sur un sous domaine en utilisant la forme particulière de la solution asymptotique.

Ce travail se déroulera comme suit : Dans le chapitre 2 et l'annexe, on a introduit quelques résultats d'existence et d'unicité pour les problèmes d'écoulements newtoniens et non newtoniens.

Le chapitre 3 propose une étude du problème de Navier-Stokes dans des structures tubulaires minces (constituées d'union finie de cylindres). De tels problèmes se posent dans la modélisation des écoulements sanguins. La solution asymptotique est construite et justifiée, les problèmes de couches limites sont étudiées enfin la M.A.P.D.D est appliquée.

Dans le chapitre 4 on étudie le problème de couplage fluide-structure. plus précisément, on considère l'écoulement non stationnaire d'un fluide visqueux à l'intérieur d'un tube mince à parois élastiques. Le problème dépend de deux paramètres ε qui mesure le rapport entre le diamètre et la longueur du tube, ainsi que γ qui mesure la rigidité des parois. Ce développement est justifié par des estimations d'erreur et des estimations *a priori*. Les termes principaux de la solution asymptotique sont comparés à ceux de la solution d'un écoulement de Poiseuille dans un tube à parois rigides. Dans le cas critique $\gamma = 3$, pour le déplacement, on obtient une équation différentielle non classique du sixième ordre.

Dans le chapitre 5, une analyse asymptotique des équations de Stokes non linéaire dans des structures tubulaires minces (union finie de tubes cylindriques avec $\varepsilon \ll 1$). On montre alors, que pour des petits nombres de Reynolds on obtient un écoulement

de Poiseuille à une certaine distance δ des extrémités des cylindres. Ces fonctions de Poiseuille sont collées par des fonctions de type couche limite aux bords des tubes cylindriques. Cette structure de la solution nous permet de justifier pour ce fluide la Méthode de Décomposition Asymptotique du Domaine(M.A.P.D.D.). En remplaçant la vitesse inconnue par les fonctions de Poiseuille à une distance δ des bords, estimée à $O(\varepsilon|\ln\varepsilon|)$.

Par conséquence, cette méthode réduit considérablement les coûts de calculs. En effet, cette approche peut être appliquée aux énormes systèmes d'écoulements de fluides comme le système de circulation sanguine. Ici, nous discutons la possibilité de paralléliser les calculs dans l'approche M.A.P.D.D. bien que cette approche ne soit justifiée rigoureusement que pour les écoulements newtoniens, nous étudions son application aux fluides non newtoniens en développant certaines expériences numériques. Enfin l'idée principale de la M.A.P.D.D consiste à faire une coupe au niveau du champ de vitesse et transmettre cette coupe à l'entrée ou à la sortie du domaine. Des résultats numériques extrêmement importants ont été mis en évidence dans le domaine décomposé.

Chapitre 2

Problèmes d'écoulement de fluides newtoniens et non newtoniens

2.1 Problème de Stokes

Le problème de Stokes est au coeur de la simulation numérique en mécanique des fluides. Une bonne compréhension des difficultés reliées à sa discrétisation par la méthode des éléments finis ouvre la voie à toute une panoplie d'applications. Cela va des écoulements de fluides fortement visqueux avec des applications à la mise en forme des polymères, aux fluides peu visqueux que nous modéliserons à l'aide des équations de Navier-Stokes pour étudier des applications en médecine par exemple l'écoulement du sang.

Introduisant en premier lieu un peu de notation. On note τ le tenseur des contraintes de Cauchy :

$$\tau = -pI + \sigma$$

où p est la pression et σ , le tenseur des extra-contraintes. L'équation d'équilibre s'écrit encore ici :

$$-\nabla \cdot \tau = f$$

où f est un vecteur de forces volumiques supposé connu.

En tout point du domaine de calcul, nous cherchons à déterminer le champ des

vitesse $u = (u_1, u_2)$ de même que la pression p . Nous nous intéressons, en particulier, au cas des fluides incompressibles pour lesquels la conservation de la masse impose que :

$$\nabla \cdot u = 0$$

Pour fermer le système, il reste à établir une relation entre le tenseur des extra-contraintes σ et le champ des vitesses u ou plus précisément le tenseur des taux de déformation $d(u) = \frac{1}{2}(\nabla u + \nabla^T u)$. Cette relation, dite loi de comportement, dépend de la nature du fluide considéré.

Le premier cas (et aussi le plus simple) concerne les fluides newtoniens pour lesquels la loi de comportement s'écrit :

$$\sigma = 2\eta d(u)$$

où η est la viscosité du fluide que l'on suppose constante. Cette loi convient dans certaines applications mais pas du tout dans d'autres. On vérifie en effet facilement que la viscosité de bon nombres de fluides n'est pas constante mais varie avec les taux de cisaillements (et la température). Plus précisément, plus un fluide est cisailé (par exemple entre deux plaques en mouvement l'une par rapport à l'autre), plus la viscosité diminue. On doit également ajouter une forte dépendance de la viscosité en fonction de la température. Dans un premier temps, nous ne nous intéressons qu'au cas où la viscosité est constante. Nous reviendrons sur un cas plus général à la prochaine section.

2.1.1 Le problème continu

Dans le cas d'un écoulement stationnaire, rampant d'un fluide newtonien, les équations de conservation de la quantité de mouvement et de la masse introduites plus haut, donnent :

$$\begin{cases} -\nabla \cdot (2\eta d(u)) + \nabla p = f, \\ \nabla \cdot u = 0 \end{cases} \quad (2.1)$$

Le problème (2.1) est communément appelé problème de Stokes. A ce système d'équations, il faut ajouter des conditions aux limites appropriées. Pour tous les détails concernant l'analyse du problème de Stokes (1.1), ainsi que sa discrétisation par la

méthode des éléments finis, on peut se référer aux travaux de Temam, Girault–Raviart, Brezzi–Fortin [17],[11],[7]. Quelques rappelles sont donnés en annexe.

Nous présentons également dans le chapitre 5 des essais numériques du (2.1) dans des géométries particulières.

2.2 Problème de Stokes non linéaire

Les fluides newtoniens, régis par le problème de Stokes, sont une approximation raisonnable de fluides plus réalistes appelées fluides non newtoniens ou quasi-newtoniens. Pour ces fluides, dont certains sont d’usage très courant (polymères, certaines huiles, pâtes alimentaires, sang, ...), la viscosité est une fonction du tenseur des taux de déformation, de la température, du temps, etc. Ils donnent lieu à des problèmes non linéaires dont l’étude pose des difficultés aussi bien au niveau mathématique que numérique.

Pour ces fluides non newtoniens, le tenseur des extra-contraintes s’écrit sous la forme générale suivante :

$$\sigma = 2\eta(|d(u)|)d(u)$$

où $|d(u)|$ désigne le second invariant du tenseur $d(u)$ défini par :

$$|d(u)|^2 = d(u) : d(u) = \sum_{i,j=1}^2 d_{i,j}(u)d_{i,j}(u), \quad d_{i,j}(u) = \frac{1}{2} \left(\frac{\partial u_i}{\partial x_j} + \frac{\partial u_j}{\partial x_i} \right), \quad \forall i, j = 1, 2.$$

La viscosité η est une fonction de $|d(u)|$ par l’intermédiaire de lois de comportement telle la loi de puissance :

$$\eta = \eta_0 |d(u)|^{m-1} \quad (2.2)$$

ou m est l’indice de pseudo plasticité et η_0 est la consistance. Cette loi est principalement utilisée pour décrire la viscoplasticité des métaux chaud. Une autre loi de comportement importante et plus réaliste est la loi de Carreau-Yasuda qui nous écrivons sous cette forme :

$$\eta = \eta_0 (c_0 + \lambda^n |d(u)|^n)^{\frac{m-1}{n}} \quad (2.3)$$

Le modèle de Carreau-Yasuda permet de prendre en compte la présence d’un plateau newtonien a faible taux de cisaillement ; η_0 désigne toujours la consistance, λ est un

temps de relaxation et m et n des indices de pseudo plasticité. En particulier si $n = 2$ on trouve le modèle classique de Carreau que nous étudions dans les prochains chapitre :

$$\eta = \eta_\infty + (\eta_0 - \eta_\infty)[1 + (\lambda d(u))^2]^{\frac{m-1}{2}} \quad (2.4)$$

Finalement, pour une viscosité variable, le problème de Stokes présenté plus haut, devient non linéaire et s'écrit :

$$\begin{cases} -\nabla \cdot (2\eta(|d(u)|)d(u)) + \nabla p = f \\ \nabla \cdot u = 0 \end{cases} \quad (2.5)$$

auxquelles il faut ajouter des conditions aux limites appropriées.

Remarque :

En annexe on a défini quelques résultats d'existence et d'unicité pour les écoulements Newtonien et non Newtonien plus un rappel sur les éléments finis P2P1.

Chapitre 3

M.A.P.D.D : Method of Asymptotic Partial Domain Decomposition

This chapter is based on the book of Grigory Panasenko : Multi-Scale Modeling for Structures and Composites. Springer, Dordrecht, 2005.

3.1 Flows in tube structures

The Navier-Stokes problem stated in tube structures (or finite rod structures), i.e. in connected finite unions of the thin cylinders with the ratio of the diameter to the height of the order $\varepsilon \ll 1$, is considered. Such problems arise in the blood circulation modelling. The asymptotic expansion of the solution is built and justified. Boundary layers are studied. The Navier-Stokes problem in one thin cylindrical domain was considered in [13].

3.1.1 Definitions. One bundle structure

In this section we are going to construct the asymptotic expansion to the solution of the Navier-Stokes problem, stated in a tube structure containing one bundle. We shall justify the error estimate . First we consider the case of right hand side functions concentrated in some neighborhoods of the nodes and then we generalize our construction for the right hand side functions which do not vanish inside of the tubes. Let us

define the tube structure containing one bundle. It is the same type of domains as finite rod structure but with more smooth boundary. We consider here two possible dimensions of the space : two and three. Let e_1, \dots, e_n be n closed segments in \mathbf{R}^s ($s = 2, 3$), which have a single common point O (i.e. the origin of the co-ordinate system), and let it be the common end point of all these segments. Let β_1, \dots, β_n be n bounded $(s-1)$ -dimensional domains in \mathbf{R}^3 , which belong to n hyper-planes containing the point O . Let β_j be orthogonal to e_j . Let β_j^ε be the image of β_j obtained by a homothetic contraction in $1/\varepsilon$ times with the center O . Denote B_j^μ the open cylinders with the bases β_j^ε and with the heights e_j , denote also $\hat{\beta}_j^\varepsilon$ the second base of each cylinder B_j^ε and let O_j be the end of the segment e_j which belongs to the base $\hat{\beta}_j^\varepsilon$. Define the bundle of segments e_j centered in O as

$$B = \cup_{j=1}^n e_j.$$

Denote below $O_0 = O$. Let γ_j^ε , $j = 0, 1, \dots, n$, be the images of the bounded domains γ_j , (such that $\bar{\gamma}_j$ contain the ends of the segments O_j and independent of ε obtained by a homothetic contraction in $1/\varepsilon$ times with the center O_j). Define the tube structure associated with the bundle B as

$$B^\varepsilon = (\cup_{j=1}^n B_j^\varepsilon) \cup (\cup_{j=0}^n \gamma_j^\varepsilon).$$

We suppose it be a domain with C^2 -smooth boundary ∂B^ε and we assume that the bases $\hat{\beta}_j^\varepsilon$ of the cylinders B_j^ε $j = 1, \dots, n$, are some parts of ∂B^ε . We add the domains

γ_j^ε , $j = 0, 1, \dots, n$, to make the boundary of the tube structure C^2 - smooth surface.

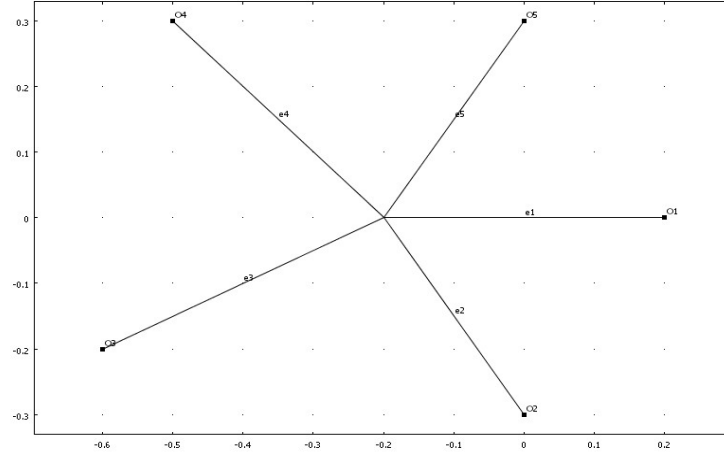


Figure 2.1.1.a) A bundle of segments .

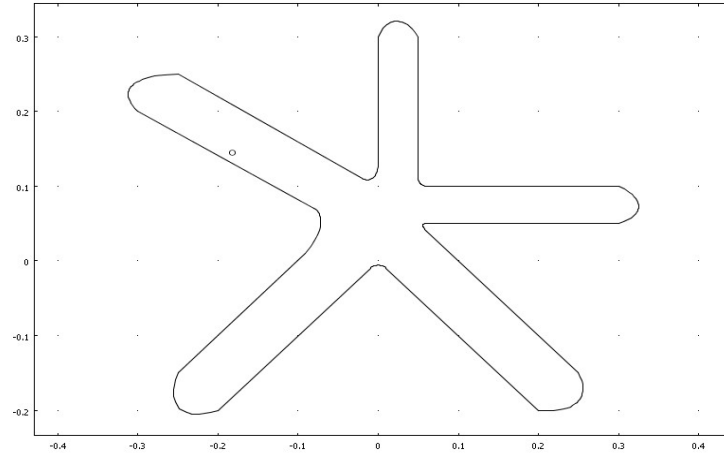


Figure 2.1.1.b). A one bundle tube structure.

Consider the Navier-Stokes system of equations

$$\eta \Delta u_\varepsilon - (u_\varepsilon, \nabla) u_\varepsilon - \nabla p_\varepsilon = f, \quad (3.1.1)$$

$$\operatorname{div} u_\varepsilon = 0, \quad x \in B^\varepsilon \quad (3.1.2)$$

with the Dirichlet condition

$$u_\varepsilon = g \quad (3.1.3)$$

on ∂B^ε . Here $g = 0$ on the lateral boundary of the cylinders composing B^ε ; moreover $g = 0$ everywhere with the exception of the bases $\hat{\beta}_j^\varepsilon$ of the cylinders B_j^ε (these bases are assumed to belong to the boundary of the tube structure); $g \in C^2(\hat{\beta}_j^\varepsilon)$, and for each j , $g = \varepsilon^2 g_j(\frac{x-O_j}{\varepsilon})$ on $\hat{\beta}_j^\varepsilon$, the vector valued function $g_j \in C^2$ do not depend on ε . The solvability condition imposes the relation

$$\int_{\partial B^\varepsilon} g n ds = 0. \quad (3.1.4)$$

In this section we will drop the subscript ε for the solution of problem (3.1.1)-(3.1.3). Consider first the case of a right hand side vector valued function f "concentrated" in some neighborhoods of the nodes O_j , i.e. assume that

$$f = f_j\left(\frac{x - O_j}{\varepsilon}\right) \quad (3.1.5)$$

in a vicinity of each O_j , $j = 0, 1, \dots, n$, and assume that the vector valued functions $f_j(\xi)$ vanish if $|\xi| > r_0$. Suppose also that these functions (and r_0) do not depend on ε . Thus we have defined f in small domains obtained from $\text{supp } f_j$ by a contraction in $1/\varepsilon$ times with the centers O_j . We define f as zero in all other points. Let $f \in C^1$, $\eta > 0$. Let $H_{div=0}(B^\varepsilon)$ be space of vector valued functions from $H^1(B^\varepsilon)$ with vanishing divergence, let $H_{div=0}^0(B^\varepsilon)$ be the subspace of $H_{div=0}(B^\varepsilon)$ of functions vanishing on the boundary. Suppose that g can be continued in B^ε as a vector valued function \hat{g} of $H_{div=0}(B^\varepsilon)$. The variational formulation is as follows : find $u \in H_{div=0}(B^\varepsilon)$ such that $u - \hat{g} \in H_{div=0}^0(B^\varepsilon)$, and such that it satisfies to the integral identity

$$-\int_{B^\varepsilon} \eta \sum_{i=1}^s \left(\frac{\partial u}{\partial x_i}, \frac{\partial \varphi}{\partial x_i} \right) dx + \int_{B^\varepsilon} \sum_{i=1}^s u_i \left(u, \frac{\partial \varphi}{\partial x_i} \right) dx = \int_{B^\varepsilon} (f, \varphi) dx,$$

for all $\varphi \in H_{div=0}^0(B^\varepsilon)$. Here $(,)$ is the symbol of the scalar product in \mathbf{R}^s , u_i is the i -th component of the vector u , i.e. $\sum_{i=1}^s u_i \left(u, \frac{\partial \varphi}{\partial x_i} \right) = (u, (u, \nabla)\varphi)$. The existence and uniqueness of the solution was proved in [14] (for sufficiently small values of ε).

We construct the asymptotic expansion in a form

$$\begin{aligned} u^a &= \sum_{l=2}^K \varepsilon^l \left\{ \sum_{e=e_j, j=1, \dots, n} u_l^e \left(\frac{x^{e,L}}{\varepsilon} \right) \chi_\varepsilon(x) + \sum_{i=0}^n u_i^{BLO_i} \left(\frac{x - O_i}{\varepsilon} \right) \right\}, \\ p^a &= \sum_{l=2}^{K+1} \varepsilon^{l-2} \sum_{e=e_j, j=1, \dots, n} p_l^e(x_1^e) \chi_\varepsilon(x) + \sum_{i=0}^n p_2^e(O_i) (1 - \chi_\varepsilon(x)) \theta_i(x) \end{aligned} \quad (3.1.6)$$

$$+ \sum_{l=2}^{K+1} \varepsilon^{l-1} \sum_{i=0}^n p_l^{BLO_i} \left(\frac{x - O_i}{\varepsilon} \right), \quad (3.1.7)$$

Here χ_ε is a function equal to zero at the distance not more than $(\hat{d}_0 + 1)\varepsilon$ from O_j , $j = 0, 1, \dots, n$; $\hat{d}_0\varepsilon = \max \{d_0\varepsilon, d_1\varepsilon\}$, $d_0\varepsilon$ is the infimum of radiuses of all spheres with the center O such that every point of it belongs only to not more than one of the cylinders B_j $j = 1, \dots, n$; d_1 is the maximal diameter of the domains $\gamma_0, \gamma_1, \dots, \gamma_n$, and

$$\theta_j(x) = 0 \text{ if } |x - O_j| > \min_i |e_i|/2,$$

$$\theta_j(x) = 1 \text{ if } |x - O_j| \leq \min_i |e_i|/2.$$

We have introduced here the local system of coordinates $Ox_1^{e_j} \dots x_s^{e_j}$ associated with a segment e_j such that the direction of the axis $Ox_1^{e_j}$ coincides with the direction of the segment OO_j , i.e. $x_1^{e_j}$ is a longitudinal coordinate. The axes $Ox_1^{e_j}, \dots, Ox_s^{e_j}$ form a cartesian coordinate system. We suppose that the function χ_ε is equal to zero on the cylinder B_j^ε if $x_1^{e_j} \leq (d_0 + 1)\varepsilon$ or if $|x_1^{e_j} - |e_j|| \leq (d_0 + 1)\varepsilon$ (here $|e_j|$ is the length of the segment e_j), we suppose that the function χ_ε is equal to one on this cylinder if $x_1^{e_j} \geq (d_0 + 2)\varepsilon$ and $|x_1^{e_j} - |e_j|| \geq (d_0 + 2)\varepsilon$, and we define χ_ε by relations $\chi_\varepsilon(x) = \chi_j(x_1^{e_j}/\varepsilon)$ if $(d_0 + 1)\varepsilon \leq x_1^{e_j} \leq (d_0 + 2)\varepsilon$, and we pose $\chi_\varepsilon(x) = \chi_j((x_1^{e_j} - |e_j|)/\varepsilon)$ if $(d_0 + 1)\varepsilon \leq |e_j| - x_1^{e_j} \leq (d_0 + 2)\varepsilon$. Here χ_j is a differentiable on \mathbf{R} function of one variable, it is independent of ε , and it is equal to zero on the segment $[-(d_0 + 1), d_0 + 1]$ and it is equal to one on the union of the intervals $(-\infty, -(d_0 + 2)) \cup ((d_0 + 2), +\infty)$. For any γ_j^ε , χ_ε is equal to zero on it. The variable $x^{e_j L} = (x_2^{e_j}, \dots, x_s^{e_j})$. Let the relation between the columns (here T is the transposition symbol) x^T and $x^{e_j, T}$ be

$$x^T = \Gamma_j x^{e_j, T} + O, \quad j = 1, \dots, n, \quad (3.1.8)$$

where Γ_i is an orthogonal matrix of passage from the canonic base to the local one (in the previous sections we used for matrices Γ_j the notation α_e^*). Then the vector valued function u_l^e and the scalar functions p_l^e are defined up to the scalar constants c_l^e, d_l^e :

$$u_l^{e_j}(\xi^L) = c_l^{e_j} \Gamma_j (\tilde{u}^{e_j}(\xi^L), 0, \dots, 0)^T, \quad p_l^{e_j}(x_1^{e_j}) = c_l^{e_j} x_1^{e_j} + d_l^{e_j}, \quad l = 2, 3, \dots \quad (3.1.9),$$

where $\xi^L = (\xi_2, \dots, \xi_s)$ and \tilde{u}^{e_j} is the solution of the problem

$$\eta \Delta_{\xi^L} \tilde{u}^{e_j} - 1 = 0, \quad \xi^L \in \beta_j, \quad \tilde{u}^{e_j}|_{\partial\beta_j} = 0, \quad j = 1, \dots, n, \quad (3.1.10)$$

and $d_2^{e_j} = 0$.

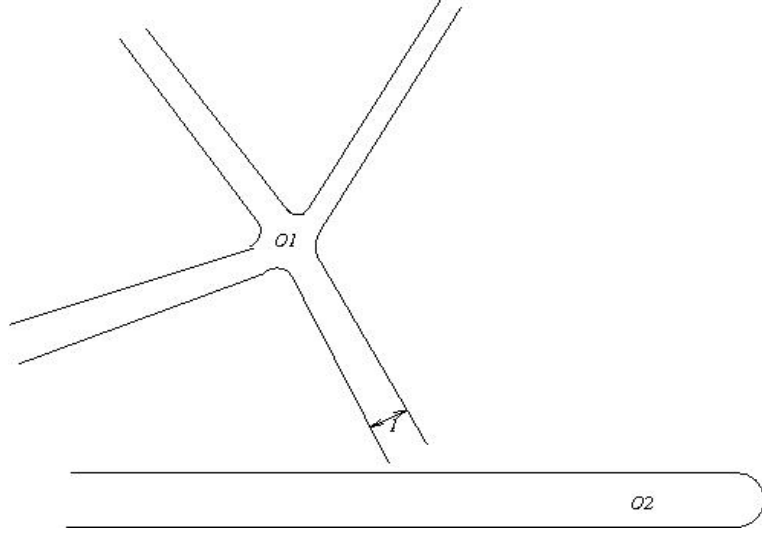


Figure 2.1.2. Dilated domains Ω_{O_j} .

The boundary layer solution is a pair constituted of a vector valued function $u_l^{BLO_j}$ and scalar function $p_l^{BLO_j}$ satisfying to the Stokes system :

$$\begin{aligned}
& \eta \Delta_\xi u_l^{BLO_0} - \nabla_\xi p_l^{BLO_0} = f_0(\xi) \delta_{l,0} + \\
& + \sum_{e=e_j, j=1, \dots, n} \{c_l^{e_j} \{-\eta \Delta_\xi (\chi_j(\xi_1^{e_j}) \Gamma_j(\tilde{u}^{e_j}(\xi^L), 0, \dots, 0)^T) \\
& \quad + \nabla_\xi (\chi_j(\xi_1^{e_j}) \xi_1^{e_j})\} + \\
& + (\sum_{p+r=l-1} c_p^{e_j} c_r^{e_j}) (\chi_j(\xi_1^{e_j}) \tilde{u}^{e_j}(\xi^L) \frac{\partial}{\partial \xi_1^{e_j}} \chi_j(\xi_1^{e_j})) \Gamma_j(\tilde{u}^{e_j}(\xi^L), 0, \dots, 0)^T + \\
& \quad + (\sum_{p+r=l-1} (u_p^{BLO_0} \cdot \nabla_\xi) u_r^{BLO_0}) + \\
& \quad + \sum_{p+r=l-1} c_p^{e_j} (\chi_j(\xi_1^{e_j}) \tilde{u}^{e_j}(\xi^L) \frac{\partial}{\partial \xi_1^{e_j}} u_r^{BLO_0} + \\
& + \sum_{p+r=l-1} c_r^{e_j} (u_p^{BLO_0} \cdot \nabla_\xi) (\chi_j(\xi_1^{e_j}) \Gamma_j(\tilde{u}^{e_j}(\xi^L), 0, \dots, 0)^T + \\
& \quad + d_{l+1}^{e_j} \nabla_\xi (\chi_j(\xi_1^{e_j}))), \tag{3.1.11}
\end{aligned}$$

$$div_\xi u_l^{BLO_0} = -div_\xi \left\{ \sum_{e=e_j, j=1, \dots, n} \{c_l^{e_j} \chi_j(\xi_1^{e_j}) \Gamma_j(\tilde{u}^{e_j}(\xi^L), 0, \dots, 0)^T\}, \quad \xi \in \Omega_{O_0} \right. \tag{3.1.12}$$

with the Dirichlet condition

$$u_l^{BLO_0}|_{\partial \Omega_{O_0}} = 0 \tag{3.1.13}$$

and for $i = 1, \dots, n$

$$\begin{aligned}
& \eta \Delta_{\hat{\xi}} u_l^{BLO_j} - \nabla_{\hat{\xi}} p_l^{BLO_j} = f_j(\hat{\xi}) \delta_{l,0} + \\
& + \hat{c}_l^{e_j} \{ -\eta \Delta_{\hat{\xi}} (\chi_j(\hat{\xi}_1^{e_j}) \hat{\Gamma}_j(\tilde{u}^{e_j}(\hat{\xi}^L), 0, \dots, 0)^T) \\
& \quad + \nabla_{\hat{\xi}} (\chi_j(\hat{\xi}_1^{e_j}) \hat{\xi}_1^{e_j}) \} + \\
& + \left(\sum_{p+r=l-1} c_p^{e_j} c_r^{e_j} \right) (\chi_j(\xi_1^{e_j}) \tilde{u}^{e_j}(\xi^L) \frac{\partial}{\partial \xi_1^{e_j}} \chi_j(\xi_1^{e_j})) \Gamma_j(\tilde{u}^{e_j}(\xi^L), 0, \dots, 0)^T + \\
& \quad + \left(\sum_{p+r=l-1} (u_p^{BLO_j} \cdot \nabla_{\xi}) u_r^{BLO_0} + \right. \\
& \quad + \sum_{p+r=l-1} c_p^{e_j} (\chi_j(\xi_1^{e_j}) \tilde{u}^{e_j}(\xi^L) \frac{\partial}{\partial \xi_1^{e_j}} u_r^{BLO_j} + \\
& \quad + \sum_{p+r=l-1} c_r^{e_j} (u_p^{BLO_j} \cdot \nabla_{\xi}) (\chi_j(\xi_1^{e_j}) \Gamma_j(\tilde{u}^{e_j}(\xi^L), 0, \dots, 0)^T + \\
& \quad \quad \left. + \hat{d}_{l+1}^{e_j} \nabla_{\hat{\xi}} (\chi_j(\hat{\xi}_1^{e_j}))), \right. \tag{3.1.14}
\end{aligned}$$

$$\operatorname{div}_{\hat{\xi}} u_l^{BLO_j} = -\operatorname{div}_{\hat{\xi}} \{ \hat{c}_l^{e_j} \chi_j(\hat{\xi}_1^{e_j}) \hat{\Gamma}_j(\tilde{u}^{e_j}(\hat{\xi}^L), 0, \dots, 0)^T \}, \quad \hat{\xi} \in \Omega_{O_j} \tag{3.1.15}$$

with the Dirichlet condition

$$u_l^{BLO_j} |_{\partial \Omega_{O_j}, \hat{\xi}_1^{e_j} = 0} = g_j \delta_{l,2}, \tag{3.1.16}$$

$$u_l^{BLO_j} |_{\partial \Omega_{O_j}, \hat{\xi}_1^{e_j} \neq 0} = 0, \tag{3.1.17}$$

where $\Omega_{O_0} = \cup_{j=1}^n \tilde{\Omega}_j \cup \gamma_0$, and $\tilde{\Omega}_i$ are the half-infinite cylinders obtained from B_j^ε by infinite extension behind the base $\hat{\beta}_j^\varepsilon$ and by homothetic dilatation in $1/\varepsilon$ times (with respect to the point O); let Ω_j be obtained from $\tilde{\Omega}_j$ by a symmetric reflection relatively the plain containing β_j^ε and let $\Omega_{O_j} = \Omega_j \cup \gamma_j^t$, where γ_j^t is obtained from γ_j by a translation (such that the point O_j becomes O). The variable $\hat{\xi}_1^{e_j}$ is opposite to $\xi_1^{e_j}$, i.e. to the first component of the vector $\Gamma_j^T \xi^{e_j, T}$. So $\hat{\xi}_1^{e_j} = \hat{\Gamma}_j^T (\xi^{e_j})^T$, where $\hat{\Gamma}_j = \hat{I} d \Gamma_j$ and $\hat{I} d$ is the diagonal matrix with the diagonal elements $-1, 1, \dots, 1$. The constants \hat{c}_l^e, \hat{d}_l^e are defined in such a way that the linear functions $p_l^{e_j}(x_1^{e_j}) = c_l^{e_j} x_1^{e_j} + d_l^{e_j}$ and $p_l^{e_j}(x_1^{e_j}) = \hat{c}_l^{e_j} (|e_j| - x_1^{e_j}) + \hat{d}_l^{e_j}$ are equal, i.e.

$$c_l^{e_j} = -\hat{c}_l^{e_j}, \quad \hat{d}_l^{e_j} = c_l^{e_j} |e_j| + d_l^{e_j}. \tag{3.1.18}$$

We suppose that every term in the sum $\sum_{e=e_j, j=1, \dots, n}$ in (3.1.12) is defined only on the branch of Ω_{O_0} , corresponding to $e = e_j$, and it vanishes in γ_0 . We seek the exponentially decaying at infinity solutions of these boundary layer problems and we choose the constants $c_l^e, \hat{c}_l^{e_j}, d_l^e, \hat{d}_l^{e_j}$ from the conditions of existence of such solutions [15]. We define first $\hat{c}_l^{e_j}$ from the condition of exponential decaying of $u_l^{BLO_j}$ at infinity :

$$\int_{\Omega_{O_j}} \operatorname{div}_{\xi}(\hat{c}_l^{e_j} \chi_j(\xi_1^{e_j}) \hat{\Gamma}_i(\tilde{u}^{e_j}(\xi^L)), 0, \dots, 0)^T d\xi = \int_{\beta_j} (\hat{\Gamma}_j^T g_j)^1 d\xi,$$

i.e.

$$- \int_{\beta_j} \tilde{u}^{e_j}(\xi^L) d\xi \hat{c}_l^{e_j} = \int_{\beta_j} (\hat{\Gamma}_j^T g_j)^1 d\xi \delta_{l,2}, \quad (3.1.19)$$

where the upper index 1 corresponds to the first component of the vector. Note that $\int_{\beta_j} \tilde{u}^{e_j}(\xi^L) d\xi$ is negative due to the principle of maximum for problem (3.1.10). Then we find $c_l^{e_j} = -\hat{c}_l^{e_j}$ and $\hat{d}_l^{e_j} = c_l^{e_j} |e_j|$. Then we determine the constants $d_{l+1}^{e_j}$ from the condition of the exponential decaying of $p_l^{BLO_0}$ at infinity. To this end we consider first the problem (3.1.11)-(3.1.13) without the last term in the equation (3.1.11), i.e.

$$\begin{aligned} & \eta \Delta_{\xi} \bar{u}_l^{BLO_0} - \nabla_{\xi} \bar{p}_l^{BLO_0} = f_0(\xi) \delta_{l,2} \\ & + \sum_{e=e_j, j=1, \dots, n} c_l^{e_j} \{ -\eta \Delta_{\xi} (\chi_j(\xi_1^{e_j}) \Gamma_j(\tilde{u}^{e_j}(\xi^L), 0, \dots, 0)^T) \\ & \quad + \nabla_{\xi} (\chi_j(\xi_1^{e_j}) \xi_1^{e_j}) \} + \\ & + \left(\sum_{p+r=l-1} c_p^{e_j} c_r^{e_j} \right) (\chi_j(\xi_1^{e_j}) \tilde{u}^{e_j}(\xi^L) \frac{\partial}{\partial \xi_1^{e_j}} \chi_j(\xi_1^{e_j}) \Gamma_j(\tilde{u}^{e_j}(\xi^L), 0, \dots, 0)^T) \\ & \quad + \left(\sum_{p+r=l-1} (u_p^{BLO_0} \cdot \nabla_{\xi}) u_r^{BLO_0} \right) + \\ & \quad + \sum_{p+r=l-1} c_p^{e_j} (\chi_j(\xi_1^{e_j}) \tilde{u}^{e_j}(\xi^L) \frac{\partial}{\partial \xi_1^{e_j}} u_r^{BLO_0} + \\ & + \sum_{p+r=l-1} c_r^{e_j} (u_p^{BLO_0} \cdot \nabla_{\xi}) (\chi_j(\xi_1^{e_j}) \Gamma_j(\tilde{u}^{e_j}(\xi^L), 0, \dots, 0)^T) + \\ & \quad + d_{l+1}^{e_j} \nabla_{\xi} (\chi_j(\xi_1^{e_j})) \}, \end{aligned} \quad (3.1.20)$$

$$\operatorname{div}_{\xi} \bar{u}_l^{BLO_0} = -\operatorname{div}_{\xi} \left\{ \sum_{e=e_j, j=1, \dots, n} \{ c_l^{e_j} \chi_j(\xi_1^{e_j}) \Gamma_j(\tilde{u}^{e_j}(\xi^L), 0, \dots, 0)^T \}, \quad \xi \in \Omega_{O_0} \right. \quad (3.1.21)$$

with the Dirichlet condition

$$\bar{u}_l^{BLO_0} |_{\partial \Omega_{O_0}} = 0. \quad (3.1.22)$$

Here the constants $c_l^{e_j}$ are just defined by (3.1.18), (3.1.19) and satisfy the condition

$$\int_{\Omega_{O_0}} \operatorname{div}_\xi \left\{ \sum_{e=e_j, j=1, \dots, n} c_l^e \chi_i(\xi_1^e) \Gamma_j(\tilde{u}^e(\xi^L), 0, \dots, 0)^T \right\} d\xi = 0,$$

i.e.

$$\sum_{e=e_j, j=1, \dots, n} \int_{\beta_j} \tilde{u}^{e_j}(\xi^L) d\xi c_l^{e_j} = 0. \quad (3.1.23)$$

Indeed, the choice of the constants $c_l^{e_j} = -\hat{c}_l^{e_j}$ and $\hat{c}_l^{e_j}$ from (3.1.19) and condition (3.1.4) give relation (3.1.23). It is known (for example [15]) that there exists the unique solution $\{\bar{u}_l^{BLO_0}, \bar{p}_l^{BLO_0}\}$ of this problem such that $\bar{u}_l^{BLO_0}$ stabilizes to zero at infinity (on every branch of Ω_{O_0}) and $\bar{p}_l^{BLO_0}$ stabilizes on every branch of Ω_{O_0} , associated with e_j , to its own constant $\bar{p}_l^{BLO_0 \infty j}$). These constants are defined uniquely up to one common additional constant, which we fix here by a condition $\bar{p}_l^{BLO_0 \infty 1} = 0$. Then we define

$$d_{l+1}^{e_j} = -\bar{p}_l^{BLO_0 \infty j}, \quad (3.1.24)$$

$$u_l^{BLO_0} = \bar{u}_l^{BLO_0}, \quad (3.1.25)$$

and

$$p_l^{BLO_0} = \bar{p}_l^{BLO_0} + d_{l+1}^{e_j} \chi_j(\xi_1^{e_j}) \quad (3.1.26)$$

on every branch of Ω_{O_0} , associated with e_j . Obviously, this pair $\{u_l^{BLO_0}, p_l^{BLO_0}\}$ satisfies equations (3.1.11)-(3.1.13). The boundary layer functions $u_l^{BLO_j}$ and $p_l^{BLO_j}$, $j = 1, \dots, n$, are not defined in the vicinity of O . Therefore we should change a little bit the formulas of u^a and p^a far from the nodes $O_j, j = 0, \dots, n$. Let $\eta_j(x_1^{e_j})$ be a smooth function defined on each segment e_j , let it be one if $|x_1^{e_j} - |e_j|/2| \geq |e_j|/4$ and let it be zero if $|x_1^{e_j} - |e_j|/2| \leq |e_j|/8$. Let $\eta(x) = \eta_j(x_1^{e_j})$ for each cylinder B_j^ε and let $\eta = 1$ on each γ_j^ε . Then we redefine u^a and p^a as

$$u^a = \sum_{l=2}^K \varepsilon^l \left\{ \sum_{e=e_j, j=1, \dots, n} u_l^e \left(\frac{x^{e,L}}{\varepsilon} \right) \chi_\varepsilon(x) + \sum_{i=0}^n u_l^{BLO_i} \left(\frac{x - O_i}{\varepsilon} \right) \eta(x) \right\}, \quad (3.1.27)$$

$$\begin{aligned} p^a = & \sum_{l=2}^{K+1} \varepsilon^{l-2} \left\{ \sum_{e=e_j, j=1, \dots, n} p_l^e(x_1^e) \chi_\varepsilon(x) + \sum_{i=0}^n p_2^e(O_i) (1 - \chi_\varepsilon(x)) \theta_i(x) \right. \\ & \left. + \sum_{l=2}^{K+1} \varepsilon^{l-1} \sum_{i=1}^N p_l^{BLO_i} \left(\frac{x - O_i}{\varepsilon} \right) \eta(x) \right\}, \end{aligned} \quad (3.1.28)$$

The consequence of this redefinition is a small discrepancy in the right hand side of the equations of order $O(\exp(-c/\varepsilon))$ with the positive constant c : now we have the relations

$$\eta\Delta\tilde{u}^a - \nabla\tilde{p}^a = f + \Phi, \quad (3.1.29)$$

$$\operatorname{div} \tilde{u}^a - (\tilde{u}^a, -\nabla)\tilde{u}^a = \Psi, \quad x \in B^\varepsilon \quad (3.1.30)$$

with the Dirichlet condition

$$\tilde{u}^a = g \quad (3.1.31)$$

on ∂B^ε , where

$$\|\Psi\|_{H^1(B^\varepsilon)} = O(\exp(-c/\varepsilon)), \quad \|\Phi\|_{L^2(B^\varepsilon)} = O(\varepsilon^{K-1+(s-1)/2}) \quad (3.1.32)$$

with a positive constant c and

$$\int_{B^\varepsilon} \Psi dx = 0, \quad (3.1.33)$$

because $\int_{\partial B^\varepsilon} (\tilde{u}^a, n) ds = \int_{\partial B^\varepsilon} (g, n) ds = 0$. We are going to prove the estimate

$$\|u - \tilde{u}^a\|_{H^1(B^\varepsilon)} = O(\varepsilon^{K-1+(s-1)/2}), \quad (3.1.34)$$

where $c_1 > 0$ does not depend on ε . First we construct a function φ such that $v = \nabla\varphi$ is a solution of the equation

$$\operatorname{div} v = \Psi, \quad x \in B^\varepsilon, \quad (v, n) = 0, \quad x \in \partial B^\varepsilon,$$

i.e. let φ be a solution of the Neumann problem

$$\Delta\varphi = \Psi, \quad x \in B^\varepsilon, \quad \frac{\partial\varphi}{\partial n} = 0, \quad x \in \partial B^\varepsilon.$$

The existence of this solution is provided by the condition $\int_{B^\varepsilon} \Psi dx = 0$. As the boundary belongs to C^2 then $\varphi \in H^2(B^\varepsilon)$. If we consider the solution with vanishing average $\int_{B^\varepsilon} \varphi dx = 0$, then we apply the Poincare inequality for B^ε (cf. Appendix 4.A.2 in [16]) :

$$\forall \varphi \in H^1(B^\varepsilon), \quad \int_{B^\varepsilon} \varphi^2 dx \leq \frac{1}{\operatorname{mes} B^\varepsilon} \left(\int_{B^\varepsilon} u dx \right)^2 + A \int_{B^\varepsilon} (\nabla\varphi)^2 dx.$$

where the constant A does not depend on ε . Thus we obtain the estimate $\|\varphi\|_{H^1(B^\varepsilon)} = O(\exp(-c/\varepsilon))$ and therefore we can use Agmon, Duglas and Nirenberg [2] theory and

obtain the estimate $\|\varphi\|_{H^2(B^\varepsilon)} = O(\exp(-c_2/\varepsilon))$, where the positive constant c_2 does not depend on ε . Therefore $v \in H^1(B^\varepsilon)$ and $\|v\|_{H^1(B^\varepsilon)} = O(\exp(-c_2/\varepsilon))$. The second step is the construction of such a function $w = \text{rot } \psi$ that $w = -v$ on ∂B^ε . This construction is described in [14] and it has a "local nature." We make a partition of unity $1 = \sum_{k=1}^N \delta_k$ on B^ε , in such a way that all supports of δ_k have the diameters of order ε and satisfy to the condition of the existence of such a change of variables that the procedure of [14] ch.1, sect. 2 can be applied and the corresponding vector valued function ψ_k can be constructed for every support, i.e. $\text{rot } \psi_k|_{\partial B^\varepsilon} = \delta_k v|_{\partial B^\varepsilon}$. All these supports have non-empty intersections Δ_k with the boundary of B^ε . Moreover we can make homothetic dilatations $\xi = (x - A_k)/\varepsilon$ in $1/\varepsilon$ times with some centers A_k for every support in such a way that its image σ_k does not depend on ε . All these σ_k can be "uniformed", i.e. can be extended up to a finite number (independent of ε) of the domains σ such that all other domains could be obtained from them by rotations and translations. The functions δ_k can be taken satisfying relation $\delta_k(x) = \tilde{\delta}_k((x - A_k)/\varepsilon)$, where the functions $\tilde{\delta}_k$ do not depend on ε . Thus the problem of construction of all vector valued functions ψ_k is reduced to a finite (independent of ε) number of problems : construct such a vector valued function $\tilde{\psi}_\alpha$ that $\text{rot}_\xi \tilde{\psi}_\alpha|_{\partial B^\varepsilon} = \tilde{\delta}_\alpha v|_{\partial B^\varepsilon}$ and take $\psi_\alpha(x) = \varepsilon \tilde{\delta}_\alpha((x - A_k)/\varepsilon)$. In this case we can estimate

$$\|\text{rot}_\xi \tilde{\psi}_\alpha\|_{H^1(\sigma)} \leq C_\alpha \|v(\varepsilon\xi + A_\alpha)\|_{H^1(\sigma)},$$

with the constants C_α uniformly bounded by a constant C independent of ε . Therefore there exists a positive constant c_1 independent of ε such that

$$\|\text{rot } \psi\|_{H^1(B^\varepsilon)} = O(\exp(-c_1/\varepsilon)),$$

and

$$\|v + w\|_{H^1(B^\varepsilon)} = O(\exp(-c_1/\varepsilon)).$$

Therefore the relation holds true :

$$U^a = \tilde{u}^a - (v + w) \in H_{\text{div}=0}(B^\varepsilon)$$

and

$$-\int_{B^\varepsilon} \eta \sum_{i=1}^s \left(\frac{\partial U^a}{\partial x_i}, \frac{\partial \varphi}{\partial x_i} \right) dx + \int_{B^\varepsilon} (U^a, (U^a, \nabla)\varphi) dx =$$

$$\begin{aligned}
&= -\eta \int_{B^\varepsilon} \sum_{i=1}^s \left(\frac{\partial(\tilde{u}^a - (v+w))}{\partial x_i}, \frac{\partial \varphi}{\partial x_i} \right) dx + \int_{B^\varepsilon} (\tilde{u}^a - (v+w), (\tilde{u}^a - (v+w), \nabla) \varphi) dx = \\
&= \int_{B^\varepsilon} (f, \varphi) dx + \int_{B^\varepsilon} (\Phi, \varphi) dx + \eta \int_{B^\varepsilon} \sum_{i=1}^s \left(\frac{\partial(v+w)}{\partial x_i}, \frac{\partial \varphi}{\partial x_i} \right) dx - \\
&\quad - \int_{B^\varepsilon} ((v+w), (\tilde{u}^a - (v+w), \nabla) \varphi) dx - \int_{B^\varepsilon} (\tilde{u}^a, (v+w, \nabla) \varphi) dx,
\end{aligned}$$

for all $\varphi \in H_{div=0}^0(B^\varepsilon)$. Now we can apply the Poincaré-Friedrichs estimate (cf. section 4.A.2 in [16]) :

$$\forall \varphi \in H_0^1(B^\varepsilon), \quad \int_{B^\varepsilon} \varphi^2 dx \leq A \int_{B^\varepsilon} (\nabla \varphi)^2 dx,$$

where the constant A does not depend on ε . (Moreover, decomposing the domain to some subdomains with diameter of order ε , in such a way that each subdomain contains a part of the boundary ∂B^ε , this estimate can be proved with the factor $\varepsilon^2 A$ instead of A). Applying this estimate as well as the a priori estimate for Navier-Stokes equation from [14],[17], we obtain :

$$\|U^a - u\|_{H^1(B^\varepsilon)} = O(\varepsilon^{K-1})$$

and

$$\|u^a - u\|_{H^1(B^\varepsilon)} = O(\varepsilon^{K-1}), \quad (3.1.35)$$

where $c_3 > 0$ does not depend on ε . This estimate can be improved in a standard way (see section 2.1) as $\|u^a - u\|_{H^1(B^\varepsilon)} = O(\varepsilon^{K+(s-1)/2})$.

Remark 2.1.1. If the right hand side function is defined on each cylinder B_j^ε as

$$f = f_j \left(\frac{x - O_j}{\varepsilon} \right) + f_0 \left(\frac{x - O}{\varepsilon} \right) + \chi_\varepsilon(x) \Gamma_j (\hat{f}_j(x_1^{e_j}), 0, \dots, 0)^T, \quad (3.1.36)$$

where \hat{f}_j are sufficiently smooth functions, and for all $\gamma_j, j = 0, \dots, n$, it is defined as earlier

$$f = f_j \left(\frac{x - O_j}{\varepsilon} \right),$$

then this case can be easily reduced to a previous type of right hand side function by a subtraction of a partial solution

$$u_{\text{partial}} = 0, \quad p_{\text{partial}} = - \int_0^{x_1^{e_j}} \hat{f}_j(t) dt = -F_j(x_1^{e_j})$$

on each cylinder B_j^ε . Indeed if u and p is the solution of problem (3.1.1)-(3.1.3) with the right hand side (3.1.36) then the pair $u, p - \chi_\varepsilon(x)F_j(x_1^{e_j})$ is the solution of the problem with the right hand side

$$\tilde{f} = f_j\left(\frac{x - O_j}{\varepsilon}\right) + f_0\left(\frac{x - O}{\varepsilon}\right) + \chi_\varepsilon(x)\Gamma_j \hat{f}_j(x_1^{e_i}, 0, \dots, 0)^T - \nabla(\chi_\varepsilon(x)F_j(x_1^{e_j})),$$

on each cylinder B_j^ε . This right hand side function has a support concentrated in the vicinities of the nodes O_j , i.e. $\text{supp } \tilde{f} \subset \text{supp } (\chi_\varepsilon - 1)$. Now we develop \hat{f}_j by the Taylor's formula in vicinities of the nodes and obtain the set of problems with the right hand side of a form (3.1.5). It can be treated as above.

3.1.2 Tube structure with m bundles of tubes

Consider now the case of m different bundles of segments

$$B_1 = \cup_{j=1}^{n_1} e_{j,1}, \dots, B_m = \cup_{j=1}^{n_m} e_{j,m}.$$

We suppose that all common points of these bundles are end points of some segments of these bundles. Let the union of all bundles be connected. Consider the tube structure B_α^ε associated with the bundle B_α . Now we do not require a base $\hat{\beta}_j^\varepsilon$ to be a part of $\partial B_\alpha^\varepsilon$ in case if it corresponds to a common point of two bundles. Let

$$B^\varepsilon = \cup_{\alpha=1}^m B_\alpha^\varepsilon$$

be a domain with C^2 -smooth boundary.

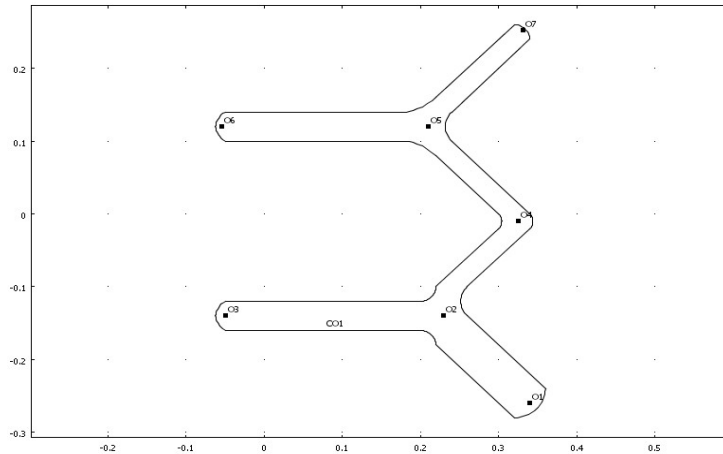


Figure 2.1.3. Tube structure with m (two) bundles of tubes.

Consider the Navier - Stokes system of equations (3.1.1)-(3.1.3) for this B^ε with the right hand side concentrated in the neighborhoods of the nodes (as above). Let us enumerate all nodes , i.e. all ends O_1, \dots, O_N of the segments and all segments e_1, \dots, e_M . For each e_j introduce local co-ordinates x^{e_j} , related to one of its ends. We seek the solution in a generalized form (3.1.27), (3.1.28), i.e.

$$\tilde{u}^a = \sum_{l=2}^K \varepsilon^l \left\{ \sum_{e=e_j, j=1, \dots, M} u_l^e \left(\frac{x^{e,L}}{\varepsilon} \right) \chi_\varepsilon(x) + \sum_{i=1}^N u_l^{BLO_i} \left(\frac{x - O_i}{\varepsilon} \right) \eta(x) \right\}, \quad (3.1.37)$$

$$\begin{aligned} \tilde{p}^a = & \sum_{l=2}^{K+1} \varepsilon^{l-2} \sum_{e=e_j, j=1, \dots, M} p_l^e(x_1^e) \chi_\varepsilon(x) + \sum_{i=1}^N p_2(O_i) (1 - \chi_\varepsilon(x)) \theta_i(x) \\ & + \sum_{l=2}^{K+1} \varepsilon^{l-1} \sum_{i=1}^N p_l^{BLO_i} \left(\frac{x - O_i}{\varepsilon} \right) \eta(x), \end{aligned} \quad (3.1.38)$$

where the terms have the same form and sense as above :

$$u_l^{e_j}(\xi^L) = c_l^{e_j} \Gamma_j(\tilde{u}^{e_j}(\xi^L), 0, \dots, 0)^T, \quad p_l^{e_j}(x_1^{e_j}) = c_l^{e_j} x_1^{e_j} + d_l^{e_j},$$

here $c_l^{e_j}, d_l^{e_j}$ are scalar constants, \tilde{u}^{e_j} is the solution of the problem (3.1.10) and the boundary value problems are stated for each domain Ω_{O_i} , related to O_i ; i.e. let O_i be one of the nodes (one of the ends of $e_{j_1}, \dots, e_{j_{q_i}}$) and let the local coordinates for each of these segments are related to O_i ; cut all cylinders $B_{j_1}^\varepsilon, \dots, B_{j_{q_i}}^\varepsilon$, associated with $e_{j_1}, \dots, e_{j_{q_i}}$ at the distance of $|e_{j_1}|/2, \dots, |e_{j_{q_i}}|/2$ respectively and consider the part of B^ε which contains O_i ; then we extend this part substituting the deleted parts of the cylinders $B_{j_1}^\varepsilon, \dots, B_{j_{q_i}}^\varepsilon$ by the half-infinite cylinders having the same cross-sections and orientations as $B_{j_1}^\varepsilon, \dots, B_{j_{q_i}}^\varepsilon$ (these half-cylinders contain only the truncated parts of $B_{j_1}^\varepsilon, \dots, B_{j_{q_i}}^\varepsilon$, but not the resting parts); then after the homothetic dilatation of this constructed domain in $1/\varepsilon$ times with respect to O_i we obtain the domain Ω_{O_i} .

Remark 2.1.2. All p_2^ε have a common value $p_2^\varepsilon(O_i)$ in O_i for all e with one of the ends O_i . The boundary layer problem is similar to (3.1.11)-(3.1.13) :

$$\begin{aligned} & \eta \Delta_\xi u_l^{BLO_i} - \nabla_\xi p_l^{BLO_i} = f_i(\xi) \delta_{l2} \\ & + \sum_{e=e_j, j=j_1, \dots, j_{q_i}} \{ c_l^{e_j} \{ -\eta \Delta_\xi (\chi_j(\xi_1^{e_j}) \Gamma_j(\tilde{u}^{e_j}(\xi^L)), 0, \dots, 0)^T \} \end{aligned}$$

$$\begin{aligned}
& + \nabla_{\xi}(\chi_j(\xi_1^{e_j})\xi_1^{e_j})\} + \\
& + \left(\sum_{p+r=l-1} c_p^{e_j} c_r^{e_j} \right) (\chi_j(\xi_1^{e_j}) \tilde{u}^{e_j}(\xi^L) \frac{\partial}{\partial \xi_1^{e_j}} \chi_j(\xi_1^{e_j})) \Gamma_j(\tilde{u}^{e_j}(\xi^L), 0, \dots, 0)^T + \\
& d_{l+1}^{e_j} \nabla_{\xi}(\chi_j(\xi_1^{e_j})) \}, \tag{3.1.39}
\end{aligned}$$

$$\operatorname{div}_{\xi} u_2^{BLO_i} = -\operatorname{div}_{\xi} \left\{ \sum_{e=e_j, j=j_1, \dots, j_{q_i}} \{c_l^{e_j} \chi_j(\xi_1^{e_j}) \Gamma_j(\tilde{u}^{e_j}(\xi^L), 0, \dots, 0)^T\}, \quad \xi \in \Omega_{O_i} \right\} \tag{3.1.40}$$

with the Dirichlet condition

$$u_l^{BLO_i} |_{\partial \Omega_{O_i}} = 0 \tag{3.1.41}$$

if O_i is not a "boundary node," i.e. if the distance from it to the support of the function g is of order of one, and with the boundary condition

$$u_l^{BLO_i} |_{\partial \Omega_{O_i}} = g_i(\xi) \tag{3.1.42}$$

if O_i is a "boundary node," i.e. if the distance from it to the support of the function g is of order of ε . We obtain for $c_l^{e_j}$ the equations of the type (3.1.4) :

$$\sum_{e=e_j, j=j_1, \dots, j_{q_i}} \int_{\beta_j} \tilde{u}^{e_j}(\xi^L) d\xi c_l^{e_j} = 0 \tag{3.1.43}$$

if O_i is not a "boundary node," or

$$\sum_{e=e_j, j=j_1, \dots, j_{q_i}} \int_{\beta_j} \tilde{u}^{e_j}(\xi^L) d\xi c_l^{e_j} = \int_{\partial \Omega_{O_i} \cap \operatorname{supp} g_i} (g_i, n) d\xi. \tag{3.1.44}$$

if O_i is a "boundary node," n is the outside normal. Now consider the problem of definition of $c_l^{e_j}$ and $d_{l+1}^{e_j}$ from (3.1.39)-(3.1.44). This problem is equivalent to the problem of definition of piecewise linear function $P_l(x)$ defined on B (linear on every e_j) satisfying conditions (3.1.43), (3.1.44) where $c_l^{e_j} = \partial P_l / \partial x_1^{e_j}$, and satisfying conditions

$$d_l^{e_j} = -\bar{p}_{l-1}^{BLO_i \infty j} + d_l^{O_i},$$

where $\bar{p}_{l-1}^{BLO_i \infty i}$ is a limit of the boundary layer function $\bar{p}_{l-1}^{BLO_i}$ constructed as above in such a way that the pair $\bar{u}_{l-1}^{BLO_i}, \bar{p}_{l-1}^{BLO_i}$ is a solution of the problem (3.1.39)-(3.1.42) for $l-1$ and without the last term of the equation (3.1.39); $d_l^{O_i}$ is a constant independent of j . This condition can be rewritten in a form

$$d_l^{e_j} = -\bar{p}_{l-1}^{BLO_i \infty i} + d_l^{e_{i_1}}. \tag{3.1.45}$$

Let Φ be a function such that it is defined on each segment e , $\partial\Phi/\partial x_1^e = 0$ in the vicinities of all nodes and such that in each node O_i its limit values $\Phi_{e_{j_1}}(O_i), \dots, \Phi_{e_{j_{q_i}}}(O_i)$ for the segments $e_{i_1}, \dots, e_{i_{q_i}}$ respectively satisfy to the relation (3.1.45), i.e.

$$\Phi_{e_j}(O_i) = -\bar{p}_{l-1}^{BLO_i \infty j} + \Phi_{e_{i_1}}(O_i). \quad (3.1.46)$$

We know that $\frac{\partial^2 \hat{P}_l}{\partial x_1^e} = 0$ and that the constants $c_l^{e_j} = \frac{\partial \hat{P}_l}{\partial x_1^e}$ satisfy relations (3.1.43), (3.1.44). Then we can reformulate the problem for $\hat{P}_l = P_l - \Phi$ as

$$\begin{aligned} & - \sum_{e=e_j, j=1, \dots, M} \int_e \rho_e \frac{\partial \hat{P}_l}{\partial x_1^e} \frac{\partial \hat{\tau}}{\partial x_1^e} dx_1^e = \\ & - \sum_{e=e_j, j=1, \dots, M} \int_e \rho_e \frac{\partial \Phi}{\partial x_1^e} \frac{\partial \hat{\tau}}{\partial x_1^e} dx_1^e \\ & - \sum_{O=O_i, \text{ boundary nodes}} \int_{\partial\Omega_{O_i}} (g_i, n) ds \tau(O_i), \end{aligned}$$

where the summation in the last term is developed over the boundary nodes, $\rho_e = \int_{\beta_e} \tilde{u}^e(\xi^L) d\xi$, τ is an arbitrary function of $H^1(B)$. Now the existence and uniqueness up to a constant of \hat{P}_l is evident (by the Lax - Milgram lemma). The justification of series (3.1.37), (3.1.38) is the same as in the case of one bundle of segments B : a function $U^a \in H_{div=0}(B^\varepsilon)$ is constructed in the same way as in section 1 and the following estimates are proved

$$\|U^a - u\|_{H^1(B^\varepsilon)} = O(\varepsilon^K), \quad \|u^a - u\|_{H^1(B^\varepsilon)} = O(\varepsilon^K). \quad (3.1.47)$$

3.2 Decomposition of a flow in a tube structure

Here below we discuss the application of MAPDD for the Navier-Stokes problem (3.1.1)-(3.1.3). For simplicity we consider the case of $g = 0$. We associate to problem (3.1.1)-(3.1.3) set in B^ε with a right hand side of form (3.1.36) the partially decomposed problem. To this end we cut the cylinders at the distance $\delta = \text{const } \varepsilon \ln(\varepsilon)$ from the nodes by the planes perpendicular to the segments and replace the inner parts of the cylinders by the corresponding parts of the segments e_j . We obtain the set $B^{\varepsilon, \delta}$. Denote $B_i^{\varepsilon, \delta}$ the connected truncated part of B^ε , containing the node O_i , e_{ij} the part of the

segment connecting $B_i^{\varepsilon,\delta}$ and $B_j^{\varepsilon,\delta}$; let S_{ij} be a cross-section of the truncated cylinder corresponding to e_{ij} , such that it belongs to $\partial B_i^{\varepsilon,\delta}$.

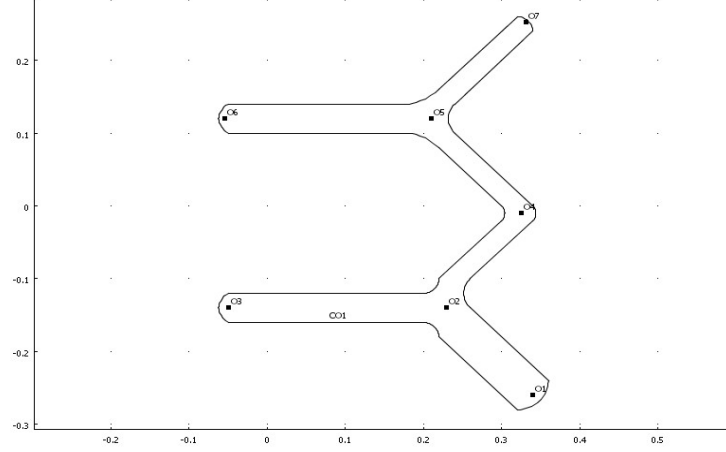


Figure 2.2.1. A tube structure.

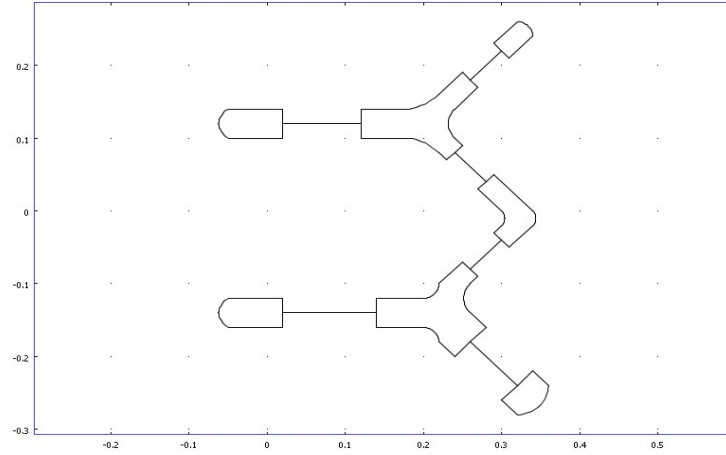


Figure 2.2.2. The asymptotically partially decomposed domain; $\delta = O(\varepsilon|\ln(\varepsilon)|)$.

Consider the equations for each $B_i^{\varepsilon,\delta}$:

$$\eta\Delta U - (U, \nabla)U - \nabla P = f, \quad (3.2.1)$$

$$\operatorname{div} U = 0, \quad x \in B_i^{\varepsilon,\delta} \quad (3.2.2)$$

$$U = 0 \quad x \in \partial B_i^{\varepsilon,\delta} \cap \partial B^\varepsilon, \quad i = 1, \dots, N, \quad (3.2.1)$$

the equation for each segment e_{j_1, j_2} :

$$-p'_{j_1, j_2} = (\Gamma_{j_1, j_2}^T f)^1 - w_{j_1, j_2} \quad (3.2.4)$$

and the interface conditions on each cross-section S_{j_1, j_2}

$$U = \varepsilon^2 w_{j_1, j_2} \Gamma_{j_1, j_2} (\tilde{u}^{e_{j_1, j_2}}, 0, \dots, 0)^T, \quad (3.2.5)$$

$$\begin{aligned} & \int_{S_{j_1, j_2}} \left(\left(\eta \frac{\partial U}{\partial n} - (U, n)U - Pn \right), \Gamma_{j_1, j_2} (\tilde{u}^{e_{j_1, j_2}}, 0, \dots, 0)^T \right) ds \\ &= - \int_{S_{j_1, j_2}} (n, \Gamma_{j_1, j_2} (\tilde{u}^{e_{j_1, j_2}}, 0, \dots, 0)^T) ds p_{j_1, j_2} \end{aligned} \quad (3.2.6)$$

where $\tilde{u}^{e_{j_1, j_2}}$ is the solution of the Dirichlet problem for Poisson equation (3.1.10) on the cross-section of the rod e_{j_1, j_2} and Γ_{j_1, j_2} is the matrix of passage to the local base corresponding to the segment e_{j_1, j_2} with the origin in O_{j_1} , w_{j_1, j_2} are unknown constants, p_{j_1, j_2} is a function of the variable $x_1^{e_{j_1, j_2}}$ defined on each segment e_{j_1, j_2} . And

$$p_{j_1, j_2}(x_1^{e_{j_1, j_2}}) = p_{j_2, j_1}(|e_{j_1, j_2}| + 2\delta - x_1^{e_{j_1, j_2}}), \quad (3.2.7)$$

$$w_{j_1, j_2} = -w_{j_2, j_1}. \quad (3.2.8)$$

Taking into account (3.2.5), relation (3.2.6) can be rewritten in a form

$$\begin{aligned} & - \int_{S_{j_1, j_2}} \left(\left(\varepsilon^4 w_{j_1, j_2}^2 \tilde{u}^{e_{j_1, j_2}} \Gamma_{j_1, j_2} (\tilde{u}^{e_{j_1, j_2}}, 0, \dots, 0)^T - \right. \right. \\ & \quad \left. \left. + Pn \right), \Gamma_{j_1, j_2} (\tilde{u}^{e_{j_1, j_2}}, 0, \dots, 0)^T \right) ds = \\ &= - \int_{S_{j_1, j_2}} (n, \Gamma_{j_1, j_2} (\tilde{u}^{e_{j_1, j_2}}, 0, \dots, 0)^T) ds p_{j_1, j_2}. \end{aligned} \quad (3.2.6')$$

Let us give the variational formulation for this problem.

Let $H_{div=0}(B_1^{\varepsilon, \delta}, \dots, B_N^{\varepsilon, \delta}, e_1, \dots, e_M)$ be the space of ordered collections

$(U_1, \dots, U_N, w_1, \dots, w_M)$, where U_i are the vector valued functions from $H_{div=0}(B_i^{\varepsilon, \delta})$, equal to zero on $\partial B_i^{\varepsilon, \delta} \cap \partial B^\varepsilon$, and w_1, \dots, w_M are the constants associated with the segments e_1, \dots, e_M such that for each e_j , containing e_{j_1, j_2} , and connecting $B_{j_1}^{\varepsilon, \delta}$ with $B_{j_2}^{\varepsilon, \delta}$, we have

$$U_{j_1} = \text{sign}(j_2 - j_1) \varepsilon^2 w_j \Gamma_{j_1, j_2} (\tilde{u}^{e_{j_1, j_2}}, 0, \dots, 0)^T, \text{ on } S_{j_1, j_2} \text{ and on } S_{j_2, j_1}. \quad (3.2.9)$$

The scalar product is defined as

$$\begin{aligned} & ((U_1, \dots, U_N, w_1, \dots, w_M), (V_1, \dots, V_N, v_1, \dots, v_M))_P = \\ & \sum_{i=1}^N \int_{B_i^{\varepsilon, \delta}} \eta \sum_{r=1}^s \left(\frac{\partial U_i}{\partial x_r}, \frac{\partial \Phi_i}{\partial x_r} \right) dx + \varepsilon^{2+(s-1)} \sum_{j=1}^M (|e_j| - 2\delta) \int_{\beta_j} (-\tilde{u}^{e_j}(\xi^L)) d\xi w_j v_j. \end{aligned}$$

Note that $\int_{\beta_j} \tilde{u}^{e_j}(\xi^L) d\xi < 0$ because $\tilde{u}^{e_j}(\xi^L) < 0$ by the principle of maximum for elliptic equation (3.1.10). The norm is defined as

$$\|(U_1, \dots, U_N, w_1, \dots, w_M)\|_P = ((U_1, \dots, U_N, w_1, \dots, w_M), (U_1, \dots, U_N, w_1, \dots, w_M))_P^{1/2}.$$

Then the variational formulation is as follows :

find $(U_1, \dots, U_N, w_1, \dots, w_M) \in H_{div=0}(B_1^{\varepsilon, \delta}, \dots, B_N^{\varepsilon, \delta}, e_1, \dots, e_M)$

and such that for any $(\Phi_1, \dots, \Phi_N, v_1, \dots, v_M) \in H_{div=0}(B_1^{\varepsilon, \delta}, \dots, B_N^{\varepsilon, \delta}, e_1, \dots, e_M)$ the integral identity holds true :

$$\begin{aligned} & - \sum_{i=1}^N \int_{B_i^{\varepsilon, \delta}} \eta \sum_{r=1}^s \left(\frac{\partial U_i}{\partial x_r}, \frac{\partial \Phi_i}{\partial x_r} \right) dx + \\ & + \sum_{i=1}^N \int_{B_i^{\varepsilon, \delta}} (U_i, (U_i, \nabla) \Phi_i) dx + \varepsilon^{2+(s-1)} \sum_{j=1}^M (|e_j| - 2\delta) \int_{\beta_j} \tilde{u}^{e_j}(\xi^L) d\xi w_j v_j \\ & = \sum_{i=1}^N \int_{B_i^{\varepsilon, \delta}} (f, \Phi) dx \\ & + \varepsilon^{2+(s-1)} \sum_{j=1}^M \int_{\beta_j} \tilde{u}^{e_j}(\xi^L) d\xi \int_{e_j \setminus \cup_{i=1}^s B_i^{\varepsilon, \delta}} (\Gamma_j^T f)^1 dx_1^{e_j} v_j. \end{aligned} \quad (3.2.10)$$

Variational formulation (3.2.10) can be obtained in a following way (cf. section 6.2 in GP2005). Consider the subspace $\hat{H}_{div=0}^0(B^\varepsilon, \delta)$ of the space $H_{div=0}^0(B^\varepsilon)$ which contains all functions \hat{U} of $\hat{H}_{div=0}^0(B^\varepsilon, \delta)$ such that for any truncated segment e_{j_1, j_2} they coincide with the Poiseuille flow $c_{j_1, j_2} \Gamma_{j_1, j_2}(\tilde{u}^{e_{j_1, j_2}}, 0, \dots, 0)^T$, on the truncated part of the cylinder forming B^ε stretched between the cross sections S_{j_1, j_2} and S_{j_2, j_1} ; c_{j_1, j_2} is a constant on

this truncated cylinder.

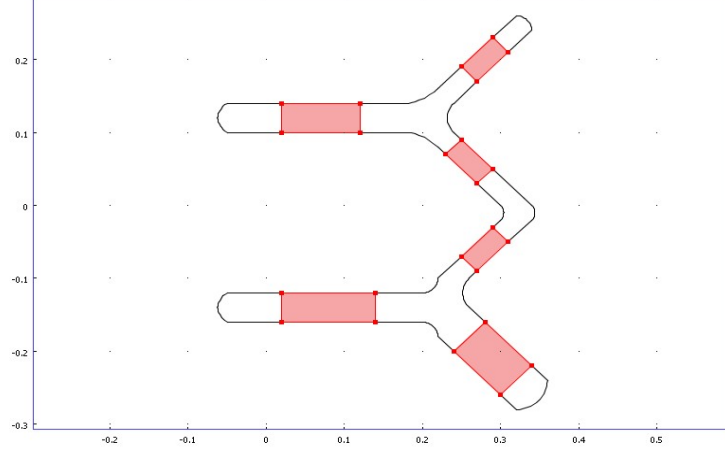


Figure 2.2.3. The structure of space $\hat{H}_{div=0}^0(B^\varepsilon \delta)$.

Consider the following partially decomposed variational problem : to find $\hat{U} \in \hat{H}_{div=0}^0(B^\varepsilon, \delta)$ such that for all $\Phi \in \hat{H}_{div=0}^0(B^\varepsilon, \delta)$

$$- \int_{B^\varepsilon} \eta \sum_{i=1}^s \left(\frac{\partial \hat{U}}{\partial x_i}, \frac{\partial \Phi}{\partial x_i} \right) dx + \int_{B^\varepsilon} (\hat{U}, (\hat{U}, \nabla) \Phi) dx = \int_{B^\varepsilon} (f, \varphi) dx. \quad (3.2.11)$$

Associating to each function $\hat{U} \in \hat{H}_{div=0}^0(B^\varepsilon, \delta)$ the ordered collection

$(U_1, \dots, U_N, w_1, \dots, w_M) \in H_{div=0}(B_1^{\varepsilon, \delta}, \dots, B_N^{\varepsilon, \delta}, e_1, \dots, e_M)$ in such way that

$\hat{U} = U_i$ on each $B_i^{\varepsilon, \delta}$, and $\hat{U} = \varepsilon^2 w_j \Gamma_j(\tilde{u}^{e_j}, 0, \dots, 0)^T$ on each truncated cylinder

forming B^ε corresponding to the segment e_j (under the convention that each e_j stretched

between O_{j_1} and O_{j_2} , $j_1 < j_2$, has the origin in O_{j_1}) we obtain (3.2.10) and respectively

(3.2.1)-(3.2.8) as an equivalent formulation of (3.2.11). It can be proved as in [14]

that for sufficiently small ε there exists a unique solution to (3.2.11) due to the fixed

point theorem and the Poincaré - Friedrichs inequality for B^ε . The a priori estimate

holds true with a constant independent of ε . Suppose that \hat{f}_i in vicinities of nodes are

approximated by Taylor's formula up to the terms $O(\varepsilon^K)$ as it was done in section 2.1.

The above asymptotic analysis of problem (3.1.1)- (3.1.3) (section 2.1) shows that U^a

satisfies the integral identity (3.2.11) with adiscrepancy

$$\int_{B^\varepsilon} \varepsilon^K (\rho, \Phi) dx, \quad (3.2.12)$$

where ρ is a bounded vector valued function. Moreover, U^a does not belong to $\hat{H}_{div=0}^0(B^\varepsilon, \delta)$ because it gives a discrepancy in condition (3.2.5) of order $O(\exp(-c\delta/\varepsilon))$, $c > 0$ in C^1 , i.e.,

$$U^a = \varepsilon^2 c_{e_{j_1, j_2}}^K \Gamma_{j_1, j_2}(\tilde{u}^{e_{j_1, j_2}}, 0, \dots, 0)^T + \exp(-c\delta/\varepsilon)r_0, \quad x \in S_{j_1, j_2}, \quad (3.2.13)$$

where r_0 is a bounded in C^1 vector valued function, $c_e^K = \sum_{l=2}^K \varepsilon^{l-2} c_l^e$. Therefore, we shall slightly change U^a in order to obtain a function of $\hat{H}_{div=0}^0(B^\varepsilon, \delta)$. The discrepancy $\exp(-c\delta/\varepsilon)r_0$ can be continued from S_{j_1, j_2} to $B_{j_1}^{\varepsilon, \delta}$ in such a way that the divergence of the extension vanishes and that this extension has an order $O(\exp(-c_1\delta/\varepsilon))$, $c_1 > 0$ in $H^1(B_{j_1}^{\varepsilon, \delta})$. Such extension exists ([14]) because $div U^a = 0$ in $B_{j_1}^{\varepsilon, \delta}$ and the constants $c_{e_j}^K = \sum_{l=2}^K \varepsilon^{l-2} c_l^{e_j}$ satisfy conditions (3.1.43), (3.1.44). Denote this extension $\delta\tilde{U}^a$. Define $\delta\tilde{U}^a = U^a - \varepsilon^2 c_{e_{j_1, j_2}}^K \Gamma_{j_1, j_2}(\tilde{u}^{e_{j_1, j_2}}, 0, \dots, 0)^T$ on truncated parts of cylinders between the cross sections S_{j_1, j_2} and S_{j_2, j_1} . Now $\tilde{U}^a = U^a - \delta\tilde{U}^a \in \hat{H}_{div=0}^0(B^\varepsilon, \delta)$, $\|\delta\tilde{U}^a\|_{H^1(B^\varepsilon)} = O(\exp(-c_2\delta/\varepsilon))$, $c_2 > 0$, and it satisfies integral identity (3.2.11) with discrepancy of order $O(\exp(-c_3\delta/\varepsilon))$, $c_3 > 0$, c_3 does not depend on small parameters, i.e.,

$$\begin{aligned} & - \int_{B^\varepsilon} \eta \sum_{i=1}^s \left(\frac{\partial \tilde{U}^a}{\partial x_i}, \frac{\partial \Phi}{\partial x_i} \right) dx + \int_{B^\varepsilon} (\tilde{U}^a, (\tilde{U}^a, \nabla) \Phi) dx = \int_{B^\varepsilon} (f, \varphi) dx + \\ & + \int_{B^\varepsilon} \eta \sum_{i=1}^s \left(\frac{\partial \delta \tilde{U}^a}{\partial x_i}, \frac{\partial \Phi}{\partial x_i} \right) dx - \int_{B^\varepsilon} (U^a, (\delta \tilde{U}^a, \nabla) \Phi) dx - \\ & - \int_{B^\varepsilon} (\delta \tilde{U}^a, (U^a - \delta \tilde{U}^a, \nabla) \Phi) dx + \int_{B^\varepsilon} \varepsilon^K (\rho, \Phi) dx = \\ & = \int_{B^\varepsilon} (f, \varphi) dx + \int_{B^\varepsilon} \sum_{i=1}^s \exp(-c_3\delta/\varepsilon) (\rho_i, \frac{\partial \Phi}{\partial x_i}) dx + \\ & + \int_{B^\varepsilon} \exp(-c_3\delta/\varepsilon) (\rho_0, \Phi) dx + \int_{B^\varepsilon} \varepsilon^K (\rho, \Phi) dx, \quad (3.2.14) \end{aligned}$$

where $\rho_i, i = 0, \dots, s$ are vector valued functions bounded in $L^2(B^\varepsilon)$ by a constant independent of the small parameters. On the other hand, for any K there exist such \hat{K} independent of ε that if $\delta = \hat{K}\varepsilon |\ln(\varepsilon)|$ then

$$\exp(-c_2\delta/\varepsilon), \exp(-c_3\delta/\varepsilon) = O(\varepsilon^K).$$

Taking into consideration the discrepancy (3.2.14) and the a priori estimate for (3.1.1)-(3.1.3) we obtain the following estimate : for any K there exist such \hat{K} independent of ε that if $\delta = \hat{K}\varepsilon|\ln(\varepsilon)|$ then

$$\|\hat{U} - \tilde{U}^a\|_{H^1(B^\varepsilon)} = O(\varepsilon^K). \quad (3.2.15)$$

Remark 2.2.1 Defining $c_{e_j}^K = \sum_{l=2}^K \varepsilon^{l-2} c_l^{e_j}$ we obtain the estimate

$$\|(u^a|_{B_1^{\varepsilon,\delta}} - U_1, \dots, u^a|_{B_N^{\varepsilon,\delta}} - U_N, c_{e_1}^K - w_1, \dots, c_{e_M}^K - w_M)\|_P = O(\varepsilon^K).$$

Combining the estimates (3.1.47) and (3.1.15) we obtain that for any K there exists such \hat{K} independent of ε that if $\delta = \hat{K}\varepsilon|\ln(\varepsilon)|$ then the estimate holds true

$$\|\hat{U} - u\|_{H^1(B^\varepsilon)} = O(\varepsilon^K). \quad (3.2.16)$$

The estimate (3.2.16) justifies the MAPDD for the Navier-Stokes problem.

Remark 2.2.2 The present section is devoted to an approximation of completely three-dimensional (two-dimensional) problem by a hybrid problem that is "mainly one-dimensional", i.e., it is of dimension 1 on the major part of the domain. On the other hand another related problem was considered recently by S.A.Nazarov and M.Specovius-Neugebauer [26],[27]. They constructed a special approximation of problems in unbounded domain by problems in bounded (truncated) domain. This approach also takes into consideration the information on asymptotic behavior of solution of the problem in unbounded domain at infinity.

Remark 2.2.3 Some numerical experiments on MAPDD were developed in case of the Stokes flow in thin domains. The comparison to the direct numerical computation of a solution of the problem shows that for the case when the viscosity η is finite, the boundary layers are very narrowly localized in the neighborhoods of the junctions, so δ can be taken almost equal to just ε . However, if the Reynolds number becomes greater (for example if the viscosity is small) then the multi-dimensional parts become also greater. The same remark holds for the flows in wavy tubes and for the extrusion process modelling. The Stokes flow in an extruder with a screw of a form presented in Figure 6.3.4 in [16] was computed by I.Sirakov using the asymptotic domain decomposition on five subdomains, as it is shown in the Figure 6.3.6. in [16] The pressure and

the particles trajectories were calculated (Figure 6.3.7) in [16].

Chapitre 4

Asymptotic analysis of a periodic flow in a thin channel with two viscoelastic walls

4.1 Introduction :

From the physical point of view, problems involving a fluid interacting with a moving or deformable structure are of great interest. This kind of problem finds practical use in many areas of engineering and pure science. Some areas of applications are : biomechanics, hydroelasticity, aeroelasticity, etc.

In the last few years, there was an increasing interest in the study of such problems : [1]-[18]-[23] are only few example of works dealing with the fluide-structure interaction. The present paper is concerned with the interaction between a viscous, incompressible fluid and a two elastic wall wich represent a part of the boundary of the flow domain. This problem can be seen as a simplified model for blood motion through a blood vessel.

Recently, some results concerning the flow through the bloodstream are published in [16],[3],[24],[25]. They considered a more complex model for the fluid motion but the flow domain had rigid walls.

Here we consider a non steady-state viscous flow in a thin channel with a two visco-

elastic wall. The fluid motion is simulated by the Stokes equations, the wall behaviour is described by the Sophie Germain fourth order in space non-steady state equation for the transversal displacements of the elastic wall (the plate model), while the longitudinal wall displacement are disregarded. The fluid-structure is simulated by the equality of the fluid velocity at the boundary and the time derivative of the wall displacement (the longitudinal velocity is taken equal to zero). The problem contains two small parameters : one of them is the ratio ε of the thickness of the channel to its length (i.e, to the period of the flow); the second, δ , is the ratio of the linear density to the stiffness of the wall. For various ratios of these two small parameters, an asymptotic expansion solution is constructed. Parameter δ is taken as some power of ε , namely, $\delta = \varepsilon^\gamma$, $\gamma \in \mathbf{N}^*$. The asymptotic expansion is different for three following cases : $\gamma > 3$ (very rigid wall), $\gamma < 3$ (soft wall), $\gamma = 3$ (critical case) and is different from case [1]. This asymptotic solutions are justified by a theorem on the error estimates and some a priori estimates, these results are different from the results obtained in [1].

4.2 The Description of the physical problem :

We consider a small parameter $\varepsilon = 1/q$, $q \in \mathbf{N}^*$ and we define the thin domain :

$$D_\varepsilon = \{(x_1, x_2) \in \mathbf{R}^2 : 0 < x_1 < 1, -\varepsilon/2 < x_2 < \varepsilon/2\}$$

let Γ_ε and $\Gamma_{-\varepsilon}$ are the elastic part of the boundary of D_ε :

$$\Gamma_\varepsilon = \{(x_1, \varepsilon/2) : 0 < x_1 < 1\}$$

and

$$\Gamma_{-\varepsilon} = \{(x_1, -\varepsilon/2) : 0 < x_1 < 1\}$$

The other part of the boundary is rigid.

We suppose that the incompressible, viscous fluid fills the domain D_ε and interacts with the elastic structure Γ_ε and $\Gamma_{-\varepsilon}$.

The interaction between the fluid and the elastic wall produces the displacement $d^+(x_1, t)$ and $d^-(x_1, t)$ of this structure in ox_2 direction. We neglect the longitudinal

displacement and we consider that the elastic boundary is clamped at the ends.

We study this problem for $t \in [0, T]$, with T an arbitrary positive constant and we assume that the wall is not very elastic so that the deformation of the boundary is small enough. Consequently, at each time t , we can consider with a good approximation the fluid flow equations in the initial configuration. For the case when the equations, for the fluid are set in the deformed configuration we can refer, for instance, to [21] for the steady state case and to [23] for the non steady state one : in this papers the existence and the uniqueness of the solution was not studied.

Let f be the exterior force applied to the fluid, $g^\pm e_2$ the exterior force applied on the elastic boundary and $(Tfn)_2$ the surface force exerted by the fluid on the structure, with T_f the stress tensor and n the outer unit normal on the boundary of the D_ε .

4.3 Modeling the problem :

Consider the following non steady state problem :

$$\left\{ \begin{array}{l} \rho_f \frac{\partial u}{\partial t} - \eta \Delta u + \nabla p = f \text{ in } D_\varepsilon \times (0, T), \\ \operatorname{div}(u) = 0 \text{ on } D_\varepsilon \times (0, T), \\ u_1 = 0, \quad u_2 = \frac{\partial d^+}{\partial t} \text{ on } \Gamma_\varepsilon \times (0, T), \\ u_1 = 0, \quad u_2 = \frac{\partial d^-}{\partial t} \text{ on } \Gamma_{-\varepsilon} \times (0, T), \\ u(x, 0) = 0 \text{ in } D_\varepsilon, \\ u \text{ 1 - periodic in } x_1, \quad p \text{ 1 - periodic in } x_1 \end{array} \right. \quad (4.1)$$

Where ρ_f and η represent positive constant, the unknowns for the system (4.1) are the fluid velocity u and the fluid pressure p .

The system (4.1) is coupled to the system (4.2) as follows :

$$\left\{ \begin{array}{l} \frac{\partial^2 d^+}{\partial t^2} + \frac{1}{\delta} \frac{\partial^4 d^+}{\partial x_1^4} + \nu \frac{\partial^5 d^+}{\partial x_1^4 \partial t} = g^+ + p \text{ sur } \Gamma_\varepsilon \times (0, T), \\ \frac{\partial^2 d^-}{\partial t^2} + \frac{\kappa}{\delta} \frac{\partial^4 d^-}{\partial x_1^4} + \nu \frac{\partial^5 d^-}{\partial x_1^4 \partial t} = g^- + p \text{ sur } \Gamma_{-\varepsilon} \times (0, T), \\ d^\pm(x_1, 0) = \frac{\partial d^\pm}{\partial t}(x_1, 0) = 0 \text{ in } (0, 1), \\ d^\pm \text{ 1 - periodic in } x_1 \end{array} \right. \quad (4.2)$$

Where κ , δ and ν represent positive constant, in connection with the properties of the materials. the positive constant h is the tickness of the elastic wall.

The action of the viscous fluid on the elastic wall is represented by the stress tensor $T_f = T_f(u, p)$ wich is defined by :

$$T_f(u, p) = pI - \eta(\nabla u + (\nabla u)^t)$$

On the boundary $\Gamma_{+\varepsilon}$ $n = (0, 1)$, hence

$$(T_f n)_2 = p - 2\eta \frac{\partial u_2}{\partial x_2} \text{ on } \Gamma_{+\varepsilon} \times (0, T)$$

On the boundary $\Gamma_{-\varepsilon}$ $n = (0, -1)$, hence

$$(T_f n)_2 = -p + 2\eta \frac{\partial u_2}{\partial x_2} \text{ on } \Gamma_{-\varepsilon} \times (0, T)$$

If we formally consider $\text{div}(u) = 0$ on $\Gamma_{\pm\varepsilon} \times (0, T)$, from (1.1)₂ it follows that

$$\frac{\partial u_2}{\partial x_2} = 0$$

Hence, the surface force exerted by the fluid on the elastic boundary can be defined by :

$$(T_f n)_2 = \pm p$$

The compatibility condition for the coupled system wich describes the physical problem is :

$$\begin{aligned} & \int_{D_\varepsilon} \text{div} u = 0 \\ 0 &= \int_{\partial D_\varepsilon} u(x, t) \cdot n ds_x = \int_0^1 u_2(x_1, \frac{\varepsilon}{2}, t) - \int_0^1 u_2(x_1, \frac{-\varepsilon}{2}, t) \\ &= \int_0^1 \frac{d}{dt} (d^+(x_1, t) - d^-(x_1, t)) dx_1 = 0 \end{aligned}$$

it follows that :

$$\int_0^1 (d^+(x_1, t) - d^-(x_1, t)) dx_1 = cst \quad \forall t \in (0, T)$$

using the initial condition for d^\pm , we obtain constant equal to zero.

Hence the compatibility condition for the above coupled system becomes :

$$\int_0^1 (d^+(x_1, t) - d^-(x_1, t)) dx_1 = 0, \quad \forall t \in (0, T)$$

4.4 Variational approach of the problem

4.4.1 Variational formulation

In this section we consider problem (4.1) and (4.2). For obtaining the variational formulation of this problem we introduce the following spaces :

$$V^\varepsilon = \{v \in (H_{per}^1(D_\varepsilon))^2 : \operatorname{div} v = 0, v = 0 \text{ sur } (\partial D_\varepsilon - (\Gamma_\varepsilon \cup \Gamma_{-\varepsilon})), v_1 = 0 \text{ sur } (\Gamma_\varepsilon \cup \Gamma_{-\varepsilon})\}$$

$$B_0 = \{(b^+, b^-) \in (H_{per}^2(0, 1))^2 : \int_0^1 (b^+(x_1) - b^-(x_1)) dx_1 = 0\}$$

and we assume that $f \in L^2(0, T; (L^2(D_\varepsilon))^2)$ and $g \in L^2((0, 1) \times (0, T))$.

Multiplying (4.1)₁ by an arbitrary function $\varphi = (\varphi_1, \varphi_2) \in V^\varepsilon$, using $\operatorname{div} \varphi = 0$ and integrant by parts on D_ε it follows :

$$\int_{D_\varepsilon} \frac{\partial u}{\partial t} \cdot \varphi + \eta \int_{D_\varepsilon} \nabla u : \nabla \varphi + \int_{\Gamma_{+\varepsilon}} p \varphi_2 - \int_{\Gamma_{-\varepsilon}} p \varphi_2 = \int_{D_\varepsilon} f \cdot \varphi$$

Multiplying the equation for d^\pm by $b \in B^0$ we get :

$$\left\{ \begin{array}{l} \int_0^1 \frac{\partial^2 d^+}{\partial t^2} b^+ + \frac{1}{\delta} \int_0^1 \frac{\partial^2 d^+}{\partial x_1^2} \frac{\partial^2 b^+}{\partial x_1^2} + \nu \int_0^1 \frac{\partial^3 d^+}{\partial x_1^2 \partial t} \frac{\partial^2 b^+}{\partial x_1^2} \\ + \int_0^1 \frac{\partial^2 d^-}{\partial t^2} b^- + \frac{\kappa}{\delta} \int_0^1 \frac{\partial^2 d^-}{\partial x_1^2} \frac{\partial^2 b^-}{\partial x_1^2} + \nu \int_0^1 \frac{\partial^3 d^-}{\partial x_1^2 \partial t} \frac{\partial^2 b^-}{\partial x_1^2} \\ = \int_0^1 g^+ b^+ + \int_0^1 p(b^+ - b^-) + \int_0^1 g^- b^- \end{array} \right.$$

Summing these two equations and choosing now $\varphi \in V_\varepsilon$ and $b \in B_0$ such that $\varphi_2 = b^\pm$ on Γ_ε^\pm and adding the two previous equalities, we obtain :

$$\left\{ \begin{array}{l} \int_{D_\varepsilon} \frac{\partial u}{\partial t} \cdot \varphi + \eta \int_{D_\varepsilon} \nabla u : \nabla \varphi + \int_0^1 \left(\frac{\partial^2 d^+}{\partial t^2} b^+ + \frac{\partial^2 d^-}{\partial t^2} b^- \right) \\ + \int_0^1 \left(\frac{1}{\delta} \frac{\partial^2 d^+}{\partial x_1^2} \frac{\partial^2 b^+}{\partial x_1^2} + \frac{\kappa}{\delta} \frac{\partial^2 d^-}{\partial x_1^2} \frac{\partial^2 b^-}{\partial x_1^2} \right) + \nu \int_0^1 \left(\frac{\partial^3 d^+}{\partial x_1^2 \partial t} \frac{\partial^2 b^+}{\partial x_1^2} + \frac{\partial^3 d^-}{\partial x_1^2 \partial t} \frac{\partial^2 b^-}{\partial x_1^2} \right) \\ = \int_0^1 g^+ b^+ + \int_0^1 g^- b^- + \int f \varphi \end{array} \right.$$

In the end the problem is to find $(u, d^+, d^-) \in L^2(0, T; V^\varepsilon) \times H^1(0, T; B_0) \times H^1(0, T; B_0)$ satisfies the following equation :

$$\left\{ \begin{array}{l} \frac{d}{dt} \int_{D_\varepsilon} u \cdot \varphi + \eta \int_{D_\varepsilon} \nabla u : \nabla \varphi + \frac{d}{dt} \int_0^1 \left(\frac{\partial d^+}{\partial t} b^+ + \frac{\partial d^-}{\partial t} b^- \right) \\ + \frac{1}{\delta} \int_0^1 \left(\frac{\partial^2 d^+}{\partial x_1^2} \frac{\partial^2 b^+}{\partial x_1^2} + \kappa \frac{\partial^2 d^-}{\partial x_1^2} \frac{\partial^2 b^-}{\partial x_1^2} \right) + \nu \int_0^1 \left(\frac{\partial^3 d^+}{\partial x_1^2 \partial t} \frac{\partial^2 b^+}{\partial x_1^2} + \frac{\partial^3 d^-}{\partial x_1^2 \partial t} \frac{\partial^2 b^-}{\partial x_1^2} \right) \\ = \int_0^1 g^+ b^+ + \int_0^1 g^- b^- + \int_{D_\varepsilon} f \varphi \end{array} \right.$$

4.5 Asymptotic approach :

Introduction :

In the sequel we introduce the asymptotic expansions and we suppose that :

$$\left\{ \begin{array}{l} f = f_1(x_1, t)e_1, f_1 \in C^\infty([0, 1] \times [0, T]), f \text{ 1-periodic in } x_1 \\ g^\pm \in C^\infty([0, 1] \times [0, T]), g^\pm \text{ 1-periodic in } x_1, \langle g^\pm \rangle(t) = 0 \forall t \in [0, T], \\ \exists 0 < t^* < T \text{ tel que } f_1(x_1, t) = g^\pm(x_1, t) = 0 \forall (x_1, t) \in (0, 1) \times [0, t^*], \end{array} \right.$$

In the sequel we take $\delta = \varepsilon^\gamma$, with $\gamma \in \mathbf{N}^*$. an asymptotic solution is written as :

$$\left\{ \begin{array}{l} u_1^{(k)}(x_1, \frac{x_2}{\varepsilon}, t) = \sum_{j=0}^k \varepsilon^{j+2} u_{1,j}(x_1, \frac{x_2}{\varepsilon}, t), \\ u_2^{(k)}(x_1, \frac{x_2}{\varepsilon}, t) = \sum_{j=0}^k \varepsilon^{j+3} u_{2,j}(x_1, \frac{x_2}{\varepsilon}, t), \\ p^{(k)}(x_1, \frac{x_2}{\varepsilon}, t) = \sum_{j=0}^k \varepsilon^{j+1} P_j(x_1, \frac{x_2}{\varepsilon}, t) + \sum_{j=0}^k \varepsilon^j q_j(x_1, t), \\ d_{(k)}^\pm(x_1, t) = \sum_{j=0}^k \varepsilon^{j+\gamma} d_j^\pm(x_1, t), \end{array} \right.$$

Introducing the asymptotic solution in (4.1) and in (4.2), identifying the coefficient of the powers of ε and denoting $\xi_2 = \frac{x_2}{\varepsilon}$

$$\left\{ \begin{array}{l} -\eta \frac{\partial^2 u_{1,j}}{\partial^2 \xi_2} + \frac{\partial p_{j-1}}{\partial x_1} - \eta \frac{\partial^2 u_{1,j-2}}{\partial t} + \rho_f \frac{\partial u_{1,j-2}}{\partial t} + \frac{\partial q_j}{\partial x_1} = f_1 \delta_{j0}, \\ -\eta \frac{\partial^2 u_{2,j-1}}{\partial^2 \xi_2} + \frac{\partial p_j}{\partial \xi_2} - \eta \frac{\partial^2 u_{2,j-3}}{\partial x_1^2} + \rho_f \frac{\partial u_{2,j-3}}{\partial t} = 0, \\ \frac{\partial u_{1,j}}{\partial x_1} + \frac{\partial u_{2,j}}{\partial \xi_2} = 0, \\ u_{1,j}(x_1, \pm 1/2, t) = 0, \\ u_{2,j}(x_1, -1/2, t) = \frac{\partial d_{j-\gamma+3}^-}{\partial t}, \\ u_{2,j}(x_1, 1/2, t) = \frac{\partial d_{j-\gamma+3}^+}{\partial t}, \end{array} \right. \quad (4.3)$$

For the coupled system we obtain :

$$\left\{ \begin{array}{l} \frac{\partial^4 d_j^+}{\partial x_1^4} + \nu \frac{\partial^5 d_{j-\gamma}^+}{\partial x_1^4 \partial t} + \frac{\partial^2 d_{j-\gamma}^+}{\partial t^2} = g^+ \delta_{j0} + q_j + p_{j-1}|_{\xi_2=\frac{1}{2}}, \\ \kappa \frac{\partial^4 d_j^-}{\partial x_1^4} + \nu \frac{\partial^5 d_{j-\gamma}^-}{\partial x_1^4 \partial t} + \frac{\partial^2 d_{j-\gamma}^-}{\partial t^2} = g^- \delta_{j0} + q_j + p_{j-1}|_{\xi_2=-1/2}, \\ \langle d_j^+ \rangle (t) = 0, \quad \langle d_j^- \rangle (t) = 0, \\ \langle q_j \rangle (t) + \langle p_{j-1}|_{\xi_2=1/2} \rangle = 0, \\ \langle q_j \rangle (t) + \langle p_{j-1}|_{\xi_2=-1/2} \rangle = 0, \end{array} \right. \quad (4.4)$$

4.6 Introducing functions :

We introduce the functions :

$$N_1(\zeta_2) = 1/2(\zeta_2^2 - 1/4)$$

wich satisfies :

$$N_1'' = 1 \text{ et } N_1(\mp 1/2) = 0$$

$$N_2(\zeta_2) = \int_{-1/2}^{\zeta_2} N_1(\tau) d\tau$$

and

$$N_2(1/2) = \int_{-1/2}^{1/2} N_1(\tau) d\tau = -1/12$$

We shall use the following notations :

$$D^{-1} : F \longmapsto \int_{-1/2}^{\zeta_2} F(x_1, \tau, t) d\tau$$

and

$$D^{-2} : F \longmapsto \int_{-1/2}^{\zeta_2} \int_{-1/2}^{\theta} F(x_1, \tau, t) d\tau d\theta - (\zeta_2 + 1/2) \int_{-1/2}^{1/2} \int_{-1/2}^{\theta} F(x_1, \tau, t) d\tau d\theta$$

4.6.1 Proposition :

The unknowns of the previous system $u_{1,j}$, $u_{2,j}$, p_j and q_j are given by the following relations :

$$\left\{ \begin{array}{l} u_{1,j} = \frac{1}{\eta} (D^{-2} (\frac{\partial p_{j-1}}{\partial x_1} - \eta \frac{\partial^2 u_{1,j-2}}{\partial x_1^2} + \rho_f \frac{\partial u_{1,j-2}}{\partial t}) + (-f_1 \delta_{j,0} + \frac{\partial q_j}{\partial x_1}) N_1(\xi_2)), \\ p_j = D^{-1} (\eta (\frac{\partial^2 u_{2,j-1}}{\partial x_2^2} + \frac{\partial^2 u_{2,j-3}}{\partial x_1^2}) - \rho_f \frac{\partial u_{2,j-3}}{\partial t}), \\ u_{2,j} = -D^{-1} (\frac{1}{\eta} (D^{-2} (\frac{\partial^2 p_{j-1}}{\partial x_1^2} - \eta \frac{\partial^3 u_{1,j-2}}{\partial x_1^3} + \frac{\partial^2 u_{1,j-2}}{\partial x_1 \partial t}))) - \frac{1}{\eta} (\frac{\partial^2 q_j}{\partial x_1^2} - (\frac{\partial f_1}{\partial x_1}) \delta_{j,0}) N_2(\xi_2) + \frac{\partial d_{j-\gamma+3}^-}{\partial t}, \\ -\frac{1}{\eta} \int_{-1/2}^{1/2} D^{-2} (\frac{\partial^2 p_{j-1}}{\partial x_1^2} - \eta \frac{\partial^3 u_{1,j-2}}{\partial x_1^3} + \frac{\partial^2 u_{1,j-2}}{\partial x_1 \partial t}) d\xi_2 - \frac{1}{12} \eta (\frac{\partial f_1}{\partial x_1} \delta_{j,0} - \frac{\partial^2 q_j}{\partial x_1^2}) = \frac{\partial d_{j-\gamma-3}^+}{\partial t} - \frac{\partial d_{j-\gamma-3}^-}{\partial t}, \end{array} \right. \quad (4.5)$$

Proof :

We integrate twice this equation :

$$\frac{\partial^2 u_{1,j}}{\partial^2 \xi_2} = \frac{1}{\eta} (\frac{\partial p_{j-1}}{\partial x_1} - \eta \frac{\partial^2 u_{1,j-2}}{\partial t} + \rho_f \frac{\partial u_{1,j-2}}{\partial t} + \frac{\partial q_j}{\partial x_1} - f_1 \delta_{j,0})$$

and using boundary condition, we get (4.5)₁.

The condition of incompressibility is given by :

$$\frac{\partial u_{1,j}}{\partial x_1} + \frac{\partial u_{2,j}}{\partial \xi_2} = 0$$

We integrate this equation with respect to ξ_2 with the boundary condition

$$u_{2,j}(x_1, \frac{-1}{2}, t) = \frac{\partial d_{j-\gamma+3}^-}{\partial t}$$

and we use the expression of $u_{1,j}$ we obtain the result.

The second equation of system (4.3) gives us :

$$\frac{\partial p_j}{\partial \xi_2} = \eta \frac{\partial^2 u_{2,j-1}}{\partial^2 \xi_2} + \eta \frac{\partial^2 u_{2,j-3}}{\partial x_1^2} - \rho_f \frac{\partial u_{2,j-3}}{\partial t}$$

We integrate this equation with respect to ξ_2 we obtain the result.

Finally the last equation is obtained by introducing the expression

$$u_{2,j}(x_1, \frac{-1}{2}, t) = \frac{\partial d_{j-\gamma+3}^-}{\partial t}$$

and

$$u_{2,j}(x_1, \frac{1}{2}, t) = \frac{\partial d_{j-\gamma+3}^+}{\partial t}$$

wich completes the proof.

4.7 Problem Resolution :

Now we consider the following system coupled :

$$\left\{ \begin{array}{l}
 u_{1,j} = \frac{1}{\eta} (D^{-2} (\frac{\partial p_{j-1}}{\partial x_1} - \eta \frac{\partial^2 u_{1,j-2}}{\partial x_1^2} + \rho_f \frac{\partial u_{1,j-2}}{\partial t}) + (-f_1 \delta_{j,0} + \frac{\partial q_j}{\partial x_1}) N_1(\xi_2)), \\
 p_j = D^{-1} (\eta (\frac{\partial^2 u_{2,j-1}}{\partial x_2^2} + \frac{\partial^2 u_{2,j-3}}{\partial x_1^2}) - \rho_f \frac{\partial u_{2,j-3}}{\partial t}), \quad (4.6) \\
 u_{2,j} = -D^{-1} (\frac{1}{\eta} (D^{-2} (\frac{\partial^2 p_{j-1}}{\partial x_1^2} - \eta \frac{\partial^3 u_{1,j-2}}{\partial x_1^3} + \frac{\partial^2 u_{1,j-2}}{\partial x_1 \partial t}))) - \frac{1}{\eta} (\frac{\partial^2 q_j}{\partial x_1^2} - (\frac{\partial f_1}{\partial x_1}) \delta_{j,0}) N_2(\xi_2) + \frac{\partial d_{j-\gamma+3}^-}{\partial t}, \\
 -\frac{1}{\eta} \int_{-1/2}^{1/2} D^{-2} (\frac{\partial^2 p_{j-1}}{\partial x_1^2} - \eta \frac{\partial^3 u_{1,j-2}}{\partial x_1^3} + \frac{\partial^2 u_{1,j-2}}{\partial x_1 \partial t}) d\xi_2 - \frac{1}{12\eta} (\frac{\partial f_1}{\partial x_1} \delta_{j,0} - \frac{\partial^2 q_j}{\partial x_1^2}) = \frac{\partial d_{j-\gamma-3}^+}{\partial t} - \frac{\partial d_{j-\gamma-3}^-}{\partial t}, \\
 \frac{\partial^4 d_j^+}{\partial x_1^4} + \nu \frac{\partial^5 d_{j-\gamma}^+}{\partial x_1^4 \partial t} + \frac{\partial^2 d_{j-\gamma}^+}{\partial t^2} = g^+ \delta_{j,0} + q_j + p_{j-1} |_{\xi_2=1/2}, \\
 \kappa \frac{\partial^4 d_j^-}{\partial x_1^4} + \nu \frac{\partial^5 d_{j-\gamma}^-}{\partial x_1^4 \partial t} + \frac{\partial^2 d_{j-\gamma}^-}{\partial t^2} = g^- \delta_{j,0} + q_j + p_{j-1} |_{\xi_2=-1/2}, \\
 \langle d_j^+ \rangle (t) = 0, \quad \langle d_j^- \rangle (t) = 0, \\
 \langle q_j \rangle (t) + \langle p_{j-1}, \xi_2 = 1/2 \rangle = 0, \\
 \langle q_j \rangle (t) + \langle p_{j-1}, \xi_2 = -1/2 \rangle = 0,
 \end{array} \right.$$

Remark :

The order of solving that system will be different, and depending on γ .

In the sequel we shall consider three different cases with respect to γ . In each case we shall solve the system (4.6) and we shall analyze the leading terms.

4.7.1 Proposition :

In the case $\gamma > 3$, the asymptotic solution of (4.6) is given by :

$$\begin{cases} u_1(x_1, x_2, t) = \frac{-\varepsilon^2}{\eta} \langle f_1 \rangle (t) N_1\left(\frac{x_2}{\varepsilon}\right) + O(\varepsilon^3), \\ u_2(x_1, x_2, t) = O(\varepsilon^4), \\ p(x_1, x_2, t) = \int_0^{x_1} \widehat{f}(s, t) ds - \langle \int_0^{x_1} \widehat{f}(s, t) ds \rangle + O(\varepsilon), \\ d^+(x_1, t) = \varepsilon^\gamma d_0^+ + O(\varepsilon^{\gamma+1}), \\ d^-(x_1, t) = \varepsilon^\gamma d_0^- + O(\varepsilon^{\gamma+1}), \end{cases} \quad (4.7)$$

Where $\widehat{f} = f_1(s, t) - \langle f_1 \rangle (t)$ and d_0^\pm are obtained as the unique solution of (4.6)_{5,6}

Proof :

The proof of this proposition is obtained by giving a $j = 0$ in the previous term. Indeed, for $j = 0$ the first term of the previous equation becomes

$$\frac{\partial^2 q_0}{\partial x_1^2} = \frac{\partial f_1}{\partial x_1}$$

The solution of this equation is of the form :

$$q_0(x_1, t) = \int_0^{x_1} \widehat{f}(s, t) ds - \langle \int_0^{x_1} \widehat{f}(s, t) ds \rangle$$

Indeed, integrating the equation

$$\frac{\partial^2 q_0}{\partial x_1^2} = \frac{\partial f_1}{\partial x_1}$$

between 0 and x_1 yields :

$$\frac{\partial q_0(x_1, t)}{\partial x_1} - \frac{\partial q_0(0, t)}{\partial x_1}(0, t) = f_1(x_1, t) - f_1(0, t)$$

Integrating the second equation between 0 and x_1 yields :

$$\begin{aligned} \int_0^{x_1} \frac{\partial q_0(s, t)}{\partial s} ds - \int_0^{x_1} \frac{\partial q_0(0, t)}{\partial s} ds &= \int_0^{x_1} f_1(s, t) - x_1 f_1(0, t) \\ q_0(x_1, t) - q_0(0, t) - x_1 \frac{\partial q_0}{\partial s} &= \int_0^{x_1} f_1(s, t) ds - x_1 f_1(0, t) \end{aligned} \quad (4.8)$$

We takes $x_1 = 1$ in the previous equation we get :

$$q_0(1, t) - q_0(0, t) - \frac{\partial q_0}{\partial x_1}(0, t) = \int_0^1 f_1(s, t) ds - f_1(0, t)$$

As $q_0(1, t) - q_0(0, t) = 0$ and $\int_0^1 f_1(s, t) ds = \langle f_1 \rangle (t)$ we get :

$$\frac{\partial q_0}{\partial x_1}(0, t) = f_1(0, t) - \langle f_1 \rangle (t)$$

By replacing the previous expression in (4.8) we obtain :

$$q_0(x_1, t) - q_0(0, t) + x_1 \langle f_1 \rangle (t) = \int_0^{x_1} f_1(s, t) ds \quad (4.9)$$

Integrating (4.9) between 0 and 1 we get :

$$\begin{aligned} \int_0^1 q_0(x_1, t) - q_0(0, t) + \frac{1}{2} \langle f_1 \rangle (t) &= \int_0^1 \left(\int_0^\tau f_1(s, t) ds \right) d\tau \\ q_0(0, t) &= \frac{1}{2} \langle f_1 \rangle (t) - \int_0^1 \left(\int_0^\tau f_1(s, t) ds \right) d\tau \\ q_0(x_1, t) - \frac{1}{2} \langle f_1 \rangle (t) + \int_0^1 \left(\int_0^\tau f_1(s, t) ds \right) d\tau + x_1 \langle f_1 \rangle (t) &= \int_0^{x_1} f_1(s, t) ds \end{aligned}$$

So :

$$q_0(x_1, t) = - \langle f_1 \rangle (t) \left(x_1 - \frac{1}{2} \right) - \int_0^1 \left(\int_0^\tau f_1(s, t) ds \right) d\tau + \int_0^{x_1} f_1(s, t) ds$$

On the other hand we have :

$$\begin{aligned} q_0(x_1, t) &= \int_0^{x_1} \widehat{f}_1(s, t) ds - \left\langle \int_0^{x_1} \widehat{f}_1(s, t) ds \right\rangle \\ &= \int_0^{x_1} f_1(s, t) ds - \int_0^{x_1} \langle f_1 \rangle (t) ds - \int_0^1 \left(\int_0^{x_1} f_1(s, t) \right) ds - \int_0^{x_1} \langle f_1 \rangle (t) ds dx_1 \\ &= \int_0^{x_1} f_1(s, t) ds - x_1 \langle f_1 \rangle (t) - \int_0^1 \left(\int_0^\tau f_1(s, t) ds \right) d\tau + \frac{1}{2} \langle f_1 \rangle (t) \end{aligned}$$

In the sequel introducing the expression of $q_0(x_1, t)$ in the expression of $u_{1,0}$ and $u_{2,0}$ yields the following result :

$$\begin{cases} u_{1,0}(x_1, \xi_2, t) = \frac{-1}{\eta} \langle f_1 \rangle (t) N_1(\xi_2), \\ u_{2,0}(x_1, \xi_2, t) = 0, \end{cases}$$

Similarly for $j = 0$ we obtain that $p_0(x_1, \xi_2, t) = 0$ which completes the proof.

4.7.2 Proposition :

In the case $\gamma < 3$, the asymptotic solution of (4.6) is given by :

$$\left\{ \begin{array}{l} u_1(x_1, x_2, t) = \frac{-\varepsilon^2}{\eta} \left(\frac{1}{2} \left(\frac{\partial g^+}{\partial x_1} + \frac{\partial g^-}{\partial x_1} \right) + f_1 \right) N_1 \left(\frac{x_2}{\varepsilon} \right) + O(\varepsilon^3), \\ u_2(x_1, x_2, t) = \frac{\varepsilon^3}{\eta} \left(\frac{1}{2} \left(\frac{\partial^2 g^+}{\partial x_1^2} + \frac{\partial^2 g^-}{\partial x_1^2} \right) + \frac{\partial f_1}{\partial x_1} \right) N_2 \left(\frac{x_2}{\varepsilon} \right) + O(\varepsilon^4), \\ p(x_1, x_2, t) = \frac{-1}{2} (g^+(x_1, t) + g^-(x_1, t)) + O(\varepsilon), \\ (d^+ - d^-)(x_1, t) = -\varepsilon^3 \frac{1}{12\eta} \int_0^t \left(\frac{1}{2} \left(\frac{\partial^2 g^+}{\partial x_1^2} + \frac{\partial^2 g^-}{\partial x_1^2} \right) + \frac{\partial f_1}{\partial x_1} \right) (x_1, s) ds + O(\varepsilon^4), \end{array} \right. \quad (4.10)$$

Proof :

We take $j = \gamma - 3$ in our problem :

Since the term $\gamma - 3 < 0$ then the left side of (4.6)₄ is zero because each index term is negative and a term of negative index is assumed to be zero, we obtain

$$\frac{\partial d_0^+}{\partial t} - \frac{\partial d_0^-}{\partial t} = 0$$

So :

$$d_0^+ - d_0^- = (d_0^+ - d_0^-)(x_1)$$

with the initial conditions are :

$$d_0^+(x_1, 0) = d_0^-(x_1, 0) = 0$$

Then we take $j = 0$ in the second equation d^+, d^- our problem we obtain $g^+ + q_0 = 0$ and $g^- + q_0 = 0$ yields :

$$q_0 = \frac{-1}{2} (g^+ + g^-)$$

Introducing this result in expressions $u_{1,0}$ and $u_{2,0}$ This gives us the desired result for u_1 and u_2 .

For p we have $p_0 = 0$.

For the displacement, the first approximation nonzero is $d_{3-\gamma}$ which is obtained by

equation (4.6)₄ with the value of $j = 0$.

$$\frac{-1}{12\eta} \left(\frac{\partial f_1}{\partial x_1} + \frac{1}{2} \left(\frac{\partial^2 g^+}{\partial x_1^2} + \frac{\partial^2 g^-}{\partial x_1^2} \right) \right) = \frac{\partial d_{3-\gamma}^+}{\partial t} - \frac{\partial d_{3-\gamma}^-}{\partial t}$$

By integrating with respect to t yields :

$$(d_{3-\gamma}^+ - d_{3-\gamma}^-)(x_1, t) = -\frac{\varepsilon^3}{12\eta} \int_0^t \left(\frac{1}{2} \left(\frac{\partial^2 g^+}{\partial x_1^2} + \frac{\partial^2 g^-}{\partial x_1^2} \right) + \frac{\partial f_1}{\partial x_1} \right) (x_1, s) ds$$

wich completes the proof.

4.7.3 Proposition :

For the case $\gamma = 3$ the system (4.6)_{4,5,6} is equivalent to the parabolic equation of the sixth order in the space variable :

$$\left\{ \begin{array}{l} \frac{\partial d_j^+}{\partial t} - \frac{\partial d_j^-}{\partial t} - \frac{1}{24\eta} \left(\frac{\partial^6 d_j^+}{\partial x_1^6} + \kappa \frac{\partial^6 d_j^-}{\partial x_1^6} \right) = \frac{-1}{12\eta} \left(\frac{1}{2} \left(\frac{\partial^2 g^+}{\partial x_1^2} + \frac{\partial^2 g^-}{\partial x_1^2} \right) + \frac{\partial f_1}{\partial x_1} \right) \delta_{j0} + \\ + \frac{\nu}{24\eta} \left(\frac{\partial^7 d_{j-3}^+}{\partial x_1^6 \partial t} + \frac{\partial^7 d_{j-3}^-}{\partial x_1^6 \partial t} \right) + \frac{1}{24\eta} \left(\frac{\partial^4 d_{j-3}^+}{\partial x_1^2 \partial t^2} + \frac{\partial^4 d_{j-3}^-}{\partial x_1^2 \partial t^2} \right) + \\ - \frac{1}{24\eta} \left(\frac{\partial^2 p_{j-1}}{\partial x_1^2} \Big|_{\xi_2 = \frac{1}{2}} + \frac{\partial^2 p_{j-1}}{\partial x_1^2} \Big|_{\xi_2 = -\frac{1}{2}} \right) - \frac{1}{\eta} \int_{-\frac{1}{2}}^{\frac{1}{2}} D^{-2} \left(\frac{\partial^2 p_{j-1}}{\partial x_1^2} - \eta \frac{\partial^3 u_{1,j-2}}{\partial x_1^3} + \frac{\partial^2 u_{1,j-2}}{\partial x_1 \partial t} \right) d\xi_2 \end{array} \right. \quad (4.11)$$

With the initial condition $d_j^\pm(x_1, 0) = 0$. Moreover the asymptotic solution in this case of our problem is given by :

$$\left\{ \begin{array}{l} u_1(x_1, x_2, t) = \varepsilon^2 \frac{1}{\eta} \left(\frac{\partial q_0}{\partial x_1} - f_1 \right) N_1 \left(\frac{x_2}{\varepsilon} \right) + O(\varepsilon^3), \\ u_2(x_1, x_2, t) = -\varepsilon^3 \frac{1}{\eta} \left(\frac{\partial^2 q_0}{\partial x_1^2} - \frac{\partial f_1}{\partial x_1} \right) N_2 \left(\frac{x_2}{\varepsilon} \right) + O(\varepsilon^4), \\ p(x_1, x_2, t) = q_0(x_1, t) + O(\varepsilon), \\ d^+(x_1, t) = \varepsilon^3 d_0^+(x_1, t) + O(\varepsilon^4), \\ d^-(x_1, t) = \varepsilon^3 d_0^-(x_1, t) + O(\varepsilon^4), \end{array} \right. \quad (4.12)$$

with d_0^\pm the solution of the following system partial differential equation,

$$\begin{cases} \frac{\partial d_0^+}{\partial t} - \frac{\partial d_0^-}{\partial t} - \frac{1}{12\eta} \frac{\partial^6 d_0^+}{\partial x_1^6} = \frac{-1}{12\eta} \left(\frac{\partial^2 g^+}{\partial x_1^2} + \frac{\partial f_1}{\partial x_1} \right) \\ \frac{\partial d_0^+}{\partial t} - \frac{\partial d_0^-}{\partial t} - \frac{\kappa}{12\eta} \frac{\partial^6 d_0^-}{\partial x_1^6} = \frac{-1}{12\eta} \left(\frac{\partial^2 g^-}{\partial x_1^2} + \frac{\partial f_1}{\partial x_1} \right) \end{cases}$$

Proof :

The first assertion of the theorem is obtained as :

we differentiate twice with respect to x (4.6)_{5,6} and multiplying with $\frac{-1}{24\eta}$ and adding the new equations of (4.6)_{4,5,6} we obtain (4.11).

Finally, (4.12) is obtained by taking $j = 0$ in (4.6)_{1,2,3}, we obtain :

$$\begin{aligned} u_{1,0} &= \frac{1}{\eta} \left(\frac{\partial q_0}{\partial x_1} - f_1 \right) N_1(\xi_2) \\ u_{2,0} &= \frac{-1}{\eta} \left(\frac{\partial^2 q_0}{\partial x_1^2} - \frac{\partial f_1}{\partial x_1} \right) N_2(\xi_2) \\ p_0 &= 0 \end{aligned}$$

By introducing these relations in the asymptotic expression of u_1 , u_2 and p we obtain the result.

4.8 A priori Estimates :

We still consider our problem :

$$\begin{cases} \rho_f \frac{\partial u}{\partial t} - \eta \Delta u + \nabla p = f \text{ in } D_\varepsilon \times (0, T), \\ \operatorname{div}(u) = 0 \text{ sur } D_\varepsilon \times (0, T), \\ u_1 = 0 \quad u_2 = \frac{\partial d^+}{\partial t} \text{ sur } \Gamma_\varepsilon \times (0, T), \\ u_1 = 0 \quad u_2 = \frac{\partial d^-}{\partial t} \text{ sur } \Gamma_{-\varepsilon} \times (0, T), \\ u(x, 0) = 0 \text{ in } D_\varepsilon, \\ \frac{\partial^2 d^+}{\partial t^2} + \frac{1}{\delta} \frac{\partial^4 d^+}{\partial x_1^4} + \nu \frac{\partial^5 d^+}{\partial x_1^4 \partial t} = g^+ + p \text{ on } \Gamma_\varepsilon^+ \times (0, T), \\ \frac{\partial^2 d^-}{\partial t^2} + \frac{\kappa}{\delta} \frac{\partial^4 d^-}{\partial x_1^4} + \nu \frac{\partial^5 d^-}{\partial x_1^4 \partial t} = g^- + p \text{ on } \Gamma_\varepsilon^- \times (0, T), \\ d^\pm(0, t) = d^\pm(1, t) = \frac{\partial d^\pm}{\partial x_1}(0, t) = \frac{\partial d^\pm}{\partial x_1}(1, t) = 0, \text{ in } (0, T) \\ d^\pm(x_1, 0) = \frac{\partial d^\pm}{\partial t}(x_1, 0) = 0 \text{ dans } (0, 1) \end{cases} \quad (4.13)$$

Let (u_i, d_i^\pm) two solution of the problem(4.13) corresponding to the data f_i, g_i $i = 1, 2$. We denote in general, $a = a_1 - a_2$. The coupled system (4.13) being linear, by subtracting the problems for $i = 1$ and $i = 2$ we obtain for the difference (u, p, d^\pm) exactly the same system (4.13). Multiplying (4.13)₁ by $u(t)$ and integrating on D_ε , we get :

$$\begin{aligned} \frac{1}{2} \frac{d}{dt} \int_{D_\varepsilon} u^2(t) dx + \eta \int_{D_\varepsilon} (\nabla u)^2(t) dx + \int_0^1 p|_{x_2=\varepsilon/2}(t) \frac{\partial d^+}{\partial t}(t) dx_1 \\ + \int_0^1 p|_{x_2=-\varepsilon/2}(t) \frac{\partial d^-}{\partial t}(t) dx_1 = \int_{D_\varepsilon} f(t) \cdot u(t) dx \end{aligned}$$

Multiplying (4.13)₆ by $\frac{\partial d^+}{\partial t}(t)$ and Multiplying (4.13)₇ by $\frac{\partial d^-}{\partial t}(t)$ it follows :

$$\left\{ \begin{aligned} & \frac{1}{2} \int_0^1 \frac{\partial}{\partial t} \left(\left(\frac{\partial d^+}{\partial t} \right)^2 \right) dx_1 + \frac{1}{\delta} \int_0^1 \frac{\partial^2 d^+}{\partial x_1^2}(t) \frac{\partial}{\partial t} \left(\frac{\partial d^+}{\partial x_1^2} \right) dx_1 \\ & + \nu \int_0^1 \left(\frac{\partial^3 d^+}{\partial x_1^2 \partial t} (t) \right)^2 dx_1 - \int_0^1 p|_{x_2=\varepsilon/2}(t) \frac{\partial d^+}{\partial t}(t) dx_1 = \int_0^1 g^+(t) \frac{\partial d^+}{\partial t}(t) dx_1, \\ & \frac{1}{2} \int_0^1 \frac{\partial}{\partial t} \left(\left(\frac{\partial d^-}{\partial t} \right)^2 \right) dx_1 + \frac{\kappa}{\delta} \int_0^1 \frac{\partial^2 d^-}{\partial x_1^2}(t) \frac{\partial}{\partial t} \left(\frac{\partial d^-}{\partial x_1^2} \right) dx_1 \\ & + \nu \int_0^1 \left(\frac{\partial^3 d^-}{\partial x_1^2 \partial t} (t) \right)^2 dx_1 - \int_0^1 p|_{x_2=-\varepsilon/2}(t) \frac{\partial d^-}{\partial t}(t) dx_1 = \int_0^1 g^-(t) \frac{\partial d^-}{\partial t}(t) dx_1, \end{aligned} \right. \quad (4.14)$$

Adding the previous three equalities we get :

$$\left\{ \begin{aligned} & \frac{1}{2} \frac{d}{dt} \int_{D_\varepsilon} u^2(t) dx + \eta \int_{D_\varepsilon} (\nabla u)^2(t) dx + \frac{1}{2} \frac{d}{dt} \int_0^1 \left(\frac{\partial d^+}{\partial t} \right)^2 \\ & + \frac{1}{2\delta} \frac{d}{dt} \int_0^1 \left(\frac{\partial^2 d^+}{\partial x_1^2} \right)^2 + \nu \int_0^1 \left(\frac{\partial^3 d^+}{\partial x_1^2 \partial t} (t) \right)^2 + \frac{1}{2} \frac{d}{dt} \int_0^1 \left(\frac{\partial d^-}{\partial t} \right)^2 + \frac{\kappa}{2\delta} \frac{d}{dt} \int_0^1 \left(\frac{\partial^2 d^-}{\partial x_1^2} \right)^2 \\ & + \nu \int_0^1 \left(\frac{\partial^3 d^-}{\partial x_1^2 \partial t} (t) \right)^2 = \int_{D_\varepsilon} f \cdot u + \int_0^1 g^+ \frac{\partial d^+}{\partial t} + \int_0^1 g^- \frac{\partial d^-}{\partial t} \end{aligned} \right. \quad (4.15)$$

Applying the Cauchy-Schwartz inequality, we obtain :

$$\left\{ \begin{aligned} & \int_{D_\varepsilon} f(t) \cdot u(t) \leq \frac{1}{2} \| u(t) \|_{L^2(D_\varepsilon)}^2 + \frac{1}{2} \| f(t) \|_{L^2(D_\varepsilon)}^2 \\ & \int_0^1 g(t)^\pm \frac{\partial d^\pm}{\partial t}(t) \leq \left(\frac{1}{2} \left\| \frac{\partial d^\pm}{\partial t}(t) \right\|_{L^2(0,1)}^2 \right) + \frac{1}{2} \| g^\pm(t) \|_{L^2(0,1)}^2 \end{aligned} \right. \quad (4.16)$$

Introducing these estimates into (4.15), we get :

$$\left\{ \begin{array}{l} \frac{d}{dt} [e^{-t} (\| u(t) \|_{L^2(D_\varepsilon)}^2 + \| \frac{\partial d^+}{\partial t}(t) \|_{L^2(0,1)}^2 + \| \frac{\partial d^-}{\partial t}(t) \|_{L^2(0,1)}^2 + \frac{1}{\delta} \| \frac{\partial^2 d^+}{\partial x_1^2}(t) \|_{L^2(0,1)}^2 \\ + \frac{\kappa}{\delta} \| \frac{\partial^2 d^-}{\partial x_1^2}(t) \|_{L^2(0,1)}^2)] + 2\eta e^{-T} \| \nabla u \|_{(L^2(D_\varepsilon))^4}^2 + 2\nu e^{-T} \| \frac{\partial^3 d^+}{\partial x_1^2 \partial t} \|_{L^2(0,1)}^2 \\ + 2\nu e^{-T} \| \frac{\partial^3 d^-}{\partial x_1^2 \partial t} \|_{L^2(0,1)}^2 \leq \| f(t) \|_{L^2(D_\varepsilon)}^2 + \| g^+(t) \|_{L^2(0,1)}^2 + \| g^-(t) \|_{L^2(0,1)}^2 . \end{array} \right. \quad (4.17)$$

Integrating this inequality from 0 to t and taking to account the initial conditions we obtain the estimates :

$$\left\{ \begin{array}{l} \| u(t) \|_{L^2(D_\varepsilon)}^2 + \| \frac{\partial d^+}{\partial t}(t) \|_{L^2(0,1)}^2 + \frac{1}{\delta} \| \frac{\partial^2 d^+}{\partial x_1^2}(t) \|_{L^2(0,1)}^2 + \| \frac{\partial d^-}{\partial t}(t) \|_{L^2(0,1)}^2 \\ + \frac{\kappa}{\delta} \| \frac{\partial^2 d^-}{\partial x_1^2}(t) \|_{L^2(0,1)}^2 + 2\eta \int_0^t \| \nabla u(s) \|_{(L^2(D_\varepsilon))^4}^2 ds + 2\nu \int_0^t \| \frac{\partial^3 d^+}{\partial x_1^2 \partial t} \|_{L^2(0,1)}^2 ds \\ + 2\nu \int_0^t \| \frac{\partial^3 d^-}{\partial x_1^2 \partial t} \|_{L^2(0,1)}^2 ds \\ \leq e^{-T} (\int_0^t \| f(s) \|_{L^2(D_\varepsilon)}^2 ds + \int_0^t \| g^+(s) \|_{L^2(0,1)}^2 ds + \int_0^t \| g^-(s) \|_{L^2(0,1)}^2 ds) . \end{array} \right. \quad (4.18)$$

4.8.1 Proposition :

We deduce from the above inequality the following a priori estimates :

$$\left\{ \begin{array}{l}
 \| u_1 - u_2 \|_{L^\infty(0,T;L^2(D_\varepsilon)^2)} \\
 \leq C(T)(\| f_1 - f_2 \|_{L^2(0,T;L^2(D_\varepsilon)^2)} + \| g_1^+ - g_2^+ \|_{L^2((0,1)\times(0,T))} + \| g_1^- - g_2^- \|_{L^2((0,1)\times(0,T))}) \\
 \| \nabla(u_1 - u_2) \|_{L^2(0,T;L^2(D_\varepsilon)^2)} \\
 \leq C(T, \eta)(\| f_1 - f_2 \|_{L^2(0,T;L^2(D_\varepsilon)^2)} + \| g_1^+ - g_2^+ \|_{L^2((0,1)\times(0,T))} + \| g_1^- - g_2^- \|_{L^2((0,1)\times(0,T))}) \\
 \| \frac{\partial(d_1^\pm - d_2^\pm)}{\partial t} \|_{L^\infty(0,T;L^2(0,1))} \\
 \leq C(T)(\| f_1 - f_2 \|_{L^2(0,T;L^2(D_\varepsilon)^2)} + \| g_1^+ - g_2^+ \|_{L^2((0,1)\times(0,T))} + \| g_1^- - g_2^- \|_{L^2((0,1)\times(0,T))}) \\
 \| \frac{\partial^2(d_1^\pm - d_2^\pm)}{\partial x_1^2} \|_{L^\infty(0,T;L^2(0,1))} \\
 \leq \delta^{1/2} C(T)(\| f_1 - f_2 \|_{L^2(0,T;L^2(D_\varepsilon)^2)} + \| g_1^+ - g_2^+ \|_{L^2((0,1)\times(0,T))} + \| g_1^- - g_2^- \|_{L^2((0,1)\times(0,T))}) \\
 \| \frac{\partial^2(d_1^- - d_2^-)}{\partial x_1^2} \|_{L^\infty(0,T;L^2(0,1))} \\
 \leq \frac{\delta^{1/2}}{\kappa^{1/2}} C(T)(\| f_1 - f_2 \|_{L^2(0,T;L^2(D_\varepsilon)^2)} + \| g_1^+ - g_2^+ \|_{L^2((0,1)\times(0,T))} + \| g_1^- - g_2^- \|_{L^2((0,1)\times(0,T))}) \\
 \| \frac{\partial^3(d_1^\pm - d_2^\pm)}{\partial x_1^2 \partial t} \|_{L^2((0,1)\times(0,T))} \\
 \leq C(T, \nu)(\| f_1 - f_2 \|_{L^2(0,T;L^2(D_\varepsilon)^2)} + \| g_1^+ - g_2^+ \|_{L^2((0,1)\times(0,T))} + \| g_1^- - g_2^- \|_{L^2((0,1)\times(0,T))})
 \end{array} \right.$$

4.9 Error estimates : rigorous justification of the asymptotic expansion

The last section deals with the error estimates between the solution exact and the asymptotic solution :

We introduce the following functions :

$$\left\{ \begin{array}{l}
 F_K(x_1, \xi_2, t) = \left(\frac{\partial u_{1,K-1}}{\partial t} - \eta \frac{\partial^2 u_{1,K-1}}{\partial x_1^2} + \frac{\partial p_K}{\partial x_1} \right) e_1 \\
 + \left(\frac{\partial u_{2,K-2}}{\partial t} - \eta \frac{\partial^2 u_{2,K-2}}{\partial x_1^2} - \eta \frac{\partial^2 u_{2,K}}{\partial \xi_2^2} \right) e_2 + \varepsilon \left(\frac{\partial u_{1,K}}{\partial t} - \eta \frac{\partial^2 u_{1,K}}{\partial x_1^2} \right) e_1 \\
 + \left(\frac{\partial u_{2,K-1}}{\partial t} - \eta \frac{\partial^2 u_{2,K-1}}{\partial x_1^2} \right) e_2 + \varepsilon^2 \left(\frac{\partial u_{2,K}}{\partial t} - \eta \frac{\partial^2 u_{2,K}}{\partial x_1^2} \right) e_2
 \end{array} \right.$$

$$G_K^\pm(x_1, t) = \begin{cases} \frac{\partial^2 d_{K+1-\gamma}^\pm}{\partial t^2} + \nu \frac{\partial^5 d_{K+1-\gamma}^\pm}{\partial x_1^4 \partial t} - p_K|_{\xi_2=1/2} + \varepsilon \left(\frac{\partial^2 d_{K+2-\gamma}^\pm}{\partial t^2} + \nu \frac{\partial^5 d_{K+2-\gamma}^\pm}{\partial x_1^4 \partial t} \right) + \\ \dots + \varepsilon^{\gamma-1} \left(\frac{\partial^2 d_K^\pm}{\partial t^2} + \nu \frac{\partial^5 d_K^\pm}{\partial x_1^4 \partial t} \right) \text{ if } \gamma > 3, \\ \frac{\partial^2 d_{K+1-\gamma}^\pm}{\partial t^2} + \nu \frac{\partial^5 d_{K+1-\gamma}^\pm}{\partial x_1^4 \partial t} - p_K|_{\xi_2=1/2} + \varepsilon^{\gamma-1} \left(\frac{\partial^2 d_K}{\partial t^2} + \nu \frac{\partial^5 d_K}{\partial x_1^4 \partial t} \right) \text{ if } \gamma < 3, \\ \frac{\partial^2 d_{K-2}^\pm}{\partial t^2} + \nu \frac{\partial^5 d_{K-2}^\pm}{\partial x_1^4 \partial t} - p_K|_{\xi_2=1/2} + \varepsilon \left(\frac{\partial^2 d_{K-1}^\pm}{\partial t^2} + \nu \frac{\partial^5 d_{K-1}^\pm}{\partial x_1^4 \partial t} \right) \\ + \varepsilon^2 \left(\frac{\partial^2 d_K^\pm}{\partial t^2} + \nu \frac{\partial^5 d_K^\pm}{\partial x_1^4 \partial t} \right) \text{ if } \gamma = 3, \\ A_K^\pm(x_1, t) = \begin{cases} - \left(\frac{\partial d_{K+4-\gamma}^\pm}{\partial t} + \dots + \varepsilon^{\gamma-4} \frac{\partial d_K^\pm}{\partial t} \right) \text{ if } \gamma > 3, \\ (u_{2,K+\gamma-2} + \varepsilon^{2-\gamma} u_{2,K})|_{\xi_2=1/2} \text{ if } \gamma < 3, \\ 0 \text{ if } \gamma = 3, \end{cases} \end{cases}$$

The next theorem gives the error estimates between the exact solution and the asymptotic solution :

4.9.1 Proposition :

Let $(u^{(K)}, p^{(K)}, d^{\pm(K)})$ be the asymptotic solution and (u, p, d) the exact solution. Then the following estimates hold :

$$\left\{ \begin{array}{l}
\| u - u^{(K)} \|_{L^\infty(0,T;(L^2(D_\varepsilon))^2)} = O(\varepsilon^{\min(K+1,K+4-\gamma/2)}), \\
\| \nabla(u - u^{(K)}) \|_{L^2(0,T;(L^2(D_\varepsilon))^4)} = O(\varepsilon^{\min(K+1,K+4-\gamma/2)}), \\
\| \frac{\partial(d^\pm - d^{\pm(K)})}{\partial t} \|_{L^\infty(0,T;(L^2(0,1)))} = O(\varepsilon^{\min(K+1,K+4-\gamma/2)}), \\
\| \frac{\partial^2(d^+ - d^{+(K)})}{\partial x_1^2} \|_{L^\infty(0,T;(L^2(0,1)))} = O(\varepsilon^{\min(K+1+\gamma/2,K+4)}), \quad (4.19) \\
\| \frac{\partial^2(d^- - d^{-(K)})}{\partial x_1^2} \|_{L^\infty(0,T;(L^2(0,1)))} = O(\varepsilon^{\min(K+1,K+4-\gamma/2)}/\kappa), \\
\| \frac{\partial^3(d^\pm - d^{\pm(K)})}{\partial x_1^2 \partial t} \|_{L^2((0,1) \times (0,T))} = O(\varepsilon^{\min(K+1,K+4-\gamma/2)}), \\
\| \nabla(p - p^{(K)}) \|_{L^2(0,T;(H^{-1}(D_\varepsilon))^2)} = O(\varepsilon^{\min(K+2-\gamma/2,K+5-\gamma)}),
\end{array} \right.$$

Proof :

In the sequel we denote $(U^K, P^K, D^K) = (u - u^{(K)}, p - p^{(K)}, d - d^{(K)})$.

Taking into account the previous equations and conditions, we obtain the following

problem for (U^K, P^K, D^K) :

$$\left\{ \begin{array}{l}
\frac{\partial U^K}{\partial t} - \eta \Delta U^K + \nabla P^K = -\varepsilon^{K+1} F_K \text{ in } D_\varepsilon \times (0, T), \\
\operatorname{div}(U^K) = 0 \text{ dans } D_\varepsilon \times (0, T), \\
U^K = \left(\frac{\partial D^{+K}}{\partial t} - \varepsilon^{\min(K+4, K+\gamma+1)} A_K^+ \right) e_2 \text{ on } \Gamma^+ \times (0, T), \\
U^K = \left(\frac{\partial D^{-K}}{\partial t} - \varepsilon^{\min(K+4, K+\gamma+1)} A_K^- \right) e_2 \text{ on } \Gamma^- \times (0, T), \\
U^K, P^K \text{ 1-periodic in } x_1, \\
U^K(x, 0) = 0 \text{ in } D_\varepsilon, \\
\frac{\partial^2 D^{+K}}{\partial t^2} + \frac{1}{\varepsilon^\gamma} \frac{\partial^4 D^{+K}}{\partial x_1^4} + \nu \frac{\partial^5 D^{+K}}{\partial x_1^4 \partial t} = p^K - \varepsilon^{K+1} G_K^+ \text{ on } \Gamma^+ \times (0, T), \\
\frac{\partial^2 D^{-K}}{\partial t^2} + \frac{\kappa}{\varepsilon^\gamma} \frac{\partial^4 D^{-K}}{\partial x_1^4} + \nu \frac{\partial^5 D^{-K}}{\partial x_1^4 \partial t} = p^K - \varepsilon^{K+1} G_K^- \text{ on } \Gamma^- \times (0, T), \\
D_\pm^K \text{ 1-periodic in } x_1, \\
D^{\pm K}(x_1, 0) = \frac{\partial D^K}{\partial t}(x_1, 0) = 0 \text{ in } (0, 1), \\
\langle D^{\pm K} \rangle(t) = 0 \text{ in } (0, T),
\end{array} \right. \quad (4.20)$$

Remark : The error estimates (4.19) will be obtained with the same technique as a priori estimates. In the sequel we obtain the error estimates (4.19) for $\gamma > 3$. The computations for $\gamma < 3$ are similar and for $\gamma = 3$ they follow directly from a priori estimates. For obtaining (4.19)₁₋₅ we compute :

$$\int_{D_\varepsilon} (4.20)_1 \cdot U^K + \int_0^1 (4.20)_7 \left(\frac{\partial D^{+K}}{\partial t} - \varepsilon^{K+4} A_K^+ \right) + \int_0^1 (4.20)_8 \left(\frac{\partial D^{-K}}{\partial t} - \varepsilon^{K+4} A_K^- \right)$$

Taking into account the following equality :

$$\int_{D_\varepsilon} \nabla P^K \cdot U^K = \int_0^1 P^K \left(\frac{\partial D^{+K}}{\partial t} - \varepsilon^{K+4} A_K^+ \right) + \int_0^1 P^K \left(\frac{\partial D^{-K}}{\partial t} - \varepsilon^{K+4} A_K^- \right)$$

It follows that :

$$\left\{ \begin{aligned}
& \frac{d}{dt} \int_{D_\varepsilon} (U^K)^2 + 2\eta \int_{D_\varepsilon} |\nabla U^K|^2 + \frac{d}{dt} \int_0^1 \left(\frac{\partial D^{+K}}{\partial t} \right)^2 + \frac{1}{\varepsilon^\gamma} \frac{d}{dt} \int_0^1 \left(\frac{\partial^2 D^{+K}}{\partial x_1^2} \right)^2 + 2\nu \int_0^1 \left(\frac{\partial^3 D^{+K}}{\partial x_1^2 \partial t} \right)^2 \\
& + \frac{d}{dt} \int_0^1 \left(\frac{\partial D^{-K}}{\partial t} \right)^2 + \frac{\kappa}{\varepsilon^\gamma} \frac{d}{dt} \int_0^1 \left(\frac{\partial^2 D^{-K}}{\partial x_1^2} \right)^2 + 2\nu \int_0^1 \left(\frac{\partial^3 D^{-K}}{\partial x_1^2 \partial t} \right)^2 \\
& = -2\varepsilon^{K+1} \int_{D_\varepsilon} F_K U^K - 2\varepsilon^{K+1} \int_0^1 G_k^+ \frac{\partial D^{+K}}{\partial t} + 2\varepsilon^{K+4} \frac{d}{dt} \int_0^1 \frac{\partial D^{+K}}{\partial t} A_K^+ \\
& - 2\varepsilon^{K+4} \int_0^1 \frac{\partial D^{+K}}{\partial t} \frac{\partial A_K^+}{\partial t} + 2\varepsilon^{K+4-\gamma} \int_0^1 \frac{\partial^2 D^{+K}}{\partial x_1^2} \frac{\partial^2 A_K^+}{\partial x_1^2} + 2\nu \varepsilon^{K+4} \int_0^1 \frac{\partial^3 D^{+K}}{\partial x_1^2 \partial t} \frac{\partial^2 A_K^+}{\partial x_1^2} \\
& + 2\varepsilon^{2K+5} \int_0^1 G_K^+ A_K^+ - 2\varepsilon^{K+1} \int_0^1 G_k^- \frac{\partial D^{-K}}{\partial t} + 2\varepsilon^{K+4} \frac{d}{dt} \int_0^1 \frac{\partial D^{-K}}{\partial t} A_K^- \\
& - 2\varepsilon^{K+4} \int_0^1 \frac{\partial D^{-K}}{\partial t} \frac{\partial A_K^-}{\partial t} + 2\kappa \varepsilon^{K+4-\gamma} \int_0^1 \frac{\partial^2 D^{-K}}{\partial x_1^2} \frac{\partial^2 A_K^-}{\partial x_1^2} + 2\nu \varepsilon^{K+4} \int_0^1 \frac{\partial^3 D^{-K}}{\partial x_1^2 \partial t} \frac{\partial^2 A_K^-}{\partial x_1^2} \\
& + 2\varepsilon^{2K+5} \int_0^1 G_K^- A_K^-
\end{aligned} \right.$$

Majorating each term of the right hand side of the above equality with standard techniques :

$$2ab \leq a^2 + b^2$$

we get :

$$\left\{ \begin{aligned}
& \frac{d}{dt} \int_{D_\varepsilon} (U^k)^2 - \int_{D_\varepsilon} (U^k)^2 + 2\eta \int_{D_\varepsilon} |\nabla U^k|^2 + \left(\frac{d}{dt} \int_0^1 \left(\frac{\partial D^{+k}}{\partial t} \right)^2 - \int_0^1 \left(\frac{\partial D^{+k}}{\partial t} \right)^2 \right) \\
& + \frac{1}{\varepsilon^\gamma} \left(\frac{d}{dt} \int_0^1 \left(\frac{\partial^2 D^{+k}}{\partial x_1^2} \right)^2 - \int_0^1 \left(\frac{\partial^2 D^{+k}}{\partial x_1^2} \right)^2 \right) + \nu \int_0^1 \left(\frac{\partial^3 D^{+k}}{\partial x_1^2 \partial t} \right)^2 + \left(\frac{d}{dt} \int_0^1 \left(\frac{\partial D^{-k}}{\partial t} \right)^2 - \int_0^1 \left(\frac{\partial D^{-k}}{\partial t} \right)^2 \right) \\
& + \frac{\kappa}{\varepsilon^\gamma} \left(\frac{d}{dt} \int_0^1 \left(\frac{\partial^2 D^{-k}}{\partial x_1^2} \right)^2 - \int_0^1 \left(\frac{\partial^2 D^{-k}}{\partial x_1^2} \right)^2 \right) + \nu \int_0^1 \left(\frac{\partial^3 D^{-k}}{\partial x_1^2 \partial t} \right)^2 \\
& \leq 2\varepsilon^{k+4} \left(\frac{d}{dt} \int_0^1 \frac{\partial D^{+k}}{\partial t} A_k^+ - \int_0^1 \frac{\partial D^{+k}}{\partial t} A_k^+ \right) + 3\varepsilon^{2k+8} \int_0^1 A_k^{+2} + 3\varepsilon^{2k+8} \int_0^1 \left(\frac{\partial A_k^+}{\partial t} \right)^2 \\
& + \varepsilon^{2k+8-\gamma} \int_0^1 \left(\frac{\partial^2 A_k^+}{\partial x_1^2} \right)^2 + \nu \varepsilon^{2k+8} \int_0^1 \left(\frac{\partial^2 A_k^+}{\partial x_1^2} \right)^2 + \varepsilon^{2k+2} \int_0^1 F_k^2 \\
& + 3\varepsilon^{2k+2} \int_0^1 G_k^{+2} + \varepsilon^{2k+5} \int_0^1 G_k^{+2} + \varepsilon^{2k+5} \int_0^1 A_k^{+2} + 2\varepsilon^{k+4} \left(\frac{d}{dt} \int_0^1 \frac{\partial D^{-k}}{\partial t} A_k^- - \int_0^1 \frac{\partial D^{-k}}{\partial t} A_k^- \right) \\
& + 3\varepsilon^{2k+8} \int_0^1 A_k^{-2} + 3\varepsilon^{2k+8} \int_0^1 \left(\frac{\partial A_k^-}{\partial t} \right)^2 + \varepsilon^{2k+8-\gamma} \int_0^1 \left(\frac{\partial^2 A_k^-}{\partial x_1^2} \right)^2 + \nu \varepsilon^{2k+8} \int_0^1 \left(\frac{\partial^2 A_k^-}{\partial x_1^2} \right)^2 \\
& + 3\varepsilon^{2k+2} \int_0^1 G_k^{-2} + \varepsilon^{2k+5} \int_0^1 G_k^{-2} + \varepsilon^{2k+5} \int_0^1 A_k^{-2}
\end{aligned} \right.$$

Multiplying this inequality by e^{-t} , integrating from 0 and t and using the initial conditions, we obtain :

$$\int_0^t e^{-s} \left(\frac{d}{ds} \int_{D_\varepsilon} (U^k)^2 - \int_{D_\varepsilon} (U^k)^2 \right) = e^{-t} \int_{D_\varepsilon} (U^k)^2$$

and :

$$e^{-T} \leq e^{-t}, \quad \forall t \in (0, T)$$

We obtain :

$$\left\{ \begin{array}{l} e^{-t} \int_{D_\varepsilon} (U^k)^2 + 2\eta e^{-T} \int_0^t \int_{D_\varepsilon} |\nabla U^k|^2 + e^{-t} \int_0^1 \left(\frac{\partial D^{+k}}{\partial t}\right)^2 + \frac{e^{-t}}{\varepsilon^\gamma} \int_0^1 \left(\frac{\partial^2 D^{+k}}{\partial x_1^2}\right)^2 \\ + e^{-T} \nu \int_0^t \int_0^1 \left(\frac{\partial^3 D^{+k}}{\partial x_1^2 \partial t}\right)^2 + e^{-t} \int_0^1 \left(\frac{\partial D^{-k}}{\partial t}\right)^2 + \frac{\kappa e^{-t}}{\varepsilon^\gamma} \int_0^1 \left(\frac{\partial^2 D^{-k}}{\partial x_1^2}\right)^2 + e^{-T} \nu \int_0^t \int_0^1 \left(\frac{\partial^3 D^{-k}}{\partial x_1^2 \partial t}\right)^2 \\ \leq 2\varepsilon^{k+4} e^{-t} \int_0^1 \frac{\partial D^k}{\partial t} A_k^+ + 2\varepsilon^{k+4} e^{-t} \int_0^1 \frac{\partial D^{-k}}{\partial t} A_k^- + O(\varepsilon^{\min(2k+2, 2k+8-\gamma)}) \end{array} \right.$$

Then :

$$\left\{ \begin{array}{l} 2\varepsilon^{k+4} e^{-t} \int_0^1 \frac{\partial D^{+k}}{\partial t} A_k^+ = 2(2\varepsilon^{k+4} \frac{e^{-t}}{2} \int_0^1 \frac{\partial D^{+k}}{\partial t} A_k^+) \leq e^{-t} 4\varepsilon^{2k+8} \int_0^1 A_k^{+2} + \frac{e^{-t}}{4} \int_0^1 \left(\frac{\partial D^{+k}}{\partial t}\right)^2 \\ et \\ 2\varepsilon^{k+4} e^{-t} \int_0^1 \frac{\partial D^{-k}}{\partial t} A_k^- = 2(2\varepsilon^{k+4} \frac{e^{-t}}{2} \int_0^1 \frac{\partial D^{-k}}{\partial t} A_k^-) \leq e^{-t} 4\varepsilon^{2k+8} \int_0^1 A_k^{-2} + \frac{e^{-t}}{4} \int_0^1 \left(\frac{\partial D^{-k}}{\partial t}\right)^2 \end{array} \right.$$

Finally we get :

$$\left\{ \begin{array}{l} e^{-t} \int_{D_\varepsilon} (U^k)^2 + 2\eta e^{-T} \int_0^T \int_{D_\varepsilon} |\nabla U^k|^2 + \frac{3}{4} e^{-t} \int_0^1 \left(\frac{\partial D^{+k}}{\partial t}\right)^2 + \frac{e^{-t}}{\varepsilon^\gamma} \int_0^1 \left(\frac{\partial^2 D^{+k}}{\partial x_1^2}\right)^2 \\ + e^{-T} \nu \int_0^t \int_0^1 \left(\frac{\partial^3 D^{+k}}{\partial x_1^2 \partial t}\right)^2 + \frac{3}{4} e^{-t} \int_0^1 \left(\frac{\partial D^{-k}}{\partial t}\right)^2 + \frac{\kappa e^{-t}}{\varepsilon^\gamma} \int_0^1 \left(\frac{\partial^2 D^{-k}}{\partial x_1^2}\right)^2 + e^{-T} \nu \int_0^t \int_0^1 \left(\frac{\partial^3 D^{-k}}{\partial x_1^2 \partial t}\right)^2 \\ \leq 4\varepsilon^{2k+8} e^{-t} \int_0^1 A_k^{+2} + 4\varepsilon^{2k+8} e^{-t} \int_0^1 A_k^{-2} + O(\varepsilon^{\min(2k+2, 2k+8-\gamma)}) \\ \leq O(\varepsilon^{\min(2k+2, 2k+8-\gamma)}) \end{array} \right.$$

Finally we get the proof of the five inequality (4.19)_{1,5}.

To obtain the last estimate (4.19)₆, we repeat the previous computations for

$$\int_{D_\varepsilon} (4.20)_1 \cdot \frac{\partial U^k}{\partial t} + \int_0^1 (4.20)_7 \left(\frac{\partial^2 D^{+K}}{\partial t^2} - \varepsilon^{K+4} \frac{A_K^+}{\partial t} \right)$$

This yields :

$$\left\| \frac{\partial(u - u^{(k)})}{\partial t} \right\|_{L^2(0,T; (L^2(D_\varepsilon))^2)} = O(\varepsilon^{\min(k+1-\frac{\gamma}{2}, k+4-\gamma)})$$

The desired estimate for the pressure is an obvious consequence of (4.20)₁ and of the last equation, which completes the proof.

Chapitre 5

Parallelization of the asymptotic partial decomposition for flows in thin structures

5.1 Introduction

An asymptotic analysis of the Stokes equations and the Navier-Stokes equations set in thin tube structures (some finite unions of thin cylinders with ratio $\varepsilon \ll 1$ of the diameter to the length) has been developed in [2]- [16]-[30]-[31]. It shows that for small Reynolds numbers the flow is approximately a Poiseuille function at some distance of the ends of the cylinders. These Poiseuille functions are glued by some boundary layer type junction functions in the neighborhoods of the ends of the cylinders. This structure of the solution allows to justify for these flows the method of asymptotic partial decomposition of domain (MAPDD) replacing the unknown velocity by the poiseuille functions at the distance δ from the "nodes" (ends points of cylinders). This δ is estimated as $O(\varepsilon|\ln\varepsilon|)$ and so this method reduces considerably the computational cost of the problem. This approach may be applied for such tremendous systems as the blood circulation system. Here we discuss the possibility to parallelise the computations in MAPDD approach. Although the MAPDD is justified rigorously only for the newtonian fluids ; we study its applicability to the non-newtonian fluids developping some

numerical experiments.

5.2 MAPDD for newtonian flows

Consider a newtonian viscous flow in a one bundle tube structure (see [16], p :215) and apply the method of asymptotic partial decomposition of the domain (MAPDD)(see [16], P :364). These methods projects the variational formulation for the fluid motion equation (for example, Navier-Stokes equations (4.5.1) – (4.5.3)) on the so called partially decomposed subspace(PDS)(see [16] $H_{div=0}^0(B^\varepsilon, \delta)$, p.368).

Generally this PDS is the subspace of the initial sobolev space, where the problem is formulated variationally, such that at every cylinder (rectangle) B_j^ε forming the tube structure the functions of this subspace are equal to the poiseuille flow functions between the sections S_{j1}^ε and S_{j2}^ε at the distance δ from the bases of the cylinder B_j^ε (see Chap III 3.1.1) ; δ is taken of order $O(\varepsilon|\ln\varepsilon|)$.

5.2.1 One-bundle tube structure

In the case of one-bundle tube structure with given velocities g_j at the bases β_j^ε of the cylinders B_j^ε (as in [16], p.218), one can calculate the flow rates for every cylinder :

$$D_j = \int_{\beta_j^\varepsilon} g(s) \cdot \vec{n} ds$$

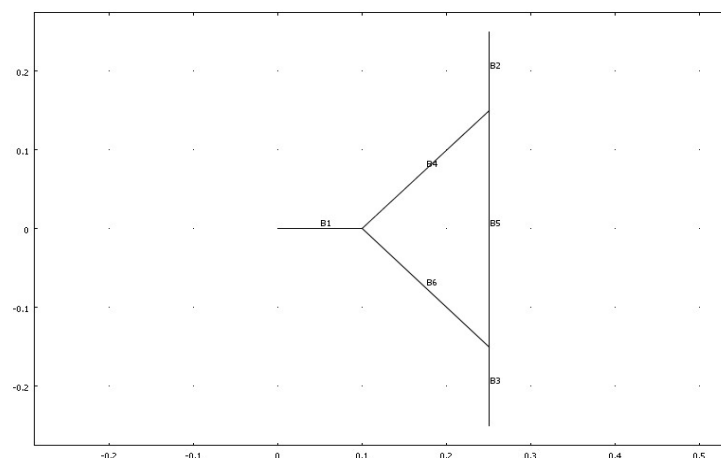
and due to the incompressibility equation, $div u = 0$, we can calculate exactly the poiseuille flow on every cylinder B_j^ε . Consequently, problem projected to the PDS is reduced to $n + 1$ decoupled problems in the truncated parts $B_i^{\varepsilon,\delta}$ of the tube structure with known (and so given) inflows, outflows on every truncated section.

5.2.2 Multi-bundle tube structure

The same result holds in the case when the tube structure is multi-bundle but the flow rates D_j for all cylinders may be calculated from the system

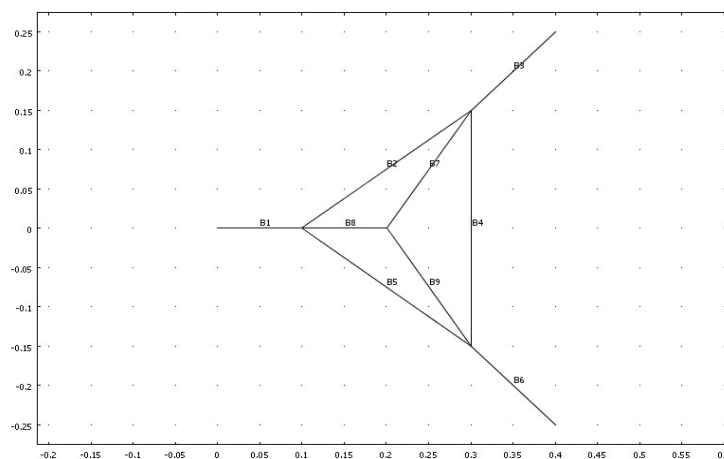
$$\sum_{j:O_i \in \partial_j} D_j = 0, \quad i = 1, \dots, N, \quad (5.1)$$

for all N end points O_i of the structure.



5.2.3 General case

In the general case, when the number of the end points is less than of the segments, as for situation presented in next figure,



the system (5.1) is not sufficient for calculation of all D_j . In this case the partially decomposed problem cannot be completely decoupled. Moreover, the asymptotic analysis shows that the leading term of the asymptotic expansion for the macroscopic pressure is continuous.

Taking into account this continuity, we can formulate the following problem for the

macroscopic pressure :

$$\begin{cases} D'_j = 0 \quad \forall e_j, \\ \sum_{j:O_i \in \bar{e}_j} D_j = 0, \quad i = 1, \dots, N, \\ D_j = k_j \frac{\partial P}{\partial x_1} e_j \quad \forall e_j. \end{cases} \quad (5.2)$$

p is continuous on the graph $B = \bigcup_j e_j$. Here k_j are the permeabilities that are the flow rates of the Poiseuille flows corresponding the unitary pressure drop. For example, in the case of 2D equation, the poiseuille function is :

$$\left(\frac{1}{2} \left(x_2^2 - \left(\frac{\varepsilon \alpha}{2} \right)^2 \right), 0 \right)^T$$

Where x_2 is the transversal component for the rectangle B_j^ε , $\varepsilon \alpha$ is its height (thickness). Then,

$$k_j = \int_{-\frac{\varepsilon \alpha}{2}}^{\frac{\varepsilon \alpha}{2}} \frac{1}{2} \left(x_2^2 - \left(\frac{\varepsilon \alpha}{2} \right)^2 \right) dx_2$$

With $x_2 = \varepsilon \alpha t$, one gets

$$k_j = (\varepsilon \alpha)^3 \int_{-\frac{1}{2}}^{\frac{1}{2}} \frac{1}{2} \left(t^2 - \left(\frac{1}{2} \right)^2 \right) dt = \frac{1}{2} (\varepsilon \alpha)^3 \left(\frac{2}{3} \frac{1}{8} - \frac{1}{4} \right).$$

And then

$$k_j = -\frac{1}{12} (\varepsilon \alpha)^3$$

Solving problem (5.2) for the graph $B = \bigcup_j e_j$ we can find all D_j (with an error of order ε and so to get an approximation of order ε to the partially decomposed problem which is decoupled.

5.3 MAPDD for non-newtonian fluid flows

Let Ω be a domain of R^2 and Γ the boundary of Ω . As, the blood is supposed to be non Newtonian incompressible fluid, we first recall the governing equations for non Newtonian fluid flows. The stationnary, non Newtonian fluid flow is governed by the set of non linear Navier–Stokes equations :

$$\begin{cases} \rho(u \cdot \nabla u) - \operatorname{div} \sigma + \nabla p = 0, \quad \text{in } \Omega, \\ \nabla \cdot u = 0, \quad \text{in } \Omega. \end{cases} \quad (5.3)$$

Where u is the fluid velocity, $\rho = 1[kg/m^3]$ the fluid density, p the pressure and $\sigma = 2\eta(|d(u)|)d(u)$, the extra stress tensor. η being the dynamic viscosity and $d(u) = (\nabla u + \nabla u^t)/2$ the rate strain tensor.

In the present study $\eta(\cdot)$ is defined as in (1.15), by the Carreau law :

$$\eta = \eta_\infty + (\eta_0 - \eta_\infty)[1 + (\lambda\gamma')^2]^{\frac{n-1}{2}}. \quad (5.4)$$

With the following chosen values of parameters :

$$\eta_\infty = 0 [Pa s], \quad \eta_0 = 7 [Pa s], \quad \lambda = 0.11 [s] \text{ and } n = 0.7.$$

For the numerical simulations of (5.3), we have adopted the classical $P2/P1$ Hood–Taylor [35] finite elements combined with triangular finite element mesh. It is well known that this choice of finite elements lead to a stable formulation satisfying the classical Babushka-Brezzi compatibility condition [33]-[34] and consequently produces a numerically stable and adequate solution strategy for Navier-Stokes flows problems. Our aim is to study the applicability of the MAPDD parallelization of computations. As mentioned above, even if the MAPDD is not already established for non Newtonian fluids, to solve non Newtonian fluid flow problems, we will develop a numerical approach based on the MAPDD.

In the case of non Newtonian fluids, the Poiseuille flow should be replaced by a quasi-Poiseuille function, that is : u is a vector valued function with all components equal to zero except for the longitudinal one. This longitudinal component $\widehat{u}_{p,\gamma}$ depends on transversal variables, $\widehat{x}' = (\widehat{x}_2^e, \dots, \widehat{x}_s^e)$, only and satisfies exactly equation (5.3).

With

$$p = \gamma \widehat{x}_1^e$$

Define the flow rate

$$D_j(\gamma) = \int \widehat{u}_{p,\gamma} d\widehat{x}$$

where the integral is taken over the section of the cylinder B_j^ε .

Assume that this $\widehat{u}_{p,\gamma}$ exist for any real γ . Then we can formulate the same algorithms of the parallelization for cases 1, 2, 3 as above, replacing the Poiseuille functions by

quasi-Poiseuille functions the third equation (5.2) should be replaced by

$$D_j = D_j\left(\frac{\partial p}{\partial \hat{x}_1^e}\right)$$

i.e.

$$\gamma = \frac{\partial p}{\partial \hat{x}_1^e}$$

5.4 Numerical simulations

5.4.1 introduction :

In the following section, we have introduced several types of bifurcations with different degrees of difficulty :

First T-type bifurcation easy to study because it has a single component for the velocity along x or along y. Second a bifurcation of type Y, difficult to solve because the velocity at the bifurcation has two components along x and along y. In the third Combining a bifurcation of type T and type Y, we increased the number of bifurcation three and four junctions. Finally we study geometry as a semi triangle and a triangle form.

5.4.2 The complete T-Geometry

We first consider a simple geometry consisting a T-geometry

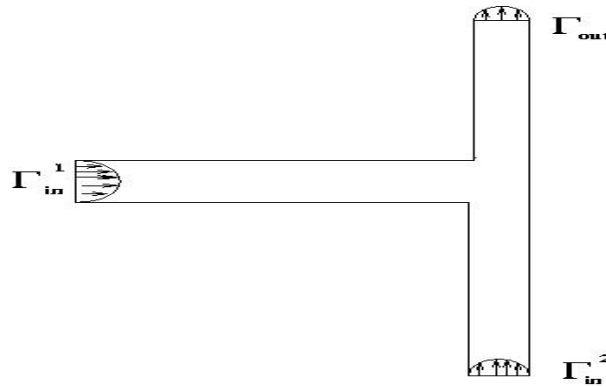


FIGURE 5.1 – T-Geometry

The blood flow enters the vessel from the left side Γ_{in}^1 and the bottom side Γ_{in}^2 with Poiseuille profiles. The amplitude of these parabolic profiles is independent of the time :

$$\Gamma_{in}^1 : \begin{cases} u_0 = 60 * Umax * s * (1 - s), \\ v_0 = 0. \end{cases} \quad \Gamma_{in}^2 : \begin{cases} u_0 = 0, \\ v_0 = 120 * Umax * s * (1 - s). \end{cases}$$

The blood flow exits the vessel from the vertical tube at Γ_{out} , following the parabolic profile :

$$\Gamma_{out} : \begin{cases} u_0 = 0, \\ v_0 = 240 * Umax * s * (1 - s). \end{cases}$$

Where $Umax = 1 [m/s]$ and s is a normalized parameter.

In the present study, the vessel walls are fixed and are not deformed by the blood flow. No-slip boundary conditions are prescribed for the fluid at the vessel walls ($u=v=0$ on $\Gamma_0 = \Gamma - (\Gamma_{in}^1 \cup \Gamma_{in}^2 \cup \Gamma_{out})$). The numerical results are described in the following figures.

- We first give the velocity vector field and the streamlines, see the following figure

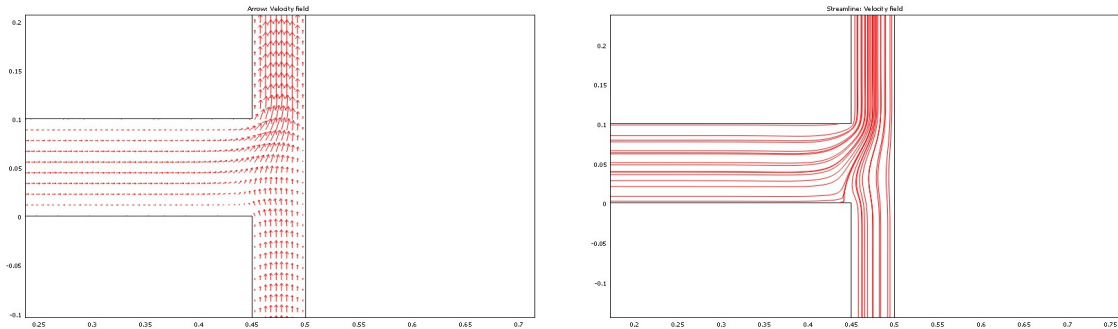


FIGURE 5.2 – Velocity vector field and Streamlines in the T-Geometry

- In the second we give the velocity profiles (x and y components),
- the surfaces and iso–pressures and contour plot (x and y components) are shown in following figure :

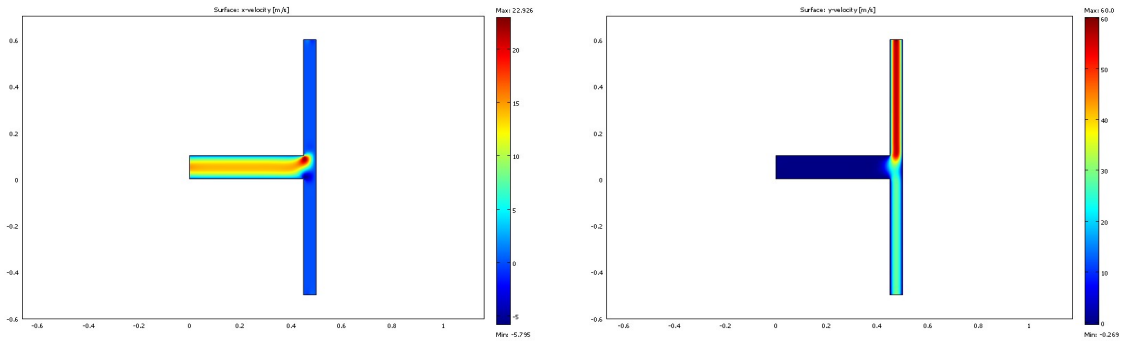


FIGURE 5.3 – The x and y velocity components in the T-Geometry

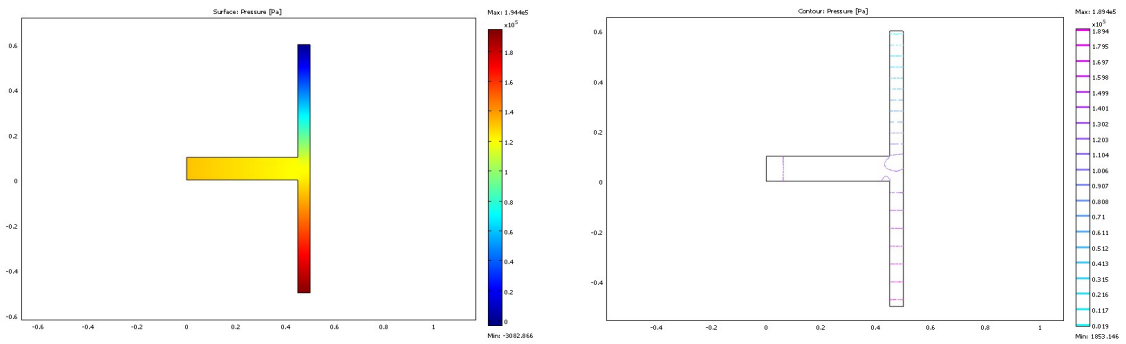


FIGURE 5.4 – Pressure profiles in T-Geometry

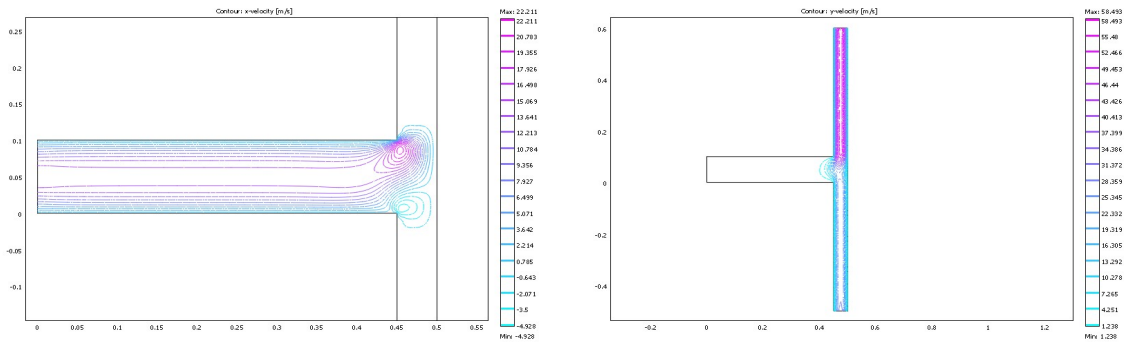


FIGURE 5.5 – Contour x and y velocity components in the T-Geometry

5.4.3 MAPDD for non-Newtonian flow in T-Geometry

The results for the T geometry complete, are consistent with what we expected. It now remains to make these calculations on a reduced geometry, obtained by reducing the size of horizontal and vertical channels according to the following figure

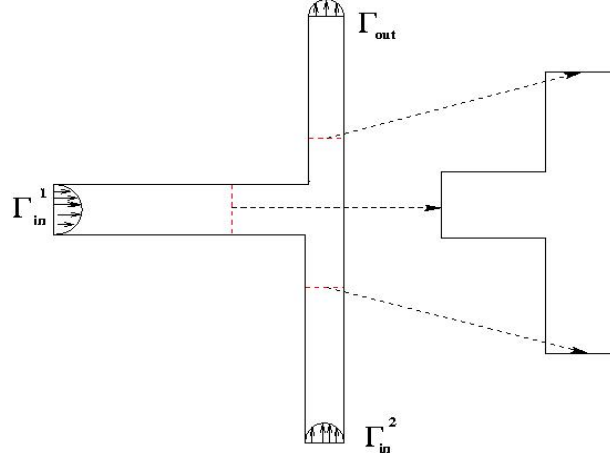


FIGURE 5.6 – domain decomposed in the T-Geometry

Three Poiseuille flow :

To solve the problem with MAPDD in reduced geometry.

A- We solve the three Poiseuille flow, with the same boundary conditions as the T-Geometry. Specifically

$$: \\ \text{Poiseuille 1 : } \Gamma_{in} \text{ and } \Gamma_{out} : \begin{cases} u_0 = 60 * Umax * s * (1 - s), \\ v_0 = 0. \end{cases} \quad \text{and } u = 0, v = 0 \text{ on } \Gamma_0.$$

$$\text{Poiseuille 2 : } \Gamma_{in} \text{ and } \Gamma_{out} : \begin{cases} u_0 = 0, \\ v_0 = 120 * Umax * s * (1 - s). \end{cases} \quad \text{and } u = 0, v = 0 \text{ on } \Gamma_0.$$

$$\text{Poiseuille 3 : } \Gamma_{in} \text{ and } \Gamma_{out} : \begin{cases} u_0 = 0, \\ v_0 = 240 * Umax * s * (1 - s). \end{cases} \quad \text{and } u = 0, v = 0 \text{ on } \Gamma_0.$$

B- The procedure, then we cut the three Poiseuille at the same distance δ of the output for the first and second and the entry for the third (see Figure (5.6)). Cuts

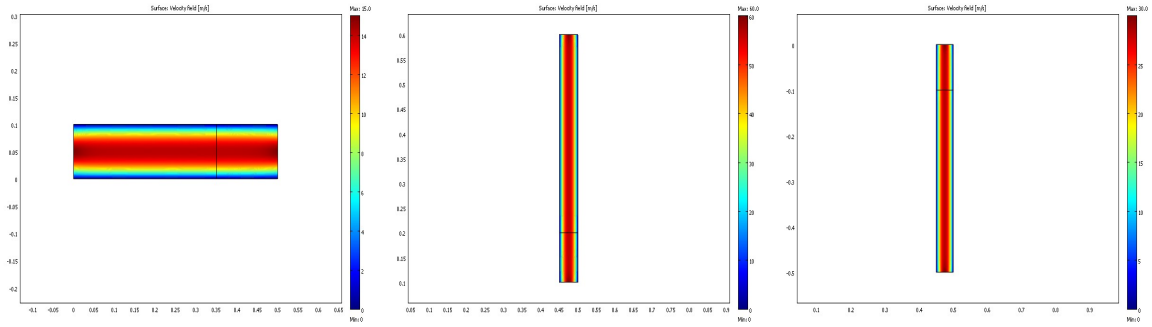


FIGURE 5.7 – Three Poiseuille in the T-Geometry

Results are then taken as boundary conditions at the entrance and exit geometry reduced. For the rest of the border, we set conditions of adherence to the walls solid Γ_0 .

Decomposed domain :

Geometry and its mesh are summarized in the following figure (see Figure(5.8)) :

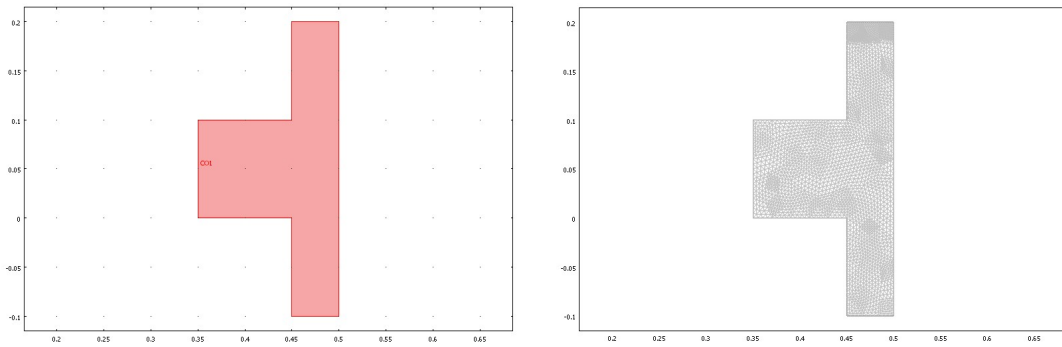


FIGURE 5.8 – The reduced T-Geometry and its mesh

The results obtained are described in the following figures. It starts by showing the components x and y of velocity (Figures (5.9) and (5.10)). It then gives the pressure profiles in Figure (5.11) and then the contour for both velocity components (Figure (5.12)).

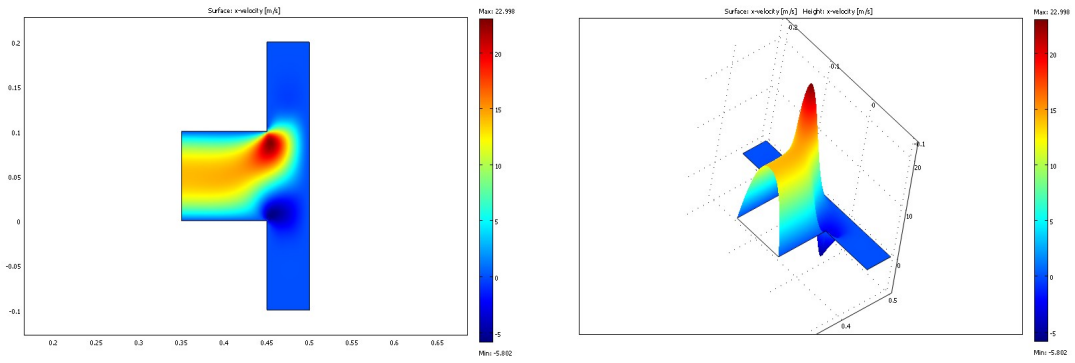


FIGURE 5.9 – surface x-velocity

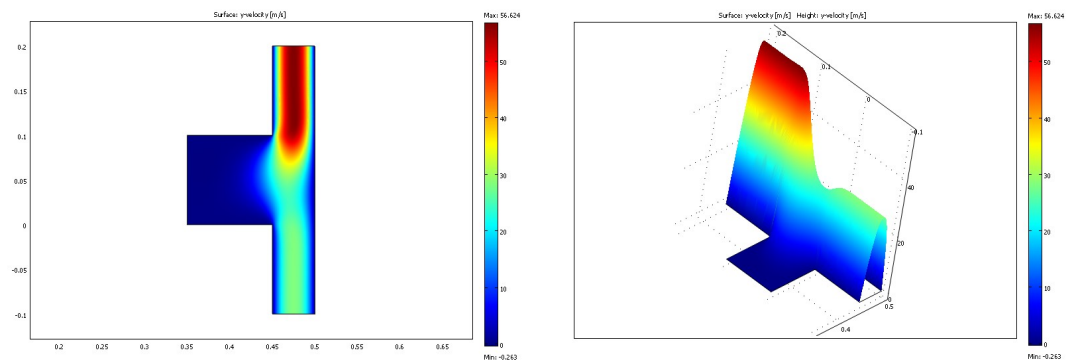


FIGURE 5.10 – surface y-velocity

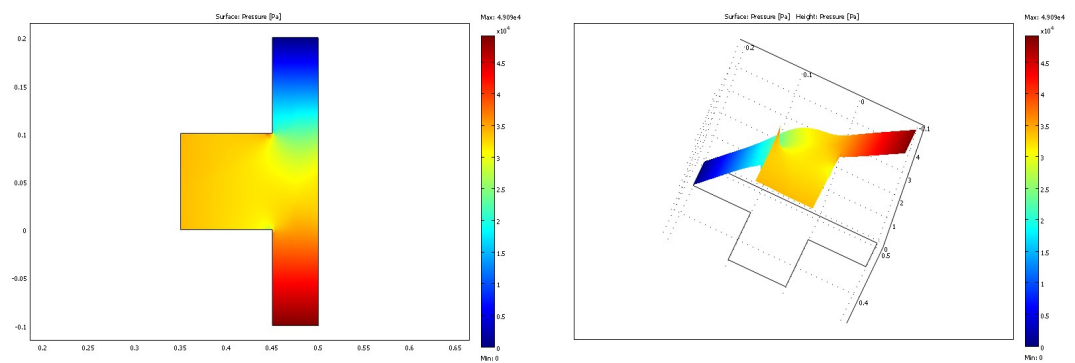


FIGURE 5.11 – surface pressure

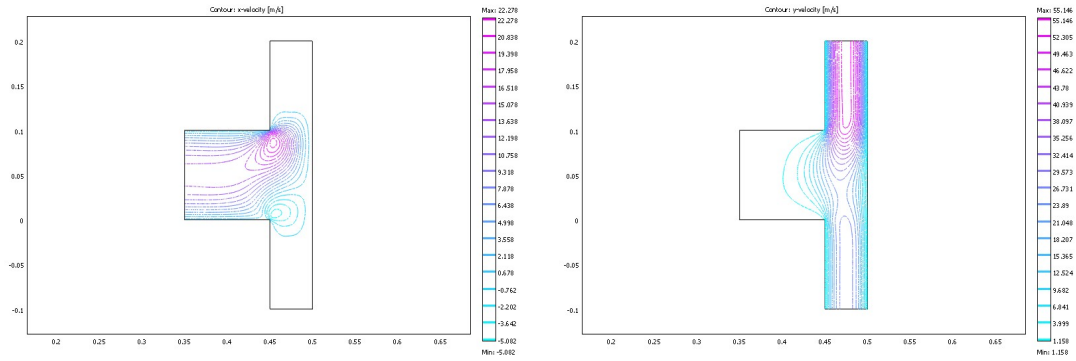


FIGURE 5.12 – Contour x-velocity and y-velocity

Comparison of profiles :

Finally, to finish with this geometry, we propose in the following figures, the comparison between the solutions obtained in the full geometry and reduced geometry. What we find most significant is to compare the velocity profile near the entrance and exit of the bifurcation.

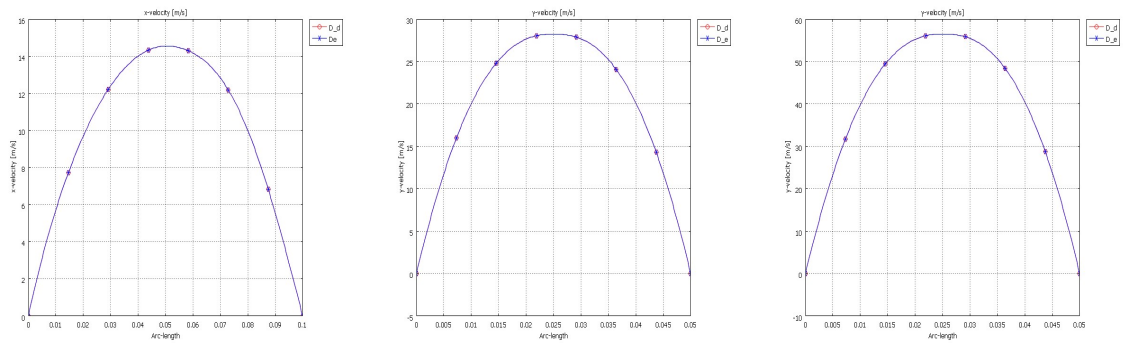


FIGURE 5.13 – Comparison profile of velocity at $x=0.4, y=0.2, y=-0.1$

5.4.4 The complete Y–Geometry

We consider a complicated geometry consisting as Y–geometry :

The blood flow enters the vessel from the left side Γ_{in}^1 with Poiseuille profiles. The

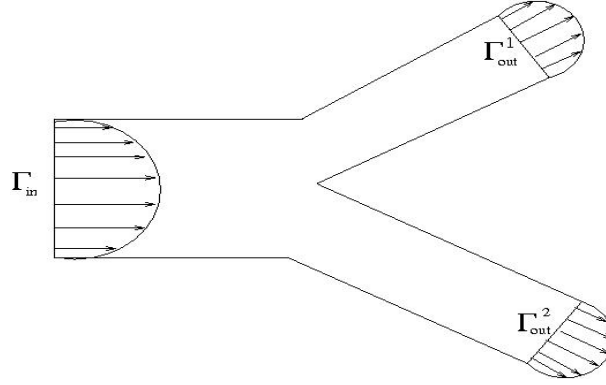


FIGURE 5.14 – Y-Geometry

amplitude of these parabolic profiles is independent of the time :

$$\Gamma_{in} : \begin{cases} u_0 = Umax * s * (1 - s), \\ v_0 = 0. \end{cases}$$

The blood flow exits the vessel from the vertical tube at Γ_{out} , following the parabolic profile :

$$\Gamma_{out}^1 : \begin{cases} u_0 = Umax * s * (1 - s), \\ v_0 = Umax * s * (1 - s). \end{cases} \quad \Gamma_{out}^2 : \begin{cases} u_0 = Umax * s * (1 - s), \\ v_0 = -Umax * s * (1 - s). \end{cases}$$

Where $Umax = 1 [m/s]$ and s is a normalized parameter. In the present study, the vessel walls are fixed and are not deformed by the blood flow. No-slip boundary conditions are prescribed for the fluid at the vessel walls ($u=v=0$ on $\Gamma_0 = \Gamma - (\Gamma_{in} \cup \Gamma_{out}^1 \cup \Gamma_{out}^2)$). The numerical results are described in the following figures :

We first give the velocity vector field and the streamlines, in the second we give the velocity profiles (x and y components), the surfaces and iso–pressures and finally contour plot (x and y components).

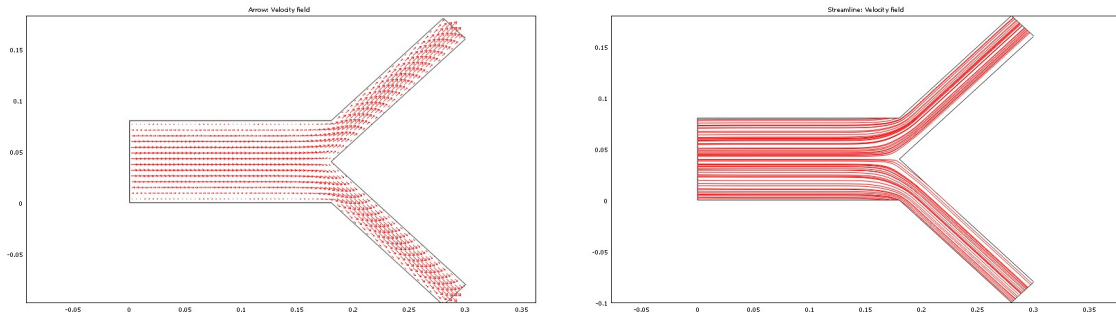


FIGURE 5.15 – Velocity vector field and Streamlines in the Y-Geometry

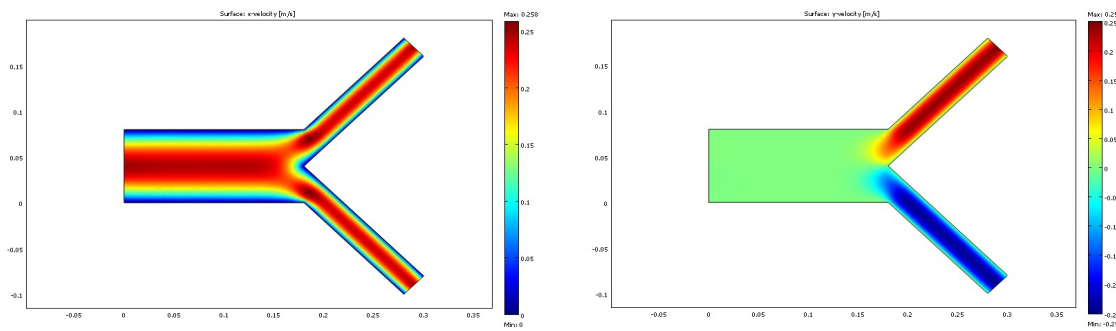


FIGURE 5.16 – The x and y velocity components in the T-Geometry

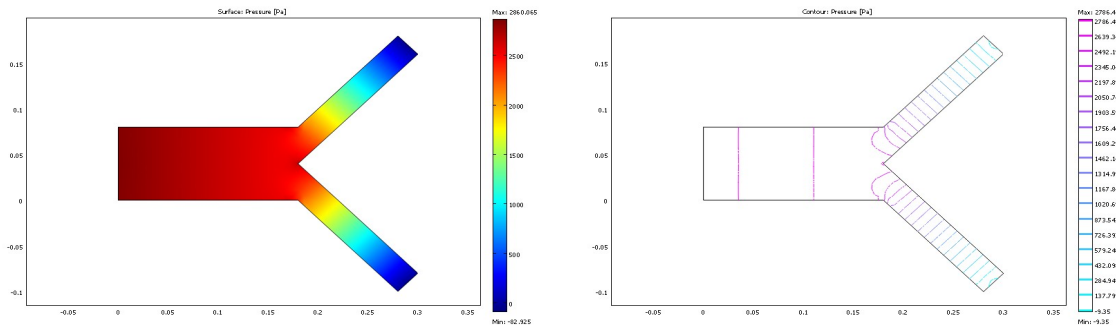


FIGURE 5.17 – Pressure profiles in Y-Geometry

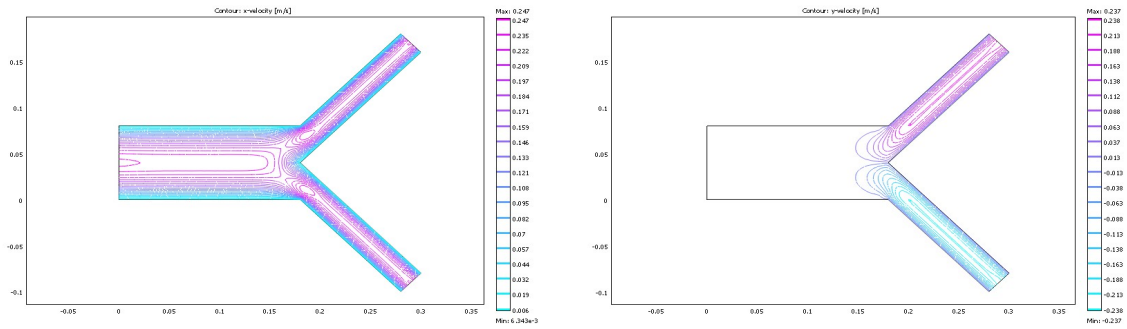


FIGURE 5.18 – Contour x and y velocity components in the Y–Geometry

5.4.5 MAPDD for non-Newtonian flow in Y–Geometry

The results for the Y–geometry complete, are consistent with what we expected. It now remains to make these calculations on a reduced geometry, obtained by reducing the size of horizontal and oblique channels according to the following figure :

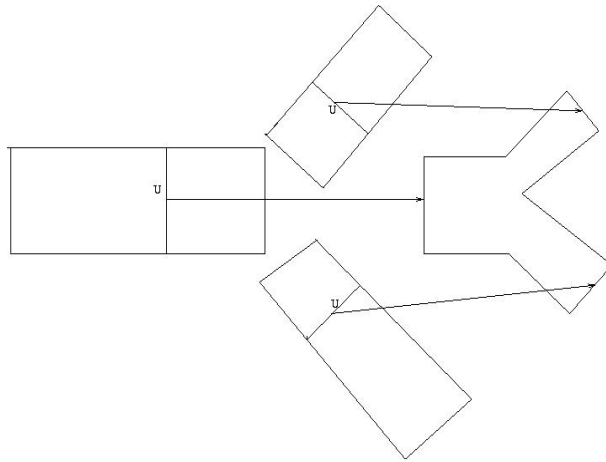


FIGURE 5.19 – Domain decomposed in the Y–Geometry

Three Poiseuille flow :

To solve the problem with MAPDD in reduced geometry :

A– We solve the three Poiseuille flow, with the same boundary conditions as the Y–Geometry. Specifically :

$$\text{Poiseuille 1 : } \Gamma_{in} \text{ and } \Gamma_{out} : \begin{cases} u_0 = Umax * s * (1 - s), \\ v_0 = 0. \end{cases} \quad \text{and } u = 0, v = 0 \text{ on } \Gamma_0.$$

$$\text{Poiseuille 2 : } \Gamma_{in} \text{ and } \Gamma_{out} : \begin{cases} u_0 = Umax * s * (1 - s), \\ v_0 = Umax * s * (1 - s). \end{cases} \quad \text{and } u = 0, v = 0 \text{ on } \Gamma_0.$$

$$\text{Poiseuille 3 : } \Gamma_{in} \text{ and } \Gamma_{out} : \begin{cases} u_0 = Umax * s * (1 - s), \\ v_0 = -Umax * s * (1 - s). \end{cases} \quad \text{and } u = 0, v = 0 \text{ on } \Gamma_0.$$

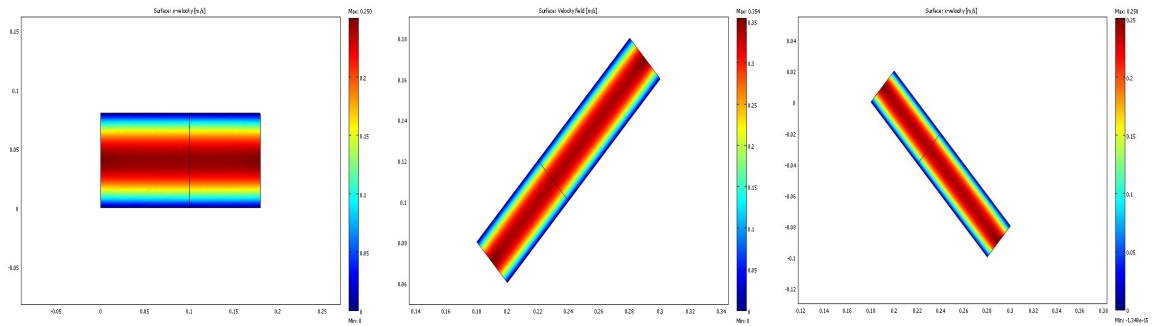


FIGURE 5.20 – Three Poiseuille in the Y–Geometry

B– The procedure, then we cut the three Poiseuille at the same distance δ of the output for the first and the entry for the second and the third (see Figure (5.20)). Cuts Results are then taken as boundary conditions at the entrance and exit geometry reduced. For the rest of the border, we set conditions of adherence to the walls solid Γ_0 .

Decomposed domain :

Geometry and its mesh are summarized in the following figure (see Figure(5.21)) :

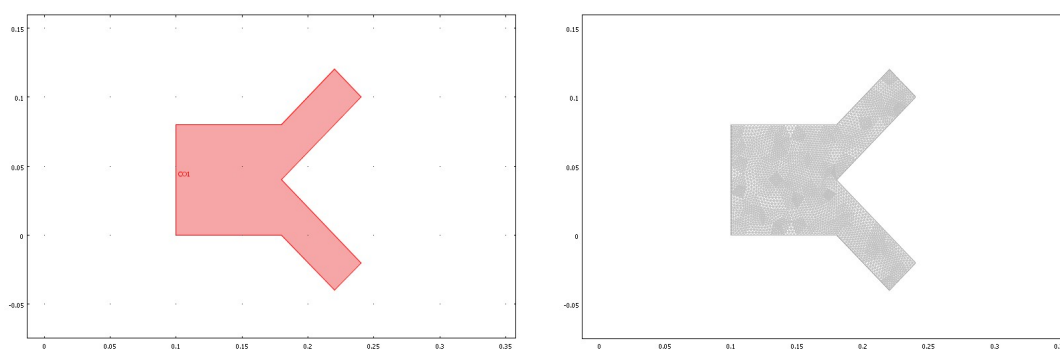


FIGURE 5.21 – The reduced Y–Geometry and its mesh

The results obtained are described in the following figures. It starts by showing the components x and y of velocity (Figures (5.22) and (5.23)). It then gives the pressure profiles in Figure (5.24) and then the contour for both velocity components (Figure (5.25)).

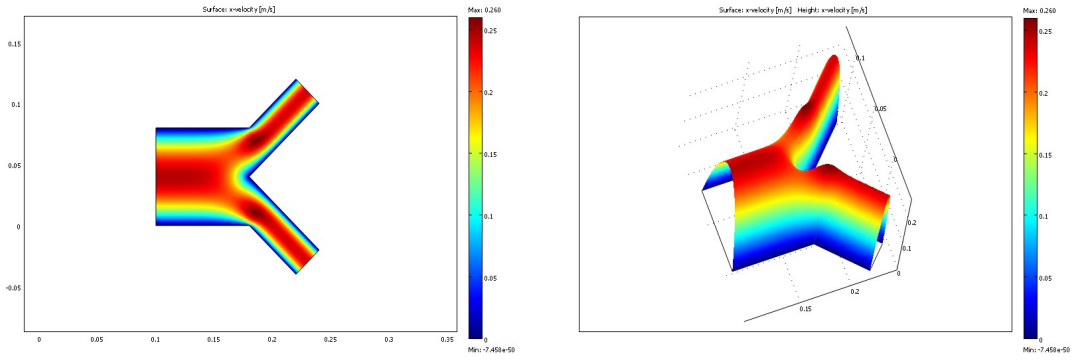


FIGURE 5.22 – Surface x-velocity

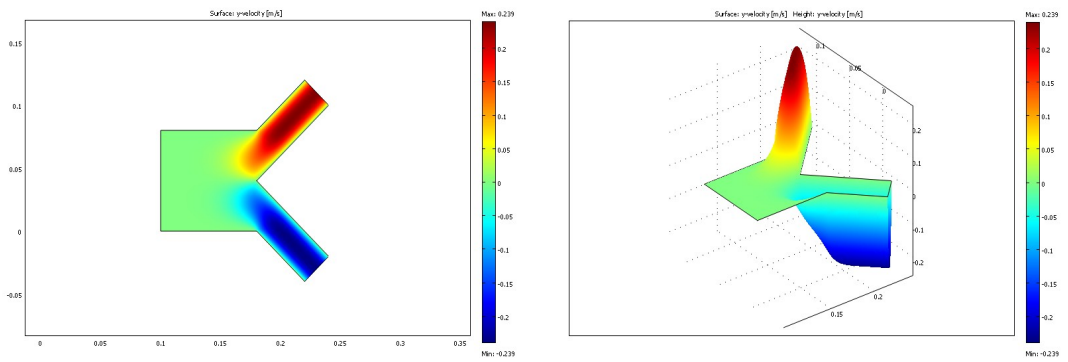


FIGURE 5.23 – Surface y-velocity

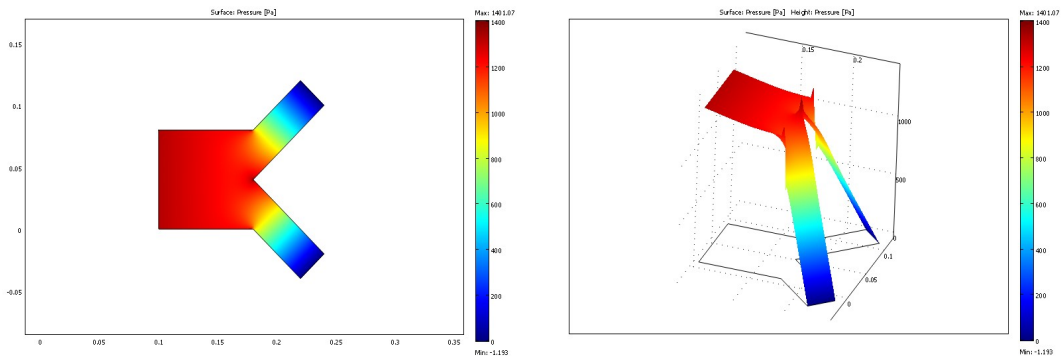


FIGURE 5.24 – Surface pressure

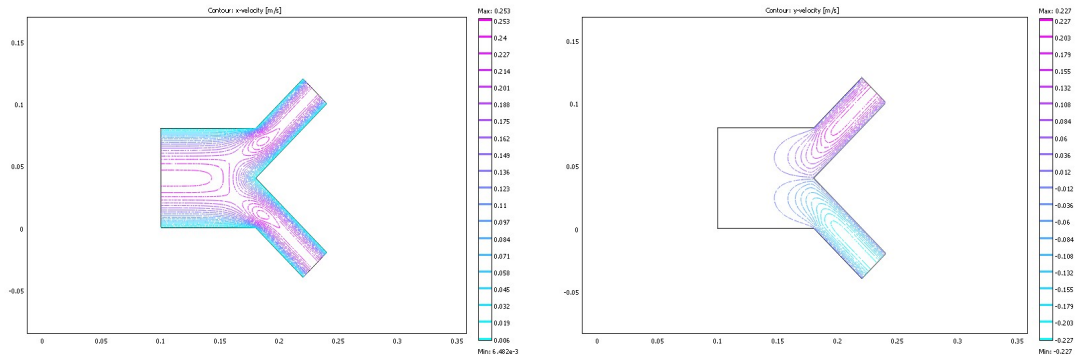


FIGURE 5.25 – Contour x-velocity and y-velocity

Comparison of profiles :

Finally, to finish with this geometry, we propose in the following figures, the comparison between the solutions obtained in the full geometry and reduced geometry. What we find most significant is to compare the velocity profile near the entrance and exit of the bifurcation.

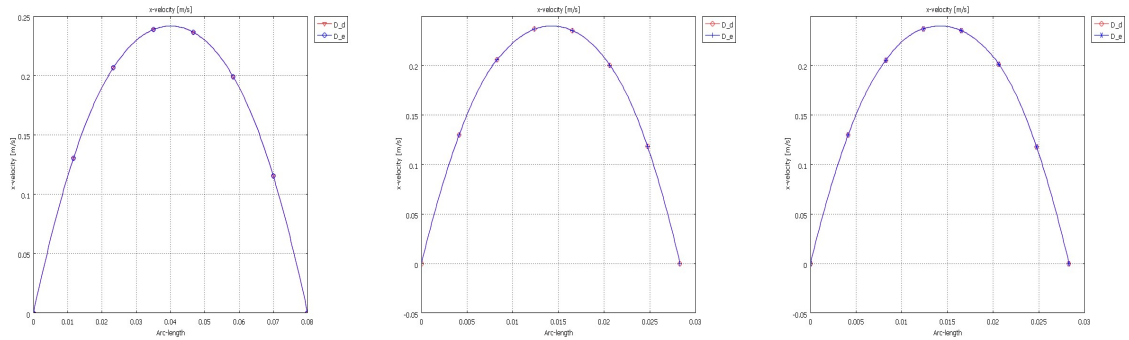


FIGURE 5.26 – Comparison profile of velocity

5.4.6 The complete T-Y-Geometry

We consider now a complicated geometry formed by Y and T (see Figure (5.27)).

The blood flow enters the vessel from the left side Γ_{in}^1 with Poiseuille profiles. The

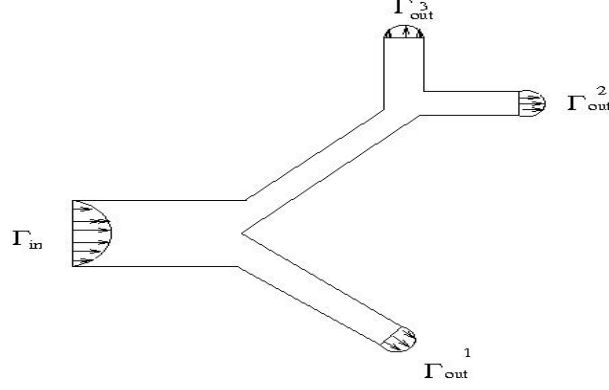


FIGURE 5.27 – T-Y-Geometry

amplitude of these parabolic profiles is independent of the time :

$$\Gamma_{in} : \begin{cases} u_0 = Umax * s * (1 - s), \\ v_0 = 0. \end{cases}$$

The blood flow exits the vessel from the vertical, horizontal and lower tube with the following parabolic profile :

$$\Gamma_{out}^1 : \begin{cases} u_0 = Umax * s * (1 - s), \\ v_0 = -Umax * s * (1 - s). \end{cases} \quad \Gamma_{out}^2 : \begin{cases} u_0 = Umax * s * (1 - s), \\ v_0 = 0. \end{cases}$$

and

$$\Gamma_{out}^3 : \begin{cases} u_0 = 0, \\ v_0 = Umax * s * (1 - s). \end{cases}$$

Where $Umax = 1 [m/s]$ and s is a normalized parameter. In the present study, the vessel walls are fixed and are not deformed by the blood flow. No-slip boundary conditions are prescribed for the fluid at the vessel walls ($u=v=0$ on $\Gamma_0 = \Gamma - (\Gamma_{in} \cup \Gamma_{out}^1 \cup \Gamma_{out}^2 \cup \Gamma_{out}^3)$). The numerical results are described in the following figures :

We first give the velocity vector field and the streamlines, in the second we give the velocity profiles (x and y components), the surfaces and iso–pressures and contour plot (x and y components).

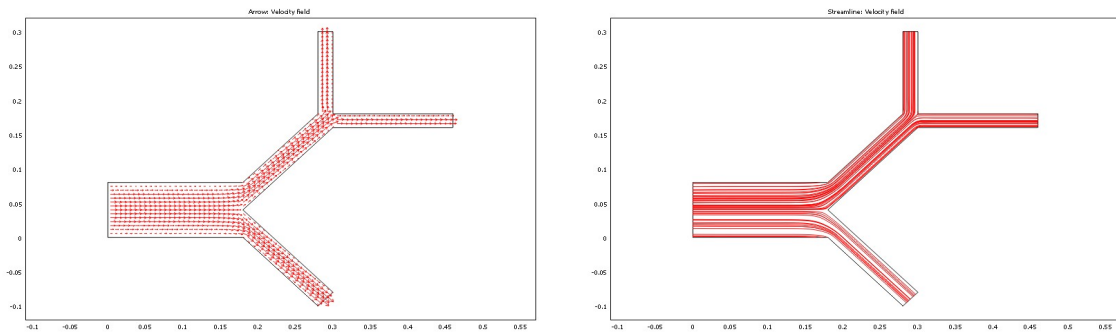


FIGURE 5.28 – Velocity vector field and Streamlines in the T-Y-Geometry

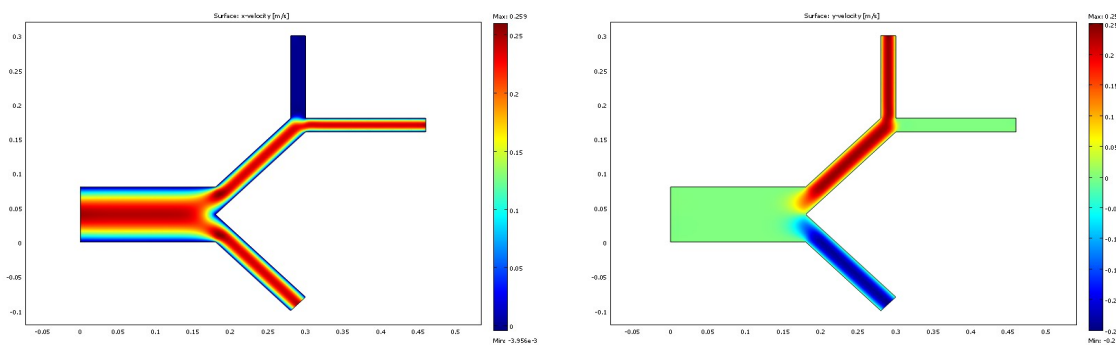


FIGURE 5.29 – The x and y velocity components in the T-Y-Geometry

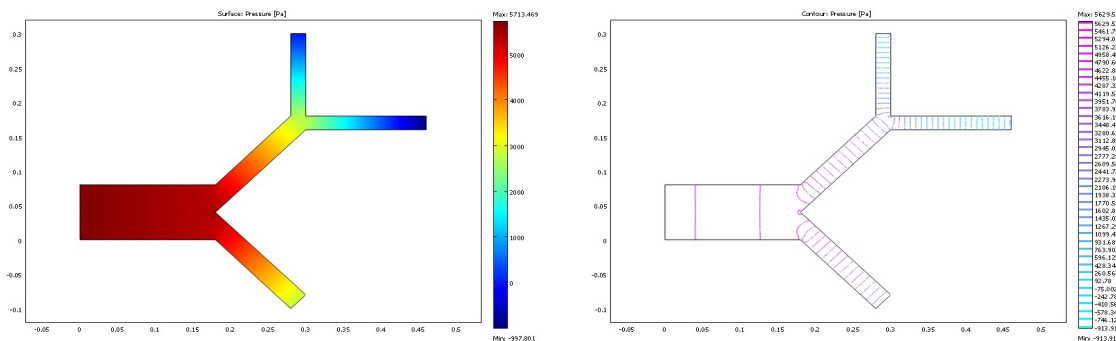


FIGURE 5.30 – Pressure profiles in T-Y-Geometry

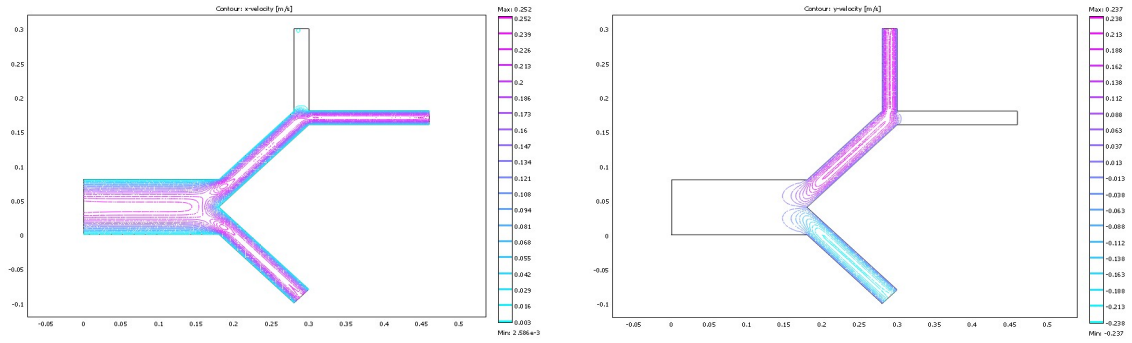


FIGURE 5.31 – Contour x and y velocity components in the T-Y-Geometry

5.4.7 MAPDD for non-Newtonian flow in T-Y-Geometry

The results for the T-Y geometry complete, are consistent with what we expected. It now remains to make these calculations on a reduced geometry, obtained by reducing the size of horizontal, obliques and vertical channels.

Decomposed domain :

Geometry and its mesh are summarized in the following figure (see Figure(5.32)) : This problem is solved with the same techniques as before. The results obtained are

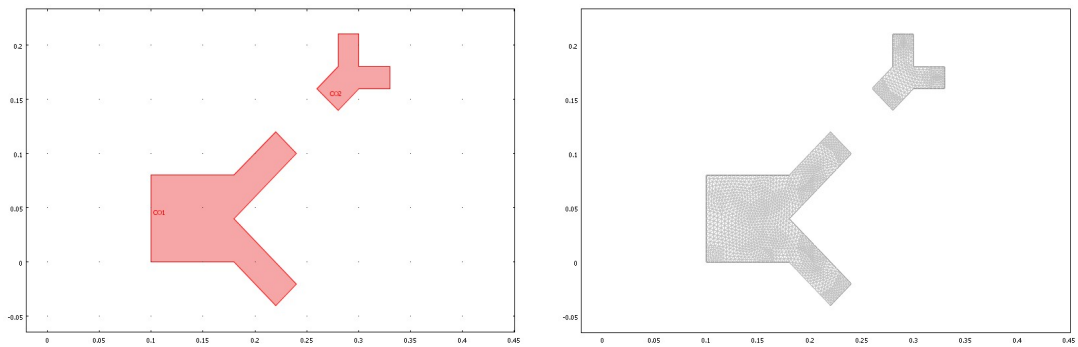


FIGURE 5.32 – The reduced T-Y-Geometry and its mesh

described in the following figures. It starts by showing the components x and y of velocity (Figures (5.33) and (5.34)). It then gives the pressure profiles in Figure (5.35) and then the contour for both velocity components (Figure (5.36)).

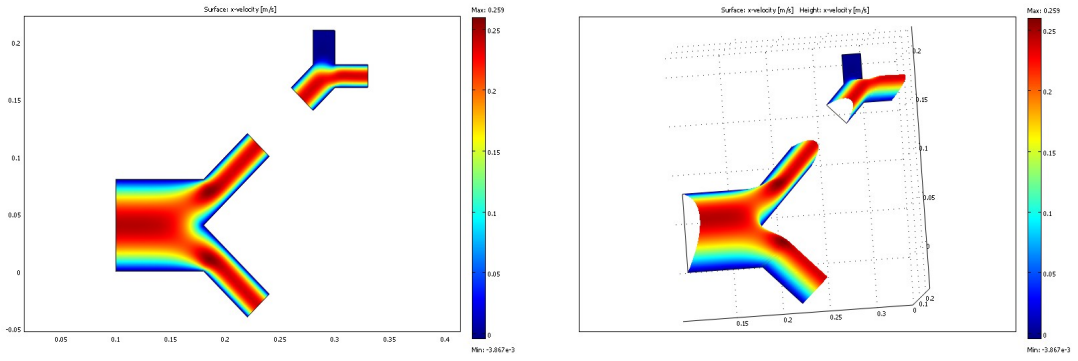


FIGURE 5.33 – Surface x-velocity

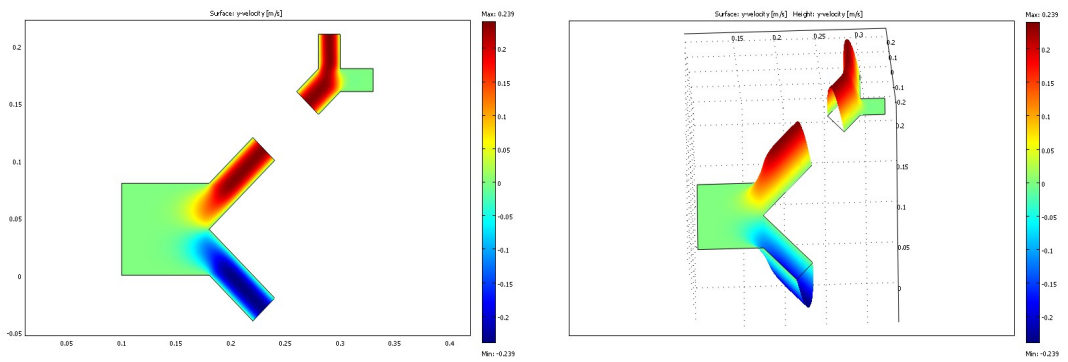


FIGURE 5.34 – Surface y-velocity

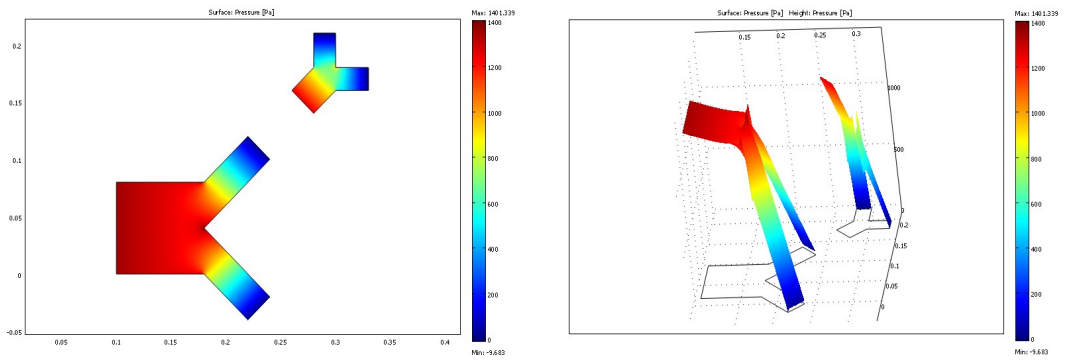


FIGURE 5.35 – Surface pressure

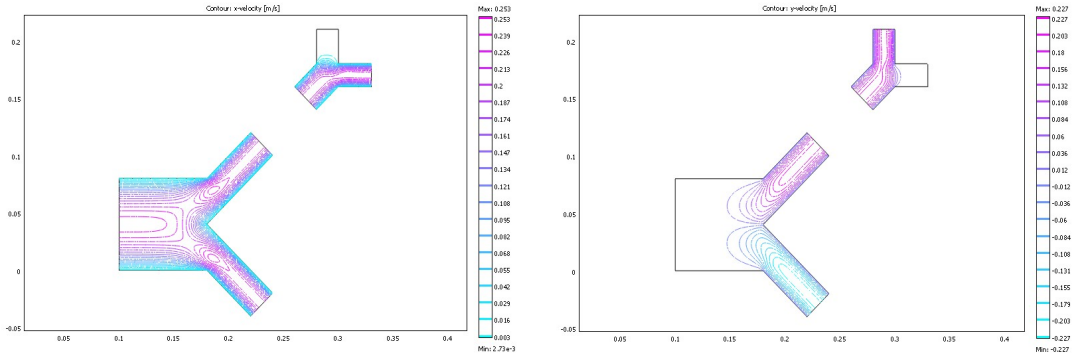


FIGURE 5.36 – Contour x-velocity and y-velocity

5.4.8 The complete Geometry of three bifurcations

Now we increase the number of bifurcation, we consider a complicated geometry formed by three bifurcations

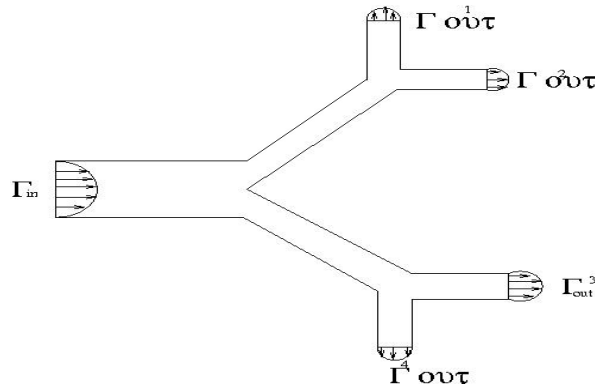


FIGURE 5.37 – Three-bif-Geometry

The blood flow enters the vessel from the left side Γ_{in}^1 with Poiseuille profiles. The amplitude of these parabolic profiles is independent of the time :

$$\Gamma_{in} : \begin{cases} u_0 = Umax * s * (1 - s), \\ v_0 = 0. \end{cases}$$

The blood flow exits the vessel from the vertical, horizontal and lower tubes with the

following parabolic profile :

$$\Gamma_{out}^1 : \begin{cases} u_0 = 0, \\ v_0 = Umax * s * (1 - s). \end{cases} \quad \Gamma_{out}^2 : \begin{cases} u_0 = Umax * s * (1 - s), \\ v_0 = 0. \end{cases}$$

and

$$\Gamma_{out}^3 : \begin{cases} u_0 = Umax * s * (1 - s), \\ v_0 = 0. \end{cases} \quad \Gamma_{out}^4 : \begin{cases} u_0 = 0, \\ v_0 = -Umax * s * (1 - s). \end{cases}$$

Where $Umax = 1 [m/s]$ and s is a normalized parameter. In the present study, the vessel walls are fixed and are not deformed by the blood flow. No-slip boundary conditions are prescribed for the fluid at the vessel walls ($u=v=0$ on $\Gamma_0 = \Gamma - (\Gamma_{in} \cup \Gamma_{out}^1 \cup \Gamma_{out}^2 \cup \Gamma_{out}^3 \cup \Gamma_{out}^4)$). The numerical results are described in the following figures :

We first give the velocity vector field and the streamlines, in the second we give the velocity profiles (x and y components), the surfaces and iso–pressures and contour plot (x and y components).

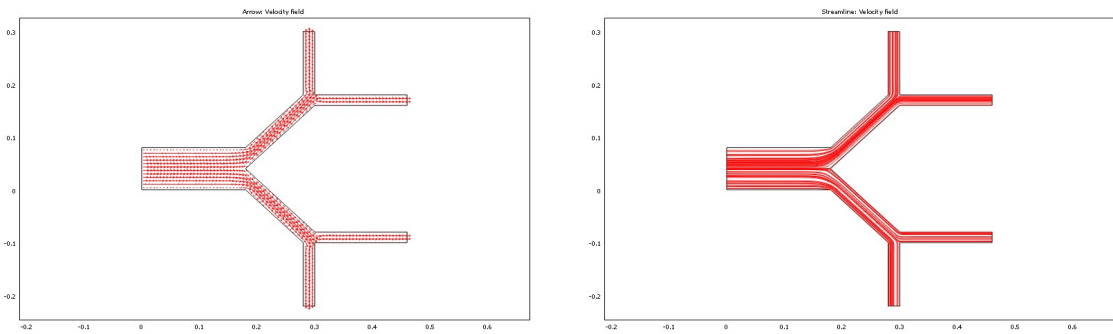


FIGURE 5.38 – Velocity vector field and Streamlines in three-bif-Geometry

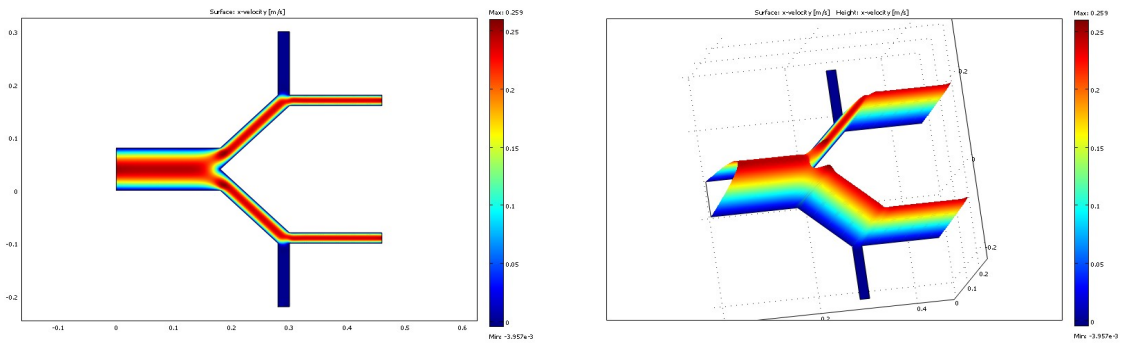


FIGURE 5.39 – The x and y velocity components in three-bif-Geometry

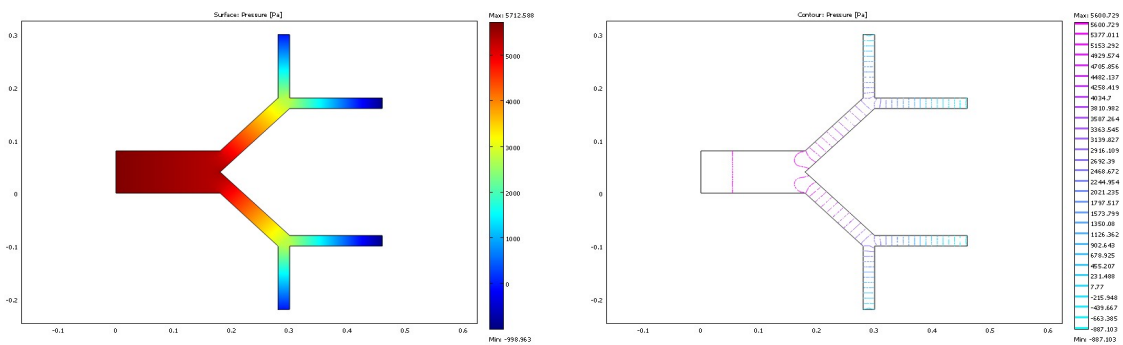


FIGURE 5.40 – Pressure profiles in three-bif-Geometry

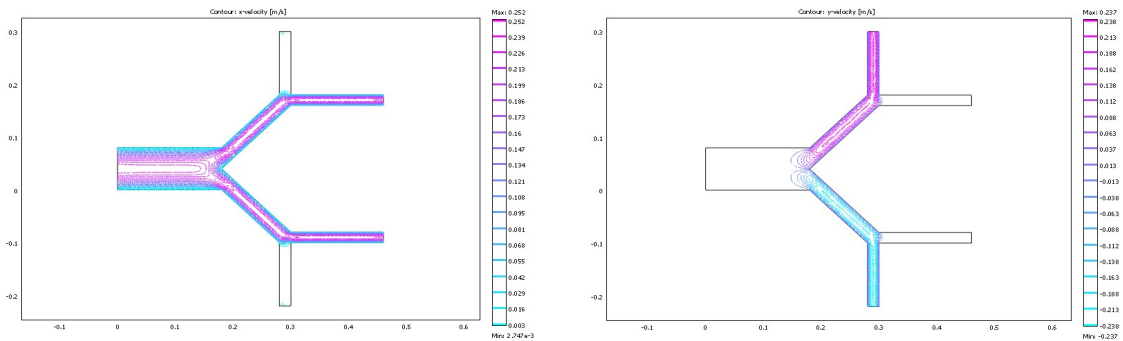


FIGURE 5.41 – Contour x and y velocity components in the three-bif-Geometry

5.4.9 MAPDD for non-Newtonian flow in three bifurcations

The results for the three bifurcations geometry complete, are consistent with what we expected. It now remains to make these calculations on a reduced geometry, obtained by reducing the size of horizontals, obliques and vertical channels.

Decomposed domain :

Geometry and its mesh are summarized in the following figure (see Figure(5.42)) : This problem is solved with the same techniques as before. The results obtained are

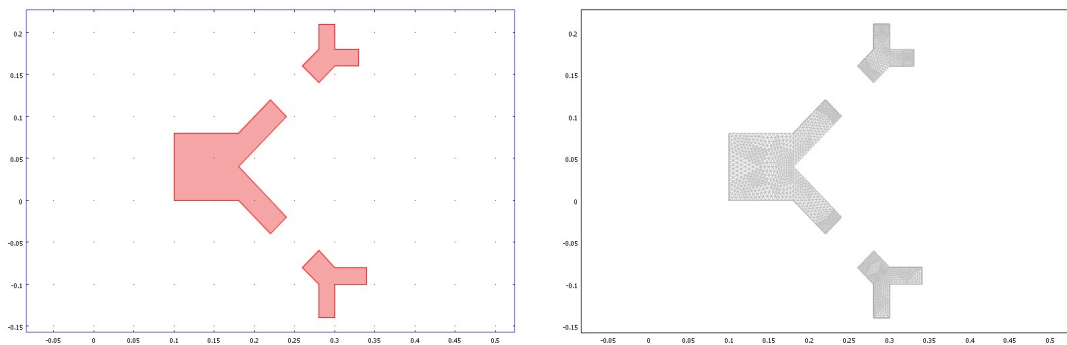


FIGURE 5.42 – The reduced three bifurcations Geometry and its mesh

described in the following figures : it starts by showing the components x and y of velocity (Figures (5.43) and (5.44)). It then gives the pressure profiles in Figure (5.45) and then the contour for both velocity components (Figure (5.46)).

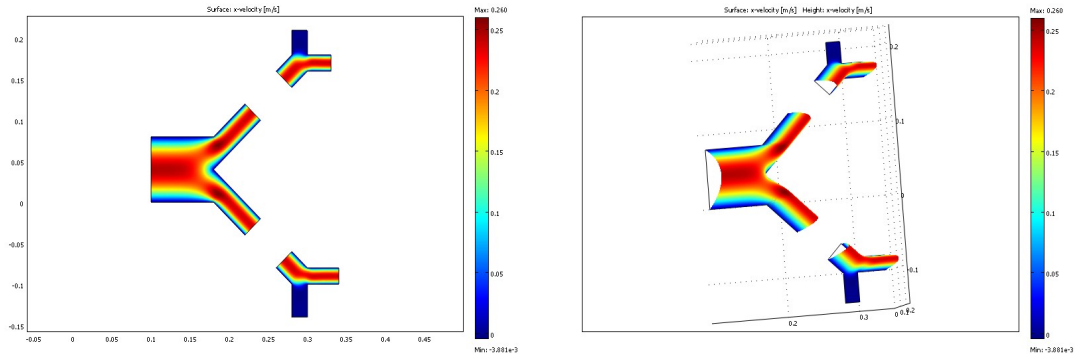


FIGURE 5.43 – Surface x-velocity

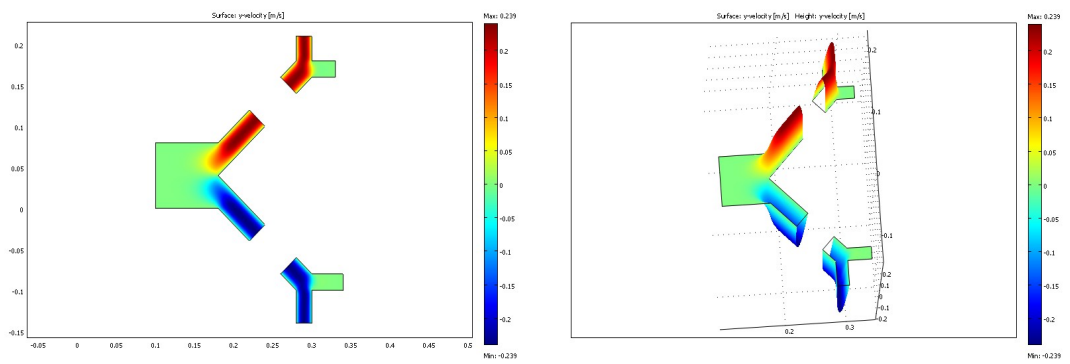


FIGURE 5.44 – Surface y-velocity

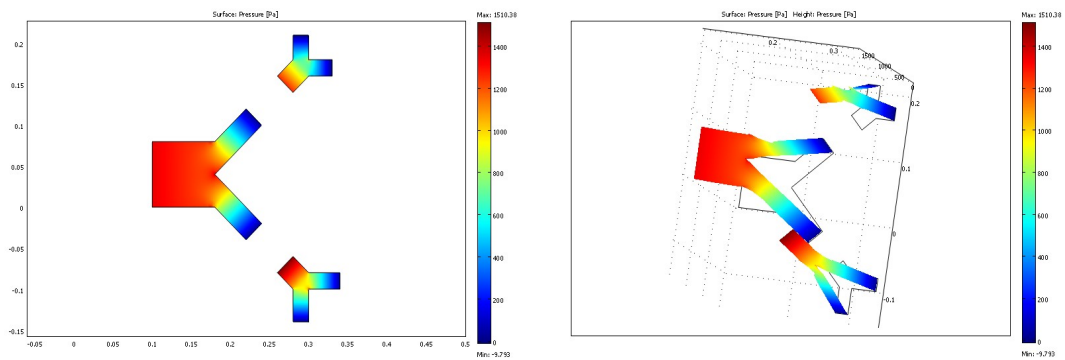


FIGURE 5.45 – Surface pressure

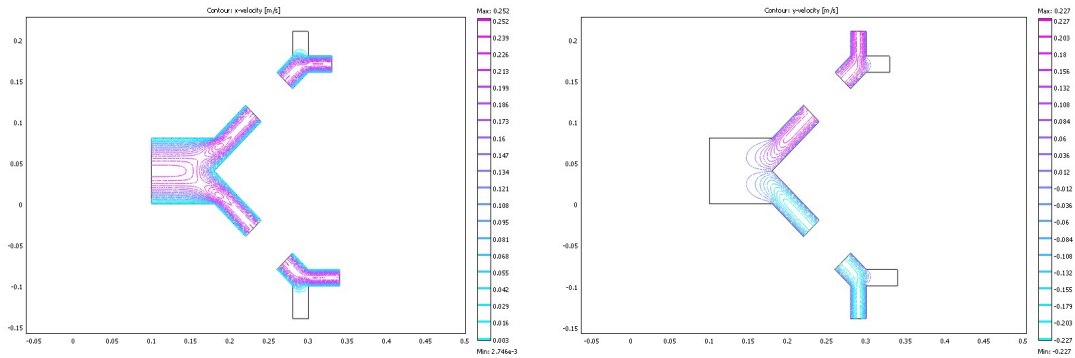


FIGURE 5.46 – Contour x-velocity and y-velocity

5.4.10 The complete Geometry of quadruple bifurcations

We consider a complicated geometry formed by quadruple bifurcations

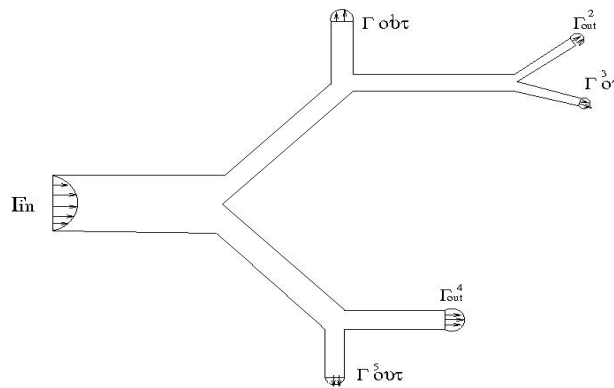


FIGURE 5.47 – Quadruple bif-Geometry

The blood flow enters the vessel from the left side Γ_{in}^1 with Poiseuille profiles. The amplitude of these parabolic profiles is independent of the time :

$$\Gamma_{in} : \begin{cases} u_0 = Umax * s * (1 - s), \\ v_0 = 0. \end{cases}$$

The blood flow exits the vessel from the verticals, horizontals and obliques tubes with

the following parabolic profile :

$$\Gamma_{out}^1 : \begin{cases} u_0 = 0, \\ v_0 = Umax * s * (1 - s). \end{cases} \quad \Gamma_{out}^2 : \begin{cases} u_0 = Umax * s * (1 - s), \\ v_0 = Umax * s * (1 - s). \end{cases}$$

$$\Gamma_{out}^3 : \begin{cases} u_0 = Umax * s * (1 - s), \\ v_0 = -Umax * s * (1 - s). \end{cases} \quad \Gamma_{out}^4 : \begin{cases} u_0 = Umax * s * (1 - s), \\ v_0 = 0. \end{cases}$$

$$\Gamma_{out}^5 : \begin{cases} u_0 = 0, \\ v_0 = -Umax * s * (1 - s). \end{cases}$$

Where $Umax = 1 [m/s]$ and s is a normalized parameter. In the present study, the vessel walls are fixed and are not deformed by the blood flow. No-slip boundary conditions are prescribed for the fluid at the vessel walls ($u=v=0$ on $\Gamma_0 = \Gamma - (\Gamma_{in} \cup \Gamma_{out}^1 \cup \Gamma_{out}^2 \cup \Gamma_{out}^3 \cup \Gamma_{out}^4 \cup \Gamma_{out}^5)$). The numerical results are described in the following figures :

We first give the velocity vector field and the streamlines, in the second we give the velocity profiles (x and y components), the surfaces and iso–pressures and contour plot (x and y components).

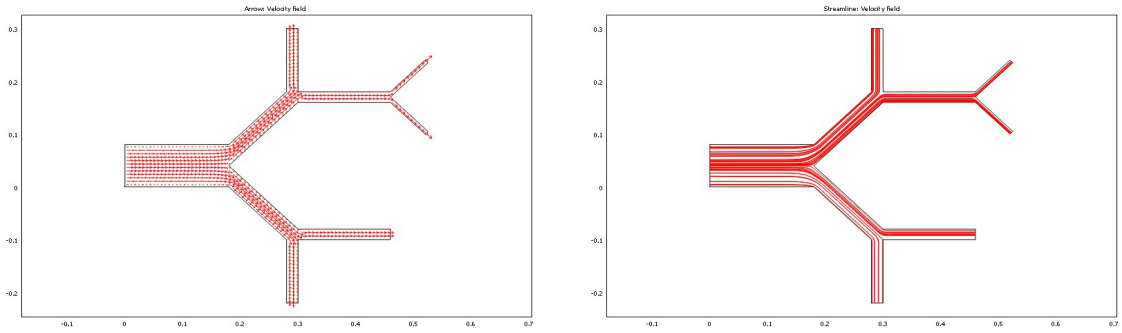


FIGURE 5.48 – Velocity vector field and Streamlines in Quadruple bif-Geometry

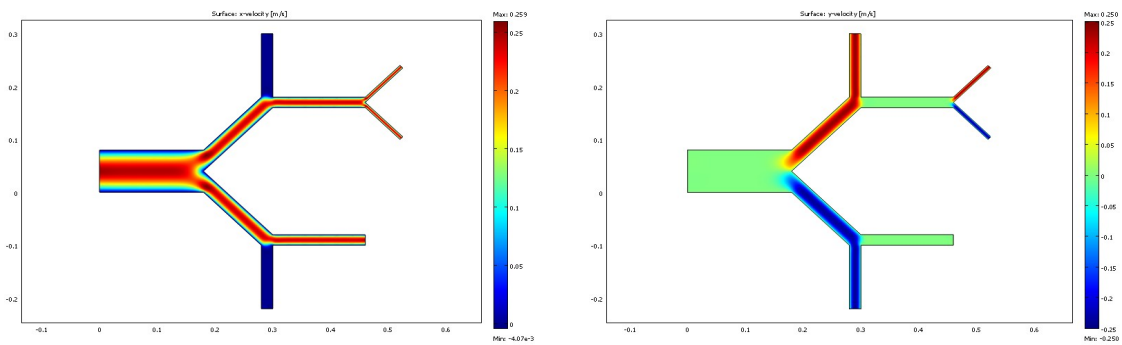


FIGURE 5.49 – The x and y velocity components in Quadruple bif-Geometry

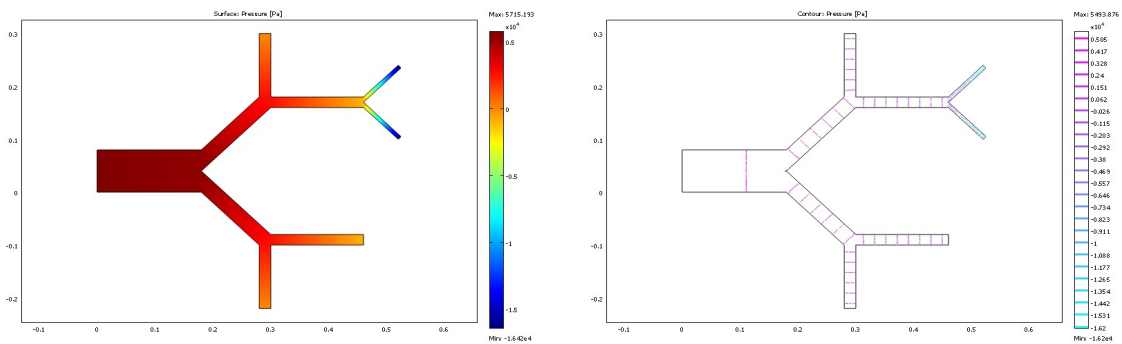


FIGURE 5.50 – Pressure profiles in Quadruple bif-Geometry

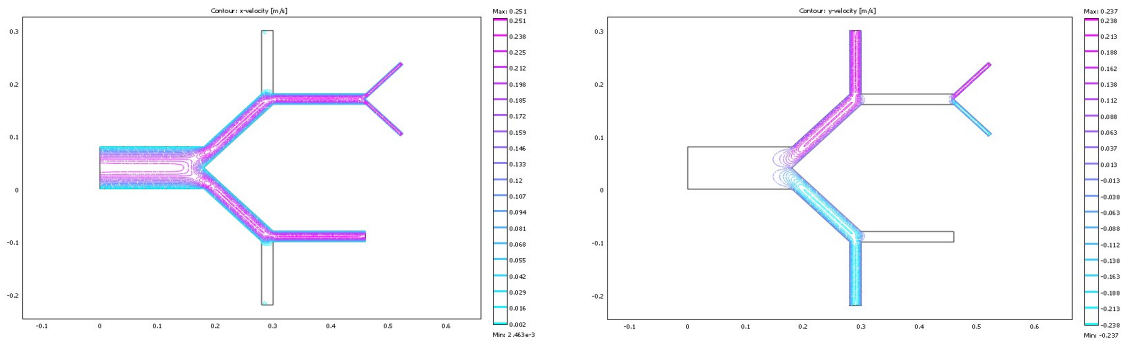


FIGURE 5.51 – Contour x and y velocity components in Quadruple bif-Geometry

5.4.11 MAPDD for non-Newtonian flow in quadruple bifurcations

The results for the quadruple bifurcations geometry complete, are consistent with what we expected. It now remains to make these calculations on a reduced geometry, obtained by reducing the size of horizontal, obliques and vertical channels.

Decomposed domain :

Geometry and its mesh are summarized in the following figure (see Figure(5.52)) : This problem is solved with the same techniques as before. The results obtained are

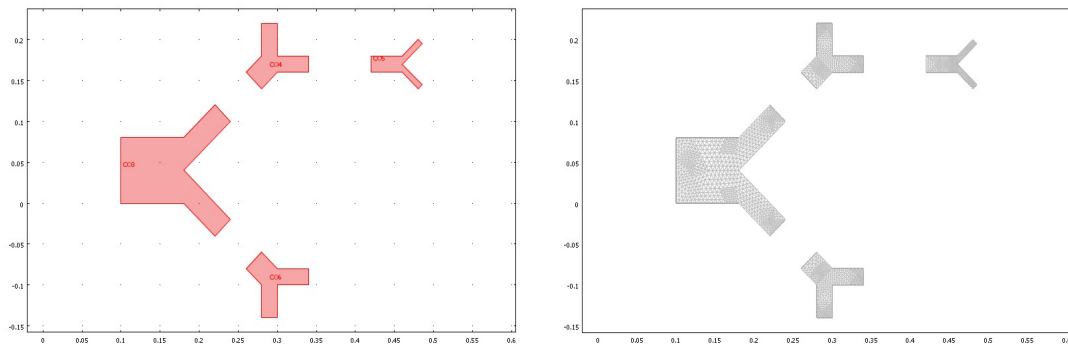


FIGURE 5.52 – The reduced quadruple bifurcations Geometry and its mesh

described in the following figures. It starts by showing the components x and y of velocity (Figures (5.53) and (5.54)). It then gives the pressure profiles in Figure (5.55)

and then the contour for both velocity components (Figure (5.56)).

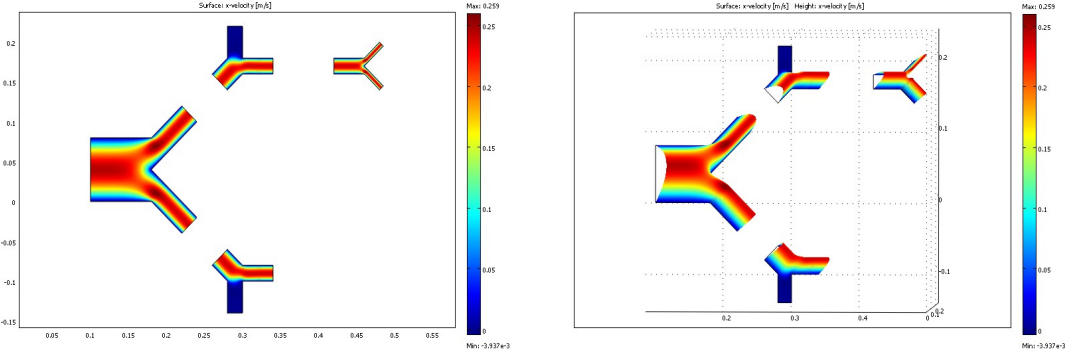


FIGURE 5.53 – Surface x-velocity

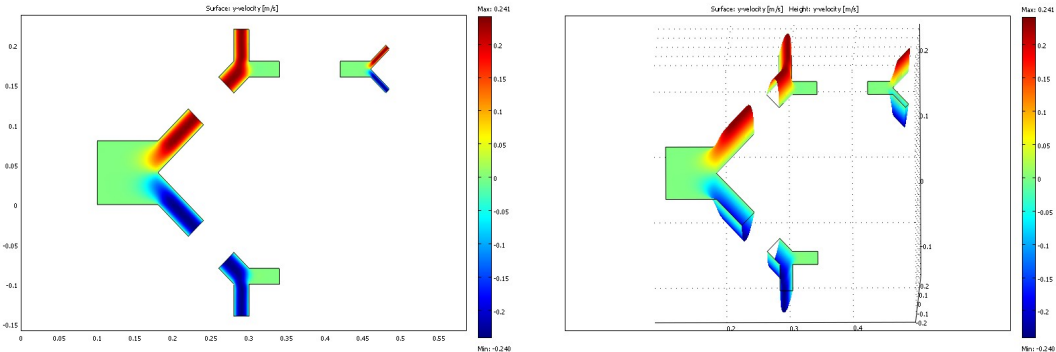


FIGURE 5.54 – Surface y-velocity

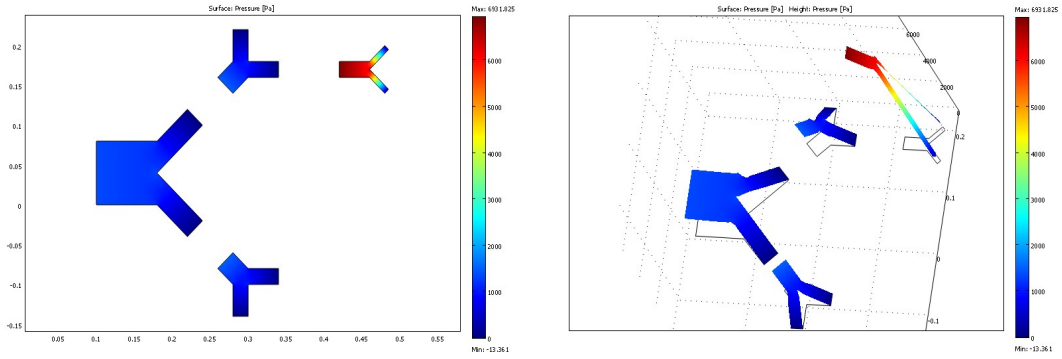


FIGURE 5.55 – Surface pressure

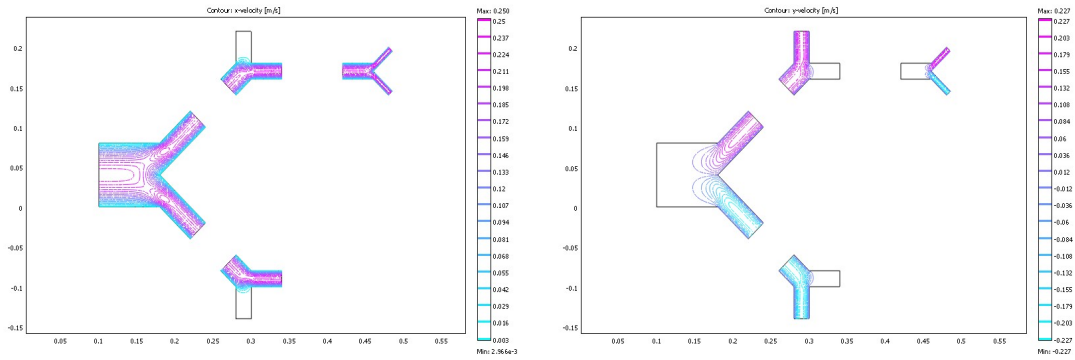


FIGURE 5.56 – Contour x-velocity and y-velocity

5.4.12 The complete Geometry of Semi-Triangle

We consider a complicated geometry formed by Semi-Triangle

The blood flow enters the vessel from the left side Γ_{in}^1 and the bottom side Γ_{in}^2 with Poiseuille profiles. The amplitude of these parabolic profiles is independent of the time :

$$\Gamma_{in}^1 : \begin{cases} u_0 = 1.5 * Umax * s * (1 - s), \\ v_0 = 0. \end{cases} \quad \Gamma_{in}^2 : \begin{cases} u_0 = 0, \\ v_0 = 2 * Umax * s * (1 - s). \end{cases}$$

The blood flow exits the vessel from the vertical, oblique tube with the following

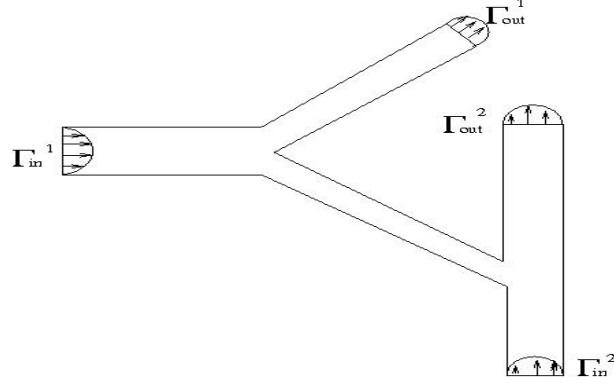


FIGURE 5.57 – Semi-Triangle-Geometry

parabolic profile :

$$\Gamma_{out}^1 : \begin{cases} u_0 = 2 * Umax * s * (1 - s), \\ v_0 = 2 * Umax * s * (1 - s). \end{cases} \quad \Gamma_{out}^2 : \begin{cases} u_0 = 0, \\ v_0 = 3 * Umax * s * (1 - s). \end{cases}$$

Where $Umax = 1 [m/s]$ and s is a normalized parameter. In the present study, the vessel walls are fixed and are not deformed by the blood flow. No-slip boundary conditions are prescribed for the fluid at the vessel walls ($u=v=0$ on $\Gamma_0 = \Gamma - (\Gamma_{in}^1 \cup \Gamma_{in}^2 \cup \Gamma_{out}^1 \cup \Gamma_{out}^2)$). The numerical results are described in the following figures :

We first give the velocity vector field and the streamlines, in the second we give the velocity profiles (x and y components), the surfaces and iso-pressures and contour plot (x and y components).

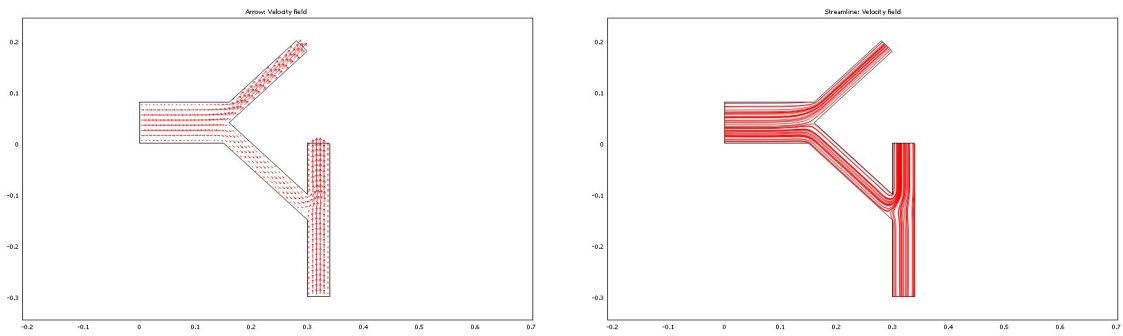


FIGURE 5.58 – Velocity vector field and Streamlines in Semi-Triangle-Geometry

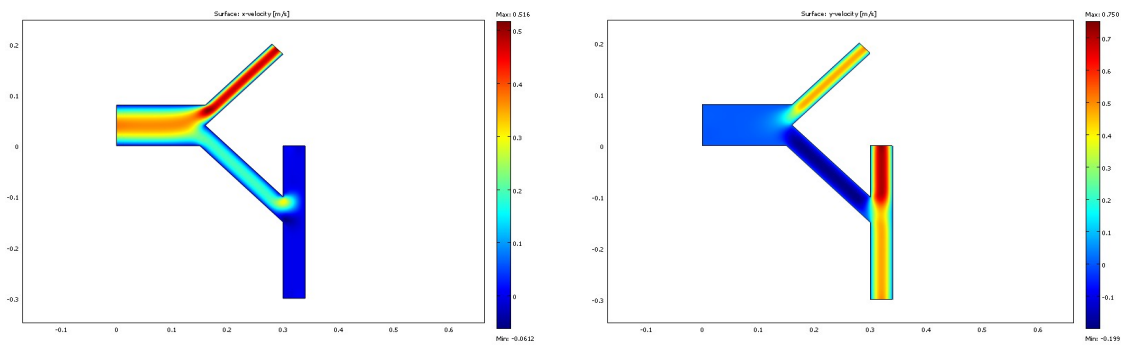


FIGURE 5.59 – The x and y velocity components in Semi-Triangle-Geometry

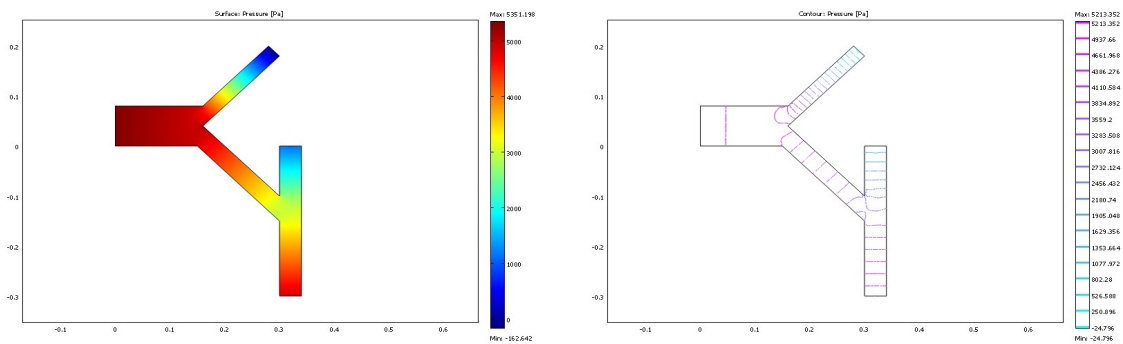


FIGURE 5.60 – Pressure profiles in Semi-Triangle-Geometry

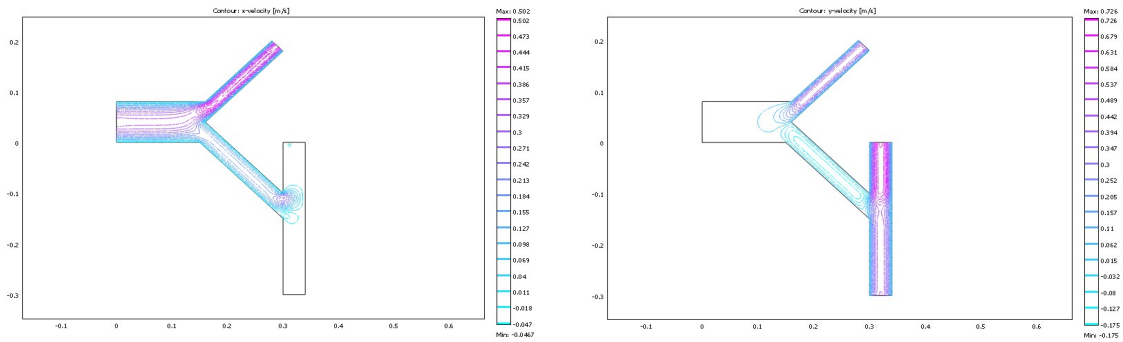


FIGURE 5.61 – Contour x and y velocity components in Semi-Triangle-Geometry

5.4.13 MAPDD for non-Newtonian flow in Semi-Triangle-Geometry

The results for the triangle geometry complete, are consistent with what we expected. It now remains to make these calculations on a reduced geometry, obtained by reducing the size of horizontal, oblique and vertical channels.

Decomposed domain :

Geometry and its mesh are summarized in the following figure (see Figure(5.62)) : This problem is solved with the same techniques as before. The results obtained are

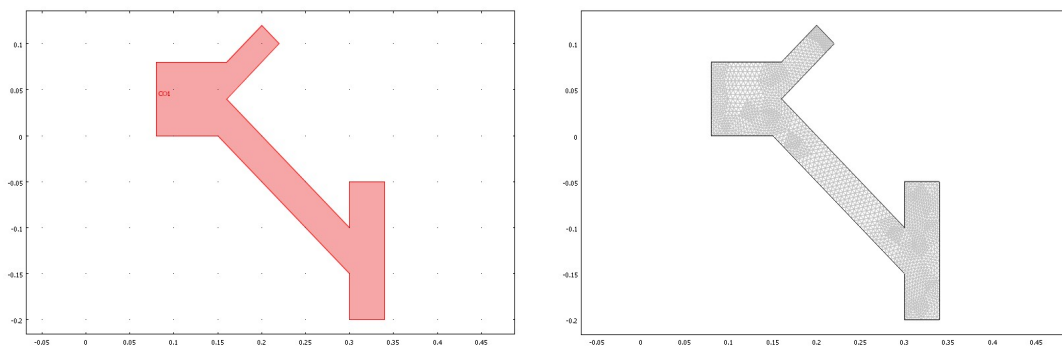


FIGURE 5.62 – The reduced Semi-Triangle Geometry and its mesh

described in the following figures. It starts by showing the components x and y of velocity (Figures (5.63) and (5.64)). It then gives the pressure profiles in Figure (5.65) and then the contour for both velocity components (Figure (5.66)).

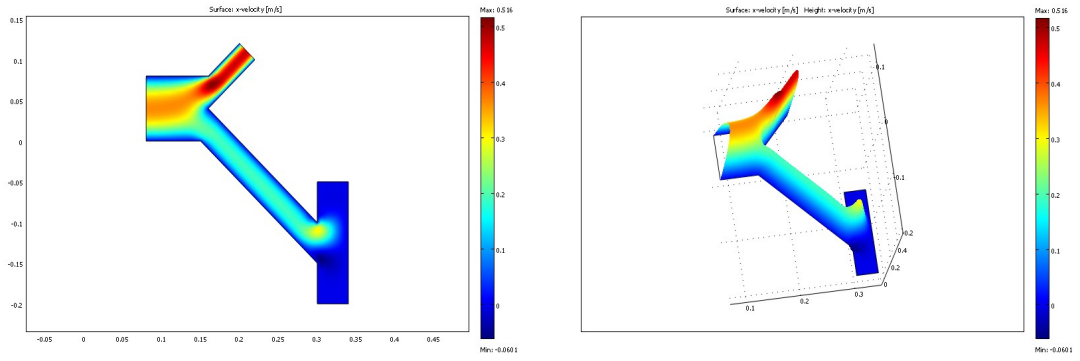


FIGURE 5.63 – Surface x-velocity

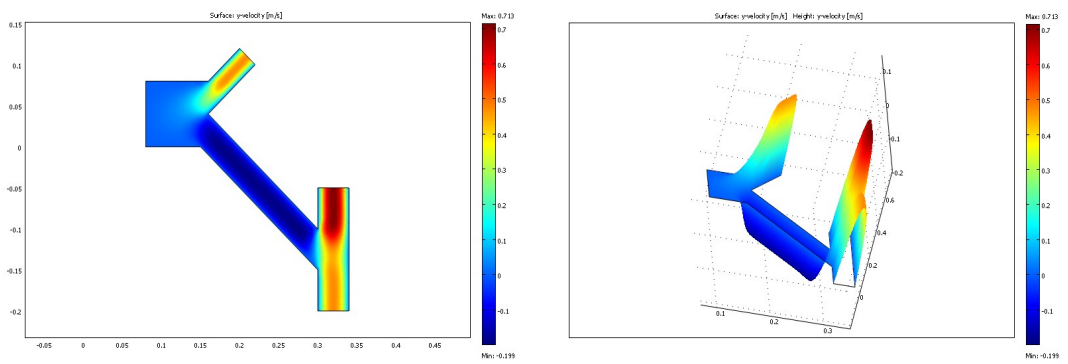


FIGURE 5.64 – Surface y-velocity

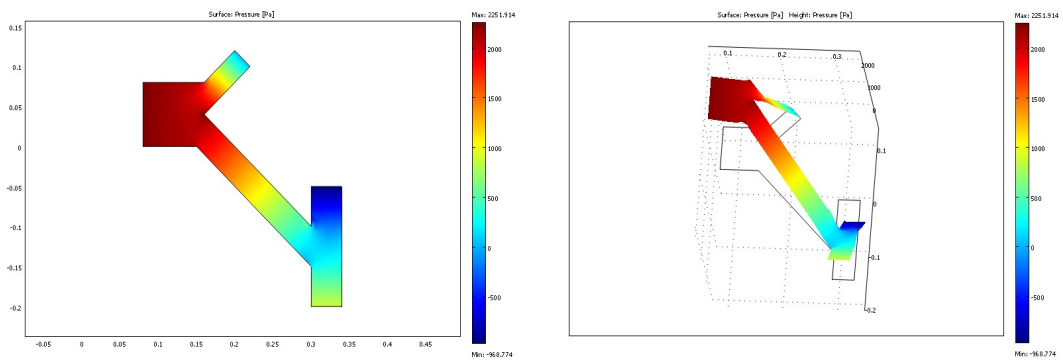


FIGURE 5.65 – Surface pressure

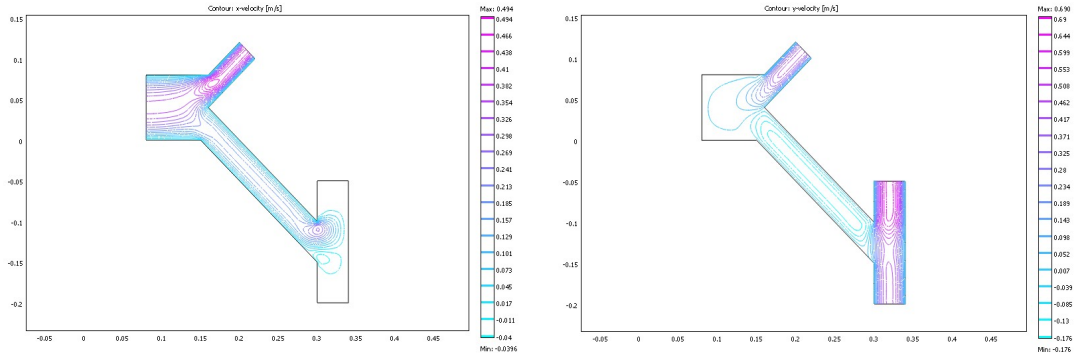


FIGURE 5.66 – Contour x-velocity and y-velocity

5.4.14 The complete Geometry of Triangle

We consider a complicated geometry formed by Triangle

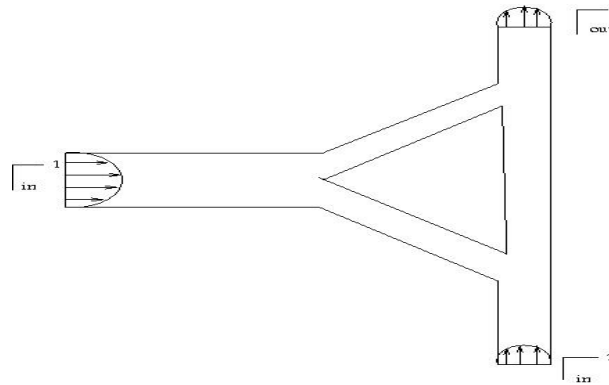


FIGURE 5.67 – Triangle-Geometry

The blood flow enters the vessel from the left side Γ_{in}^1 and the bottom side Γ_{in}^2 with Poiseuille profiles. The amplitude of these parabolic profiles is independent of the time :

$$\Gamma_{in}^1 : \begin{cases} u_0 = 1.5 * Umax * s * (1 - s), \\ v_0 = 0. \end{cases} \quad \Gamma_{in}^2 : \begin{cases} u_0 = 0, \\ v_0 = 2 * Umax * s * (1 - s). \end{cases}$$

The blood flow exits the vessel from the vertical tube with the following parabolic

profile :

$$\Gamma_{out}^1 : \begin{cases} u_0 = 0, \\ v_0 = 4 * Umax * s * (1 - s). \end{cases}$$

Where $Umax = 1 [m/s]$ and s is a normalized parameter. In the present study, the vessel walls are fixed and are not deformed by the blood flow. No-slip boundary conditions are prescribed for the fluid at the vessel walls ($u=v=0$ on $\Gamma_0 = \Gamma - (\Gamma_{in}^1 \cup \Gamma_{in}^2 \cup \Gamma_{out}^1)$). The numerical results are described in the following figures :

We first give the velocity vector field and the streamlines, in the second we give the velocity profiles (x and y components), the surfaces and iso-pressures and contour plot (x and y components).

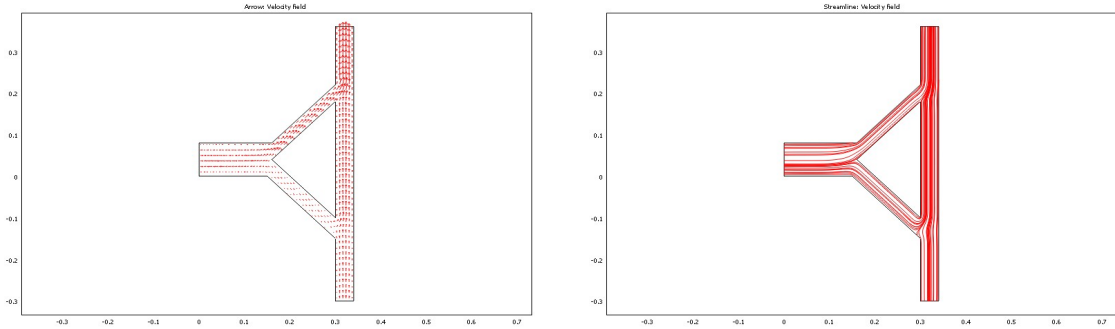


FIGURE 5.68 – Velocity vector field and Streamlines in Triangle-Geometry

5.4.15 MAPDD for non-Newtonian flow in Triangle-Geometry

The results for the Triangle geometry complete, are consistent with what we expected. It now remains to make these calculations on a reduced geometry, obtained by reducing the size of horizontal, oblique and verticals channels.

Decomposed domain :

Geometry and its mesh are summarized in the following figure (see Figure(5.72)) :

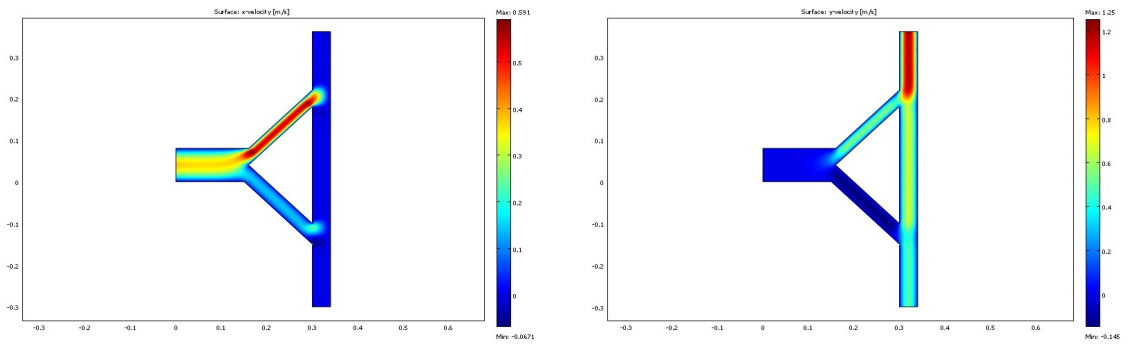


FIGURE 5.69 – The x and y velocity components in Triangle-Geometry

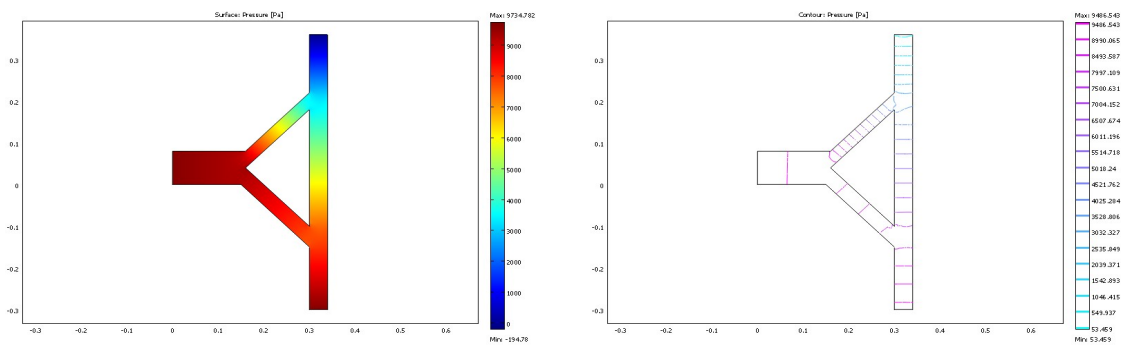


FIGURE 5.70 – Pressure profiles in Triangle-Geometry

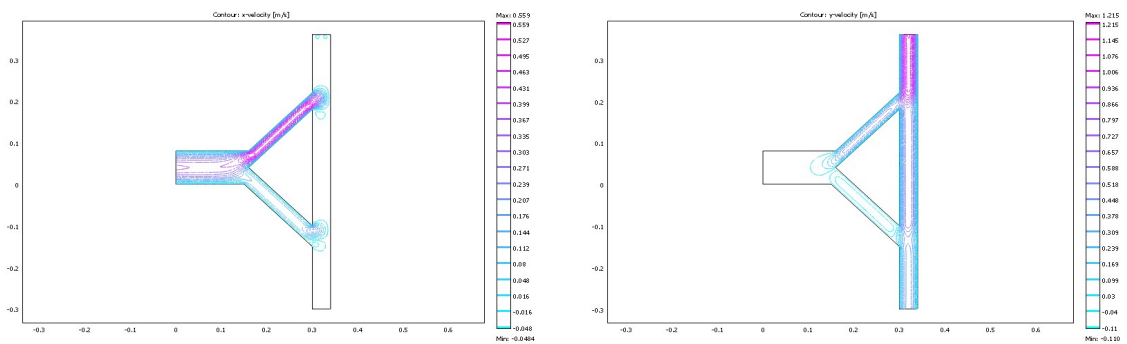


FIGURE 5.71 – Contour x and y velocity components in Triangle-Geometry

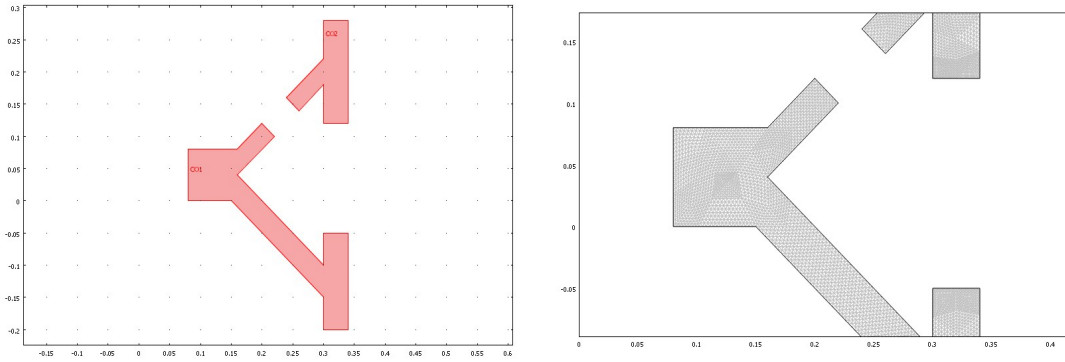


FIGURE 5.72 – The reduced Triangle-Geometry and its mesh

This problem is solved with the same techniques as before. The results obtained are described in the following figures. It starts by showing the components x and y of velocity (Figures (5.73) and (5.74)). It then gives the pressure profiles in Figure (5.75) and then the contour for both velocity components (Figure (5.76)).

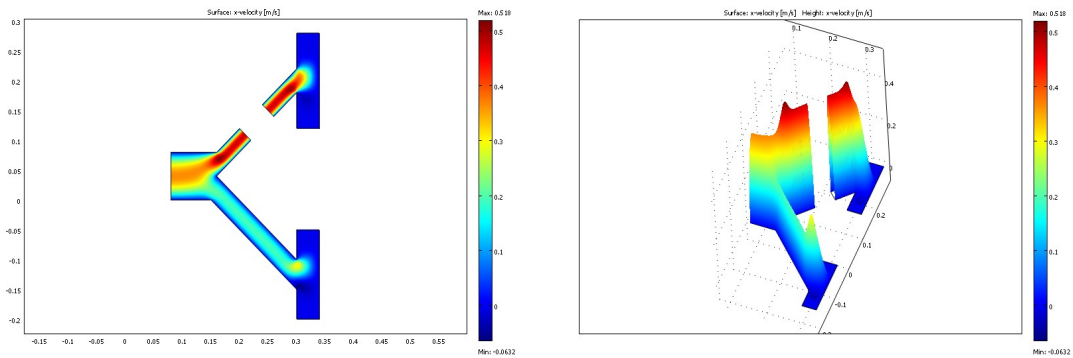


FIGURE 5.73 – Surface x-velocity

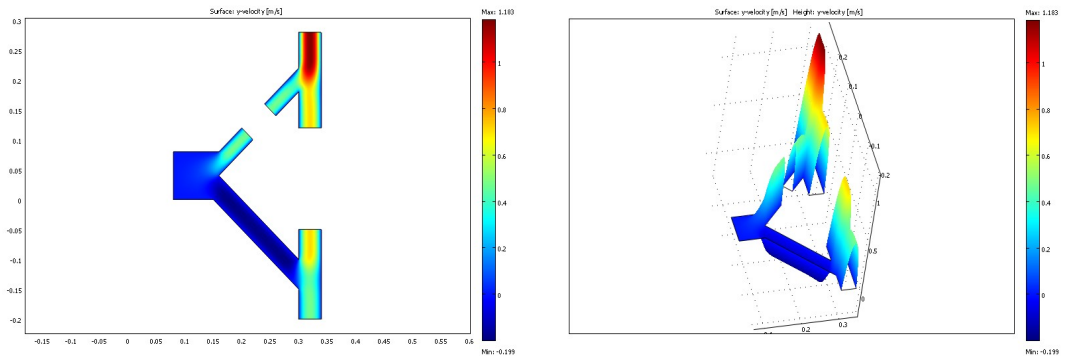


FIGURE 5.74 – Surface y-velocity

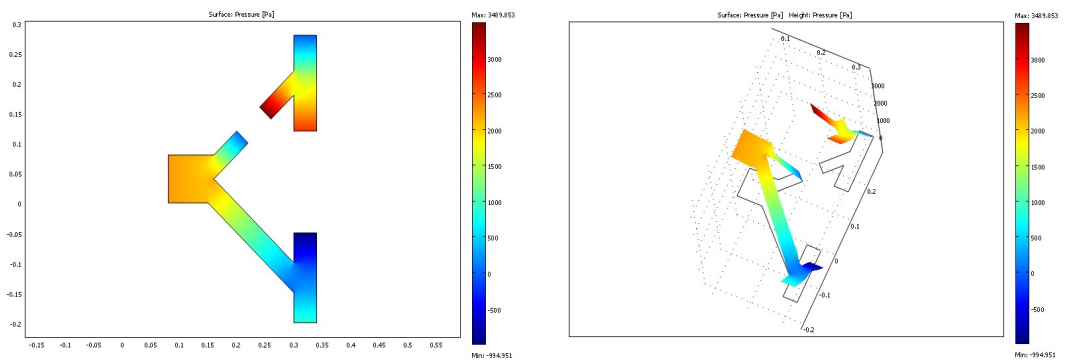


FIGURE 5.75 – Surface pressure

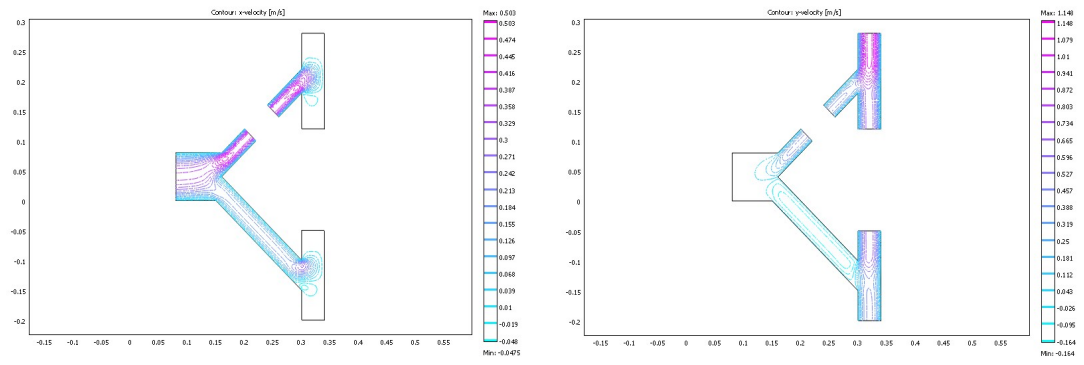


FIGURE 5.76 – Contour x-velocity and y-velocity

Annexe A

Rappels sur la discrétisation des problèmes de Stokes linéaire et non linéaire

A.1 Problème de Stokes linéaire

La résolution par la méthode des éléments finis nécessite l'obtention d'une formulation variationnelle du problème (2.1). On multiplie ces deux équations respectivement par des fonctions test $w \in V$ et $q \in Q$ où V et Q sont des espaces fonctionnels appropriés qu'il n'est pas nécessaire de spécifier pour le moment. On intègre ensuite par parties sur le domaine Ω de frontière Γ et on obtient ainsi $\forall w \in V$ et $\forall q \in Q$:

$$\begin{cases} \int_{\Omega} (2\eta d(u) : d(w) - p \nabla \cdot w) dx = \int_{\Omega} f \cdot w dx + \int_{\Gamma} ((-pI + 2\eta d(u))n) \cdot w ds \\ \int_{\Omega} q \nabla \cdot u dx = 0 \end{cases} \quad (A.1)$$

Nous supposons dans la suite les conditions aux limites suivantes ($u = 0$) partout sur la frontière Γ on obtient la formulation suivante :

$$\begin{cases} \int_{\Omega} (2\eta d(u) : d(w)) dx - \int_{\Omega} (p \nabla \cdot w) dx = \int_{\Omega} f \cdot w dx \quad \forall w \in V \\ \int_{\Omega} q \nabla \cdot u dx = 0 \quad \forall q \in Q \end{cases} \quad (A.2)$$

On introduit maintenant les formes bilinéaires a et b définies respectivement sur $V \times V$ et $V \times Q$ de sorte qu'on peut écrire :

$$\begin{cases} a(u, w) + b(v, p) = (f, w) \quad \forall w \in V \\ b(u, q) = 0 \quad \forall q \in Q \end{cases} \quad (A.3)$$

A.1.1 Cadre fonctionnel :

L'analyse numérique du système (A.1) est relativement complexe. Tout d'abord, les espaces fonctionnels sont $V = (H_0^1(\Omega))^2$ et $Q = L_0^2(\Omega)$. La forme bilinéaire b définit implicitement deux opérateurs linéaires. Le premier, que nous noterons B , est définie sur V à valeurs dans Q' le dual de Q :

$$B : V \longrightarrow Q'$$

$$w \longmapsto Bw$$

par :

$$\langle Bw, q \rangle = b(w, q) = - \int_{\Omega} q \nabla \cdot w \, dv \quad \forall q \in Q$$

On peut aussi définir le noyau de B (noté $\ker B$) par :

$$\begin{aligned} \ker B &= \{w \in V \mid Bw = 0\} = \{w \in V \mid \langle Bw, q \rangle = b(w, q) = 0 \quad \forall q \in Q\} \\ &= \{w \in (H_0^1(\Omega))^2 \mid \int_{\Omega} q \nabla \cdot w \, dv = 0 \quad \forall q \in Q\} = \{w \in (H_0^1(\Omega))^2 \mid \nabla \cdot w = 0\} \end{aligned}$$

Remarque 1.1

Si $u \in (H_0^1(\Omega))^2$, on remarque que $\nabla \cdot u \in L^2(\Omega)$ et que la deuxième équation du système (A.1) est parfaitement équivalente à imposer $\nabla \cdot u = 0$

On peut définir un deuxième opérateur linéaire, cette fois de Q à valeur dans V' , dual de V , que nous noterons B^T :

$$B^T : Q \longrightarrow V'$$

$$q \longrightarrow B^T q$$

défini Comme précédemment, par :

$$\langle B^T q, w \rangle = \langle bw, q \rangle = - \int_{\Omega} q \nabla \cdot w dv \quad \forall w \in V$$

De même, on pose :

$$\begin{aligned} \ker B^T &= \{q \in Q \mid B^T q = 0\} \\ &= \{q \in Q \mid \langle w, B^T q \rangle = b(w, q) = 0 \quad \forall w \in V\} \\ &= \{q \in Q \mid \int_{\Omega} q \nabla \cdot w dv = 0, \quad \forall w \in (H_0^1(\Omega))^2\} \end{aligned}$$

En intégrant par parties (puisque les fonctions de $(H_0^1(\Omega))^2$ s'annulent au bord), on a :

$$\ker B^T = \{q \in Q \mid \int_{\Omega} \nabla q \cdot w dv = 0 \quad \forall w \in (H_0^1(\Omega))^2\}$$

ce qui entraîne que $\nabla q = 0$ et donc que $\ker B^T$ est constitué par des fonctions constantes sur Ω .

A.1.2 Existence et unicité :

Les théorèmes qui suivent, et que nous ne démontrons pas, sont d'une grande importance théorique.

Théorème 1 (Existence et unicité du problème continu)

Sous les conditions suivantes :

- Les formes bilinéaires a et b sont continues respectivement sur $V \times V$ et $V \times Q$;
- la forme bilinéaire a est coercive sur $\ker B$ cad :

$$a(w, w) \geq \alpha \|w\|_{1,\Omega}^2 \quad \forall w \in \ker B$$

- Il existe une constante positive β telle que la forme bilinéaire b vérifie :

$$\inf_{q \in Q} \sup_{w \in V} \frac{b(w, q)}{\|q\|_{0,\Omega} \|w\|_{1,\Omega}} \geq \beta$$

alors la solution (u, p) du problème de Stokes (A.1) est unique dans $V \times Q / \ker B^T$.

Démonstration : Voir Brezzi-Fortin[33].

A.1.3 Le problème discret :

La discrétisation par éléments fins du problème de Stokes suit les étapes habituelles. On approxime (u, p) par des fonctions $(u_h, p_h) \in V_h \times Q_h$. Les sous espaces V_h de V et Q_h de Q sont de dimension finie et seront déterminés plus précisément plus loin. Le problème discrétisé s'écrit alors :

$$\begin{cases} a(u_h, w_h) + b(w_h, p_h) = (r, w_h) & \forall w_h \in V_h \\ b(u_h, q_h) = 0 & \forall q_h \in Q_h \end{cases} \quad (A.4)$$

La condition d'incompressibilité discrétisée s'écrit maintenant :

$$-\int_{\Omega} q_h \nabla \cdot w_h dv = 0 \quad \forall q_h \in Q_h$$

et n'est pas équivalente à $\nabla \cdot w_h = 0$. Pour que l'on puisse conclure que $\nabla \cdot w_h = 0$, il faudrait que q_h parcourt tout l'espace Q et pas seulement un sous-espace Q_h . Comme dans le cas continu, on peut définir :

$$\ker B_h = \{w_h \in V_h \mid -\int_{\Omega} q_h \nabla \cdot w_h dv = 0 \quad \forall q_h \in Q_h\}$$

De même, si on pose :

$$\ker B_h^T = \{q_h \in Q_h \mid -\int_{\Omega} q_h \nabla \cdot w_h dv = 0 \quad \forall w_h \in V_h\}$$

Théorème 2 (Existence et unicité du problème discret)

Sous les conditions suivantes :

-La forme bilinéaire a est coercive sur $\ker B_h$:

$$a(w_h, w_h) \geq \alpha \|w_h\|_{1,\Omega}^2 \quad \forall w_h \in \ker B_h$$

-La forme bilinéaire b vérifie :

$$\inf_{q_h \in Q_h} \sup_{w_h \in V_h} \frac{b(w_h, q_h)}{\|q_h\|_{0,\Omega} \|w_h\|_{1,\Omega}} \geq \beta_h$$

alors la solution (u_h, p_h) du problème de Stokes discret (A.4) est unique dans $V_h \times Q_h / \ker B_h^T$.

Démonstration : Voir Brezzi-Fortin.

Condition de Brezzi-Babuska :

La condition de Brezzi-Babuska se présente sous cette forme :

$$\inf_{q_h \in Q_h} \sup_{w_h \in V_h} \frac{b(w_h, q_h)}{\|q_h\|_{0,\Omega} \|w_h\|_{1,\Omega}} \geq \beta_0 > 0 \quad (A.5)$$

ou la constante β_0 est cette fois indépendant de h . Cette condition est nommée parfois par la condition inf-sup.

Théorème 3 (Convergence)

Sous les hypothèses d'existence et d'unicité des solutions (u, p) et (u_h, p_h) des problèmes de Stokes continu et discret et si la condition de Brezzi-Babuska (A.5) est vérifiée, alors :

$$\|u - u_h\|_{1,\Omega} + \|p - p_h\|_{0,\Omega} \leq C[\inf_{w_h \in V_h} \|u - w_h\|_{1,\Omega} + \inf_{q_h \in Q_h} \|p - q_h\|_{0,\Omega}]$$

Remarque 1.2 :

La constante C apparaissant dans le théorème précédent dépend entre autres chose de $\frac{1}{\alpha}$ et de $\frac{1}{\beta_0}$ d'où l'importance de la condition inf-sup.

Théorème 4 (Ordre de convergence)

Sous les mêmes hypothèses qu'au théorème précédent et si de plus le sous-espace V_h contient les polynômes de degré k et le sous espace Q_h contient les polynômes de degré $(k - 1)$, alors :

$$\|u - u_h\|_{1,\Omega} + \|p - p_h\|_{0,\Omega} \leq Ch^k (\|u\|_{k+1,\Omega} + \|p\|_{k,\Omega})$$

Remarque 1.3 :

Il est important de remarquer qu'il ne suffit pas de prendre des polynômes de degré k pour la vitesse et de degré $k - 1$ pour la pression pour avoir une discrétisation convergente, mais la condition de Brezzi-Babuska doit aussi être vérifiée.

A.2 Problème de Stokes non linéaire

La résolution par la méthode des éléments finis nécessite l'obtention d'une formulation variationnelle du problème. On multiplie ces deux équations respectivement par des fonctions test $w \in V$ et $q \in Q$ où V et Q sont des espaces fonctionnels appropriés

choisis , $V = W_0^{1,r}(\Omega)^N$ et $Q = L_0^{r'}(\Omega)$ avec $\frac{1}{r} + \frac{1}{r'} = 1$

On intègre ensuite par parties sur le domaine Ω de frontière Γ et on obtient ainsi $\forall w \in V$ et $\forall q \in Q$

$$\left\{ \begin{array}{l} \int_{\Omega} (-\nabla \cdot 2\eta(|d(u)|)d(u)) \cdot w + \nabla p \cdot w \, dx = \int_{\Omega} f \cdot w \, dx \\ \int_{\Omega} q \nabla \cdot u \, dx = 0 \end{array} \right. \quad (A.6)$$

Si on utilise le théorème de la divergence, l'équation (A.6) devient :

$$\left\{ \begin{array}{l} \int_{\Omega} (2\eta(|d(u)|)d(u) : \nabla w) \, dx - \int_{\Gamma} (2\eta(|d(u)|)d(u)) \cdot n \cdot w \, ds + \\ - \int_{\Omega} p \nabla \cdot w \, dx + \int_{\Gamma} (pn) \cdot w \, ds = \int_{\Omega} f \cdot w \, dx \\ \int_{\Omega} q \nabla \cdot u \, dx = 0 \end{array} \right. \quad (A.7)$$

c'est -à-dire :

$$\left\{ \begin{array}{l} \int_{\Omega} (2\eta(|d(u)|)d(u) : \nabla w) \, dx - \int_{\Omega} p \nabla \cdot w \, dx \\ - \int_{\Gamma} [(-pI + 2\eta(|d(u)|)d(u))n] \cdot w \, ds = \int_{\Omega} f \cdot w \, dx \\ \int_{\Omega} q \nabla \cdot u \, dx = 0 \end{array} \right. \quad (A.8)$$

étant donné que nous considérons le cas des conditions aux limites de Dirichlet homogène, on aura $v|_{\Gamma} = 0$. On obtient donc la formulation variationnelle dans le cas des fluides non newtoniens, en supposons que la viscosité est donnée par (A.8). La formulation variationnelle du problème de Stokes devient dans ce cas :

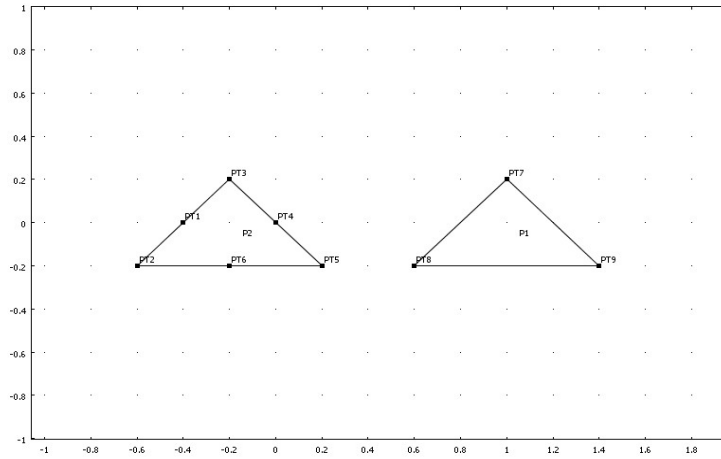
$$\left\{ \begin{array}{l} \int_{\Omega} (2\eta_0(c_0 + \lambda^n |d(u)|^n)^{\frac{m-1}{n}} d(u) : d(w) - \int_{\Omega} p \nabla \cdot w) \, dx = \int_{\Omega} f \cdot w \, dx \quad \forall w \in V \\ \int_{\Omega} q \nabla \cdot u \, dx = 0 \quad \forall q \in Q \end{array} \right. \quad (A.9)$$

A.2.1 Remarque :

L'existence est l'unicité a été approuvée par Jacques Baranger et Khalid Najib. dans [28].

A.3 Choix des éléments :

Il existe plusieurs choix possibles et nous on va s'intéresser à l'élément de Taylor-Hood souvent appelé $P_2 - P_1$, en raison de l'approximation quadratique P_2 des composantes de vitesse et de l'approximation de P_1 de la pression (voir figure si dessous). Les noeuds de calcul sont situées au sommet (vitesse et pression) et aux milieux des arêtes (vitesse seulement). Cet élément converge à l'ordre 2 ($O(h^2)$) en vertu du théorème 4 car l'approximation en vitesse contient les polynômes en degré deux et l'approximation en pression contient ceux d'ordre 1.



A.3.1 élément finis P2-P1 de Taylor-Hood :

On désigne par P_1 (piecewise linear continuous finite element) :

$$P1_h = \{v \in H^1(\Omega) | \forall K \in \mathcal{T}_h, v|_K \in P_1\}$$

. On désigne par P_2 (piecewise P_2 continuous finite element) :

$$P2_h = \{v \in H^1(\Omega) | \forall K \in \mathcal{T}_h, v|_K \in P_2\}$$

Pour la solution en éléments finis de l'équation (A.9), je discrétise le domaine et la solution en utilisant l'élément triangulaire P2-P1 (voir Figure ci dessus). Les vitesses sont présentées par les valeurs aux six points nodales, et sont interpolées par des po-

lynômes de degré deux. Par contre la pression est présentée par les valeurs aux trois points nodales, et sont interpolées par des polynômes linéaires.

A.3.2 Base nodale pour la pression :

Si on note B_p la base nodale relativement à la pression, alors cet ensemble est défini par :

$$B_p = \{\phi_i(x, y) | i \text{ indice nodale de la pression}\}$$

La fonction ϕ_i a pour valeur 1 au node n_i et 0 aux autres points nodales. Par conséquent, notre fonction de base est sous la forme d'une tente.

Si on désigne par n_j, n_k les autres points nodales de notre élément e , on sait alors que $\phi_i(x, y) = 0$ aux points nodales n_j et n_k comme ϕ_i est linéaire alors elle est nulle en tous points entre n_i et n_k , si on note les points N_i, N_j, N_k les points correspondant et N un point entre les points N_j, N_k alors les vecteurs :

$N_j N_k$ est colinéaire au vecteur $N_j N$ ce qui permet de conclure l'égalité suivante :

$$\frac{y_k - y_j}{x_k - x_j} = \frac{y - y_j}{x - x_j}$$

On pose :

$$g(x, y) = (x - x_j)(y_k - y_j) - (x_k - x_j)(y - y_j)$$

On sait que

$$g(x, y) = 0$$

en tout point entre les points nodales n_j et n_k on suppose que notre triangle est non dégénéré alors

$$g(x_i, y_i) \neq 0$$

car N_i n'appartient pas à $N_j N_k$.

En fin, si on pose

$$\phi_i(x, y) = \frac{g(x, y)}{g(x_i, y_i)}$$

On voit bien ϕ_i satisfait la base convenable, d'une manière explicite on obtient :

$$\phi_i(x, y) = \frac{(x - x_j)(y_k - y_j) - (x_k - x_j)(y - y_j)}{(x_i - x_j)(y_k - y_j) - (x_k - x_j)(y_i - y_j)}$$

Remarque :

La somme $\phi_i + \phi_j + \phi_k = 1$ car ils représentent l'aire des trois sous triangles du triangle e .

Expression analytique :

L'expression analytique est donnée par :

$$\phi_1(x, y) = 1 - x - y$$

$$\phi_2(x, y) = x$$

$$\phi_3(x, y) = y$$

et p peut s'écrire en fonction de sa base nodale :

$$p(x, y) = \sum_{i=1}^3 \phi_i p_i$$

ou les p_i sont les valeurs nodales correspondants.

A.3.3 Base nodale pour la vitesse :

Si on note B_v la base nodale relativement à la vitesse, alors cet ensemble est défini par :

$$B_v = \{\psi_i(x, y) | i \text{ indice nodale de la vitesse}\}$$

Dans ce cas on écrit $\mathbf{u}(x, y) = \sum_{i=1}^6 u_i \psi_i(x, y)$.

Pour définir les fonctions de base quadratiques relativement à la vitesse on raisonne de la même manière que précédemment pour les fonctions de base linéaire pour la pression. Pour cela on considère deux types de points nodales : les noeuds (sommets de l'élément) et les noeuds intermédiaire.

Base nodale pour les noeuds (sommets) :

Pour le noeud N_i on pose la fonction ψ_i la fonction de base associée à N_i , Même raisonnement que précédemment on se donne la fonction

$$g(x, y) = (x - x_j)(y_k - y_j) - (x_k - x_j)(y - y_j)$$

tel que $g(N_j) = g(N_k) = 0$ de plus par linéarité $g(N_{jk}) = 0$.

D'une manière analogue on construit pour les les points nodales N_{ij}, N_{ik} une fonction h tel que $h(N_{ij}) = h(N_{ik}) = 0$ cette fonction sera définie par

$$h(x, y) = (x - x_{ij})(y_{ik} - y_{ij}) - (x_{ik} - x_{ij})(y - y_{ij})$$

En fin pour le point nodale N_i on a $g(N_i) \neq 0$ et $h(N_i) \neq 0$ donc le produit $g(N_i)h(N_i) \neq 0$ est égale à zéro aux autres cinq points.

Définition :

On définit la fonction $\psi_i(x, y)$ comme produit de g par h sur le produit de g par h au point N_i de plus on a $\psi_i(N_i) = 1$,

$$\psi_i(x, y) = \frac{g(x, y)h(x, y)}{g(n_i)h(n_i)}$$

Remarque :

Pour les autres points nodales N_k et N_j on définit d'une manière similaire les deux autres fonctions de bases.

Base nodale pour les noeuds intermédiaires :

D'une manière analogue on détermine les fonctions de bases pour les noeuds intermédiaire on obtient des fonctions

$$\psi_{ij} = \frac{g(x, y)h(x, y)}{g(x_{ij}, y_{ij})h(x_{ij}, y_{ij})}$$

En effet, soit les droites N_iN_k et N_jN_k pour chaque droite on associée respectivement les deux fonctions suivantes comme précédemment g et h .

g à la forme suivante

$$g(x, y) = (x - x_k)(y_i - y_k) - (x_i - x_k)(y - y_k)$$

et h à la forme suivante

$$h(x, y) = (x - x_k)(y_j - y_k) - (x_j - x_k)(y - y_k)$$

De plus tous les points respectivement de la droite N_iN_k et N_jN_k vérifient $g(x, y) = 0$ (resp $h(x, y) = 0$). Comme le point n_{ij} n'appartient pas à ces deux droites alors on a

$g(n_{ij}) \neq 0$ et $h(n_{ij}) \neq 0$ donc $g(n_{ij})h(n_{ij}) \neq 0$

Définition :

On définit la fonction de base nodale relativement au noeud intermédiaire n_{ij} par :

$$\psi_{ij}(x, y) = \frac{g(x, y)h(x, y)}{g(n_{ij})h(n_{ij})}$$

De plus on a $\psi_{ij}(n_{ij}) = 1$.

Remarque :

Cet élément P2-P1 nous assure la continuité de la vitesse et la pression, et nous satisfait la condition inf-sup.

Expression analytique :

Pour la vitesse, on obtient les six fonctions de bases suivantes :

$$\psi_1(x, y) = 1 - 3x - 3y + 2x^2 + 4xy + 2y^2$$

$$\psi_2(x, y) = -x + 2x^2$$

$$\psi_3(x, y) = -y + 2y^2$$

$$\psi_4(x, y) = 4xy$$

$$\psi_5(x, y) = 4x - 4xy - 4y^2$$

$$\psi_6(x, y) = 4y - 4xy - 4x^2$$

Par conséquent la vitesse peut être exprimées en fonctions de sa base nodale respectivement :

$$u(x, y) = \sum_{i=1}^6 \psi_i u_i$$

$$v(x, y) = \sum_{i=1}^6 \psi_i v_i$$

ou u_i et v_i sont les valeurs nodales correspondants.

Bibliographie

- [1] **G.P.Panasenko, R.Stavre**, *Asymptotic analysis of a periodic flow in a thin channel with visco elastic wall*, J.Math.Pures Appl.,85,no. 4, 558-579, 2006.
- [2] **F. Blanc, O. Gipouloux, G. Panasenko and A. Zine** *Asymptotic Analysis and Partial Asymptotic Decomposition of Domain for Stokes Equation in Tube Structure*, Maths. Models and Methods in Applied Science, 99 : 1351–1378, 1999.
- [3] **D.Dupuy. G.P.Panasenko, R.Stavre**,*Asymptotic analysis for micropolar fluids*, C.RAcad Sci. Paris, Sér. Iib332(1)(2004)31-36.
- [4] **Bartle, R.G.** *The elements of integration*. Wiley, New York, 1966.
- [5] **Bathe, K. J.** *Finite Element Procedures*. Prentice Hall, 1996.
- [6] **Bonet, J. et D. R. Wood***Nonlinear continuum mechanics for finite element analysis*. Cambridge,1997.
- [7] **Brezzi, F. et M. Fortin** *Mixed and Hybrid Finite Element Methods*. Springer-Verlag, 1991.
- [8] **Ciarlet, P.G.** *The Finite Element Method for Elliptic problems*. North-Holland, Amsterdam,1986.
- [9] **A.Fortin. et A.Garon** *les éléments finis de la théorie à la pratique*. polycopie 1997-2011.Université Laval Québec.
- [10] **A.Quateroni and L.Formaggia**. *Mathematical Modelling and Numerical simulation of the cardiovascular system*.In *Modelling of living systems, Handbook of Numerical Analysis*, Series.N.Ayache editor,2002.

- [11] **Vivette Girault, Pierre-Arnaud Raviart.** *Finite Element Methods for Navier-Stokes Equations, Theory and Algorithms*, Spriger-Verlag, Berlin Heidelberg New York Tokyo, 1986.
- [12] **John. Burkardt.** *Finite Element Treatment of the Navier Stokes Equations*, Part II. School of Computational Science ; Florida State University.
- [13] **S.A.Nazarov.** *Asymptotic solution of the Navier-Stokes problem on the flow in thin layer fluid.* Siberian Math. Journal, 31 :296-307, 1990.
- [14] **O.A.Ladyznskaya.** *The Mathematical Theory of viscous Incompressible Flow.* New York/Londo/Paris : Gordon and Breach Sc.Publ, 1969.
- [15] **S.A.Nazarov, B.A.Plamenevski.** *Elliptic Problems in Domains with Piecewise Smooth Boundaries.* Berlin-New York : Walter de Gruyter, 1994.
- [16] **G.Panasenko.** *Multi-scale Modelling for Structure and Composites*, Springer-verlag, Berlin/New York, 2005.
- [17] **R.Temam.** *Navier Stokes Equations.* Amsterdam : North-Holland, 1979.
- [18] **B.Desjardins, M.J.Esteban, C.Grandmont, P.le talec,** *Weak solutions for fluid-structure interaction model*, Pev. Mat. comput. 14(2)(2001) 523-538.
- [19] **B.Desjardins, M.J.Esteban,** *On weak solutions for fluid-rigid structure interaction : compressible and incompressible models*, Comm. Partial Differential Equations 25(7-8) (2000) 1399-1413.
- [20] **F.Flori, P.Orenga,** *Fluid-structure interaction : analysis of 3-D compressible model*, ANN. Inst.H.Poincaré, Anal. Non linéaire 17(6)(2000) 753-777.
- [21] **C.Grandmont,** *Existence et unicité de solutions d'un problème de couplage fluide- structure bidimensionnel stationnaire*, C,R. Acad. Sci.Paris Série I 326(5)(1998)651-656.
- [22] **C.Grandmont, Y.Maday,** *Existence for an unsteady fluid-structure interaction problem.* M^2AN Math. Model. Numer. Anal. 34(3)(2000) 609-636.
- [23] **A.Chambolle, B.Desjardins, M.J.Esteban, C.Grandmont,** *Existence of weak solutions for an unsteady fluid-plate interaction problem*, Ceremade-UMR 7354-Université Paris-Dauphine, no. 0245, 2002.

- [24] **D.Dupuy. G.P.Panasenko, R.Stavre**, *Asymptotic methods for micropolar flows in tube structure*, Math.Mod.Meth.Appl.Sci.14(5)(2004)735-758.
- [25] **D.Dupuy. G.P.Panasenko, R.Stavre**, *Multiscale modeling for micropolar flows in a tube structure with one bundle of tubes*, Int.J.Multiscale comput.Eng.2(3)(2004)461-475.
- [26] **S.A.Nazarov, M.Specovius Neugebauer**. *Approximation of unbounded domain by bounded domains. Boundary value problems for lame operator*. St.Petersburg Math. Journal, 8(5) :879-912, 1997.
- [27] **M.Specovius Neugebauer**. *Approximation of stokes problem in unbounded domain*, preprint, university of Paderborn, 1997.
- [28] **Jacques.Baranger and Khalid. Najib**. *Analyse numerique des ecoulements quasi-Newtoniens dont la viscosite obeit a la loi puissance ou la loi de carreau* Numerische Mathematik Volume 58, Number 1, 35-49, DOI : 10.1007/BF01385609.
- [29] **Luca Formaggia, Alessandro Veneziani, Alfio M. Quarteroni** *Cardiovascular Mathematics : Modeling and simulation of the circulatory system* Volume 1 May 2009.
- [30] **G.P.Panasenko**, *Asymptotic expansion of the solution of Navier-Stokes equations in tubes structure*. CRAS, Seri IIb, 326 :867-872, 1998.
- [31] **G.P.Panasenko**, *Asymptotic decomposition of domain : Navier-Stokes equations in tubes structure*. CRAS, Seri IIb, 326 :893-898, 1998.
- [32] **Girault.V, Raviart.P.A**, *Finite Element Methods for Navier-Stokes Equations*, Springer, Berlin, 1986.
- [33] **Brezzi.F, Fortin.M**, *Mixed and Hybrid Finite Element Methods*, Springer, New York, 1991.
- [34] **I. Babushka**, *The finite element method with Lagrangian multipliers*, Numer. Math. 20, pp 179-192. (1973).
- [35] **P. Hood and C. Taylor**, *Navier Stokes equations using mixed interpolation, in Finite Element Methods in Flow Problems*, J. T. Oden, R. H. Gallagher, O. C.

Zienkiewicz, and C. Taylor, eds., University of Alabama in Huntsville Press, 1974, pp. 121-132.

[36] **Giovanni P. Galdi** , *An Introduction To The Mathematical Theory Of The Navier-Stokes Equations : Volume 1 : Nonlinear Steady Problems*, Springer, 2 Rev ed, English.

[37] **Giovanni P. Galdi** , *An Introduction To The Mathematical Theory Of The Navier-Stokes Equations : Volume 2 : Nonlinear Steady Problems*, Springer, 2 Rev ed, English.